Institute of Paper Science and Technology

STATUS REPORTS

To The

PAPERMAKING

PROJECT ADVISORY COMMITTEE

April 4, 1991
Institute of Paper Science and Technology
Atlanta, GA

Atlanta, Georgia

INSTITUTE OF PAPER SCIENCE AND TECHNOLOGY

Antitrust Notice

Guidelines for Meetings

Neither the Institute of Paper Science and Technology nor any committee or activity of the Institute shall be used or include discussions for the purpose of bringing about or attempting to bring about any understanding or agreement, written or oral, formal or informal, expressed or implied, among competitors with regard to prices, terms or conditions of sale, distribution, volume of production, or allocation of territories, customers, or suppliers.

No IPST activity shall involve exchange or collection and dissemination among competitors of any information regarding prices, pricing methods, costs or production, sales, marketing, or distribution.

Neither IPST nor any committee thereof shall make any effort to bring about the standardization of any product for the purpose of or with the effect of preventing the manufacture or sale of any product not conforming to a specified standard.

The Institute does not become involved in any product standards or endorsements. IPST policy as a tax exempt educational institution expressly precludes the establishment of product standards or the endorsement of any product or process and general provisions incorporated in IPST research contracts so stated.

Rev. 10/90

STATUS REPORTS

To The

PAPERMAKING

PROJECT ADVISORY COMMITTEE

April 4, 1991
Institute of Paper Science and Technology
Atlanta, GA

AGENDA

PAPERMAKING

PROJECT ADVISORY COMMITTEE

Thursday--April 4
Wyndam Hotel Midtown
Atlanta, Georgia

8:00	Coffee and Rolls	
8:20	Introduction	B. Thorp
8:30	Project 3674--Fundamentals of Coating Systems	C. Aidun
9:20	Project 3680--Displacement Dewatering	J. Lindsay
10:05	Break	
10:15	Project 3470--Fundamentals of Drying	D. Orloff
11:30	New Projects	
12:00	Lunch	
1:00	Project 3470--Funamentals of Drying	D. Orloff
2:00	Project 3480/3680--Fundamentals of Water Removal Processes	J. Lindsay
2:45	Break	
3:00	Project 3674--Fundamentals of Coating Systems	C. Aidun
4:00	Adjournment	

March 15, 1991

TO: MEMBERS OF THE PAPERMAKING PROJECT ADVISORY COMMITTEE

Attached for your review are the Status Reports for the projects to be discussed at the Papermaking Project Advisory Committee meeting scheduled for April 4, 1991, in Atlanta.

We look forward to seeing you on April 4, 1991. Best regards.

Sincerely,

R J Ellis

Richard Ellis, Director
Engineering and Paper Materials Division

Attachment

RE/at

Institute of Paper Science and Technology, Inc.

575 14th Street, N.W.
Atlanta, GA 30318

Formerly The Institute of Paper Chemistry
Appleton, Wisconsin

Telephone 404-853-9500
FAX # 404-853-9510

PAPERMAKING
PROJECT ADVISORY COMMITTEE

IPST LIAISON: RICHARD ELLIS

Mr. Benjamin A. Thorp (*Chairman*)
Senior Vice President Engineering
James River Corporation
Post Office Box 2218
Richmond, VA 23217-2218
(804) 649-4335
(804) 343-8592 FAX

Mr. Jack F. Brown
Manager Paper & Coatings
Boise Cascade Corporation
4435 North Channel Avenue
Portland, OR 97217-0000
(503) 286-7418
(503) 286-7467 FAX

Dr. David S. Dillard, Jr.
Director of Research and Development
Georgia-Pacific Corporation
100 Wisconsin River Drive
Port Edwards, WI 54469-0000
(715) 887-5111
(715) 887-5555 FAX

Mr. Robert V. LaBruzzo
Technical Manager
Tennessee River Pulp and Paper
Post Office Box 33
Counce, TN 38326
(901) 689-5199

Mr. Steve Smith
#1 Machine Supervisor
Westvaco Corporation
5600 Virginia Avenue
Charleston, SC 29411-2905
(803) 745-3211
(803) 745-3318 FAX

Mr. John W. Stolarz
Group Leader Papermaking
Mead Corporation
Eighth & Hickory Streets
Chillicothe, OH 45601-0000
(614) 772-3441
(614) 772-3595

Mr. James C. West
Containerboard Manufacturing Manager
Weyerhaeuser Paper Company
5410 79th Avenue Court
West Tacoma, WA 98467
(206) 924-2345

Mr. Allen Rosen
Section Leader Processes
Research & Development Division
Union Camp Corporation
Post Office Box 3301
Princeton, NJ 08543-3301
(609) 896-1200

TABLE OF CONTENTS

AGENDA

PAPERMAKING
PROJECT ADVISORY COMMITTEE

April 4, 1991
Wyndam Hotel Midtown
Atlanta, GA

THURSDAY--April 4

PROJECT

3674	Fundamentals of Coating Systems
3680	Displacement Dewatering
3480	Fundamentals of Water Removal Processes
3470	Fundamentals of Drying

FUNDAMENTALS OF DRYING

STATUS REPORT

FOR

PROJECT 3470

April 4, 1991

Institute of Paper Science and Technology

Atlanta, Georgia

Project Summary Form

Project Title:	FUNDAMENTALS OF DRYING
Project Number:	3470
Project Staff:	David Orloff
FY Budget:	\$200,000
Project Goal:	Reduction of the "necessary minimum" complexity in number and/or sophistication of process steps.

OBJECTIVE:

To develop an understanding and a database sufficient for the commercialization of advanced water removal systems, based on high intensity drying principles. This new technology will reduce capital costs, increase machine productivity, reduce the amount of energy used, and improve properties.

CURRENT FISCAL BUDGET:

\$200,000 from Institute funds, plus \$200,000 through a Department of Energy grant (as Project 3595). The Department of Energy has budgeted \$1.4 million over five years, this being the first of the five budget periods for the project. Additional funding is also anticipated from the Electric Power Research Institute.

SUMMARY OF RESULTS FOR THIS REPORTING PERIOD:

(December 1990 - February 1991)

We have continued to concentrate our efforts on solving the delamination problem which is a major technical barrier to the commercialization of impulse drying. A low thermal mass press roll coating has been invented to achieve this objective. For background it is helpful to review some of our previous laboratory scale findings.

* There are two regions of delamination. The first occurs at a dwell time of about 20ms, while the dwell time where the second region begins depends on: basis weight, felt moisture and platen thermal properties.

* Impulse drying results in enhanced water removal compared to conventional single felted hot pressing. Sheet preheat improves water removal at all platen temperatures.

* For short dwell times of 20ms, water removal is dependent on platen surface temperature and peak pressure while independent of platen thermal properties.

* For short dwell times of 20ms, the prototype low thermal mass platen can be operated at substantially higher temperatures and peak pressures without causing sheet delamination. Sheets impulse dried with the prototype platen exhibit a substantial increase in density and strength.

During the current reporting period our research program has consisted of two major objectives; 1) Demonstrate and evaluate the pilot scale impulse drying of 42 pound liner board using a prototype low thermal mass coated press roll. 2) Develop an understanding of the mechanism of operation of low thermal mass surfaces by measuring the heat flux during impulse drying.

PILOT SCALE DEMONSTRATION AND EVALUATION:

The prototype ceramic coated prototype press roll was installed on the first nip of the pilot impulse dryer as shown on Figure 1. In order to control the ingoing surface temperature of the roll, an infrared sensor was also installed. In addition, a steam box in combination with a vacuum box were used to preheat the web prior to introduction into the first press nip. The steam box was instrumented with a temperature and pressure compensated vortex flow meter to record steam mass flow rate. The temperature and pressure just prior to exiting the box were also recorded along with the vacuum box operating pressure.

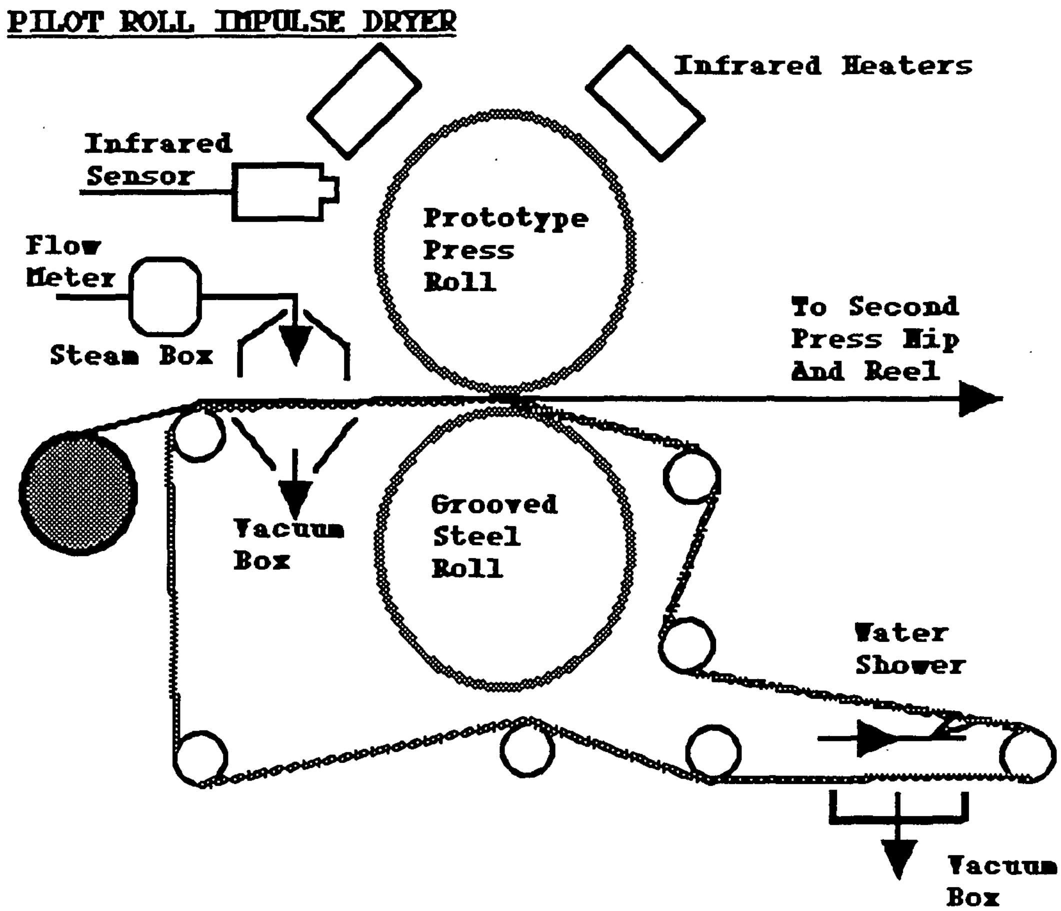

Figure 1. First nip of the pilot scale two nip impulse dryer.

Forty-two pound liner (205 gsm) was made from an unbleached softwood kraft (KAPPA No. of 73.5) refined to 650CSF. In order to achieve a range of ingoing solids from 30 to 50%, the linerboard was formed on the IPST web former, unwound and cold pressed on the second nip of the pilot dryer to the desired dryness level. Measurements of z - direction sheet permeability showed that rolls pressed to higher solids tended to have higher permeability than rolls pressed to a lower solids. It was speculated that surface drying during repeated re-winding may have contributed to this effect.

As steam preheating adds water to the sheet, a series of experiments were performed to quantify this effect over a range of ingoing solids. Pre-weighed sheets were placed onto the felt, upstream of the steam box, and retrieved for weighing at the exit of the steam box. The important variables were; steam flow rate, steam temperature, vacuum box pressure and dryer speed. Figure 2 shows the increase in sheet moisture resulting from steam preheating at a steam flow rate of 214 kg/h, a steam temperature of 112°C, a vacuum of 28 cm Hg at pilot dryer speeds of 30 m/min and 60 m/min. Using the results of Figure 2, thermodynamic calculations suggest that web temperatures will be 100°C over the range of pilot dryer speeds of 30 to 60 m/min for 205 gsm liner entering the steam box at dryness between 30% and 50%. Experimental verification of sheet preheat temperatures are planned.

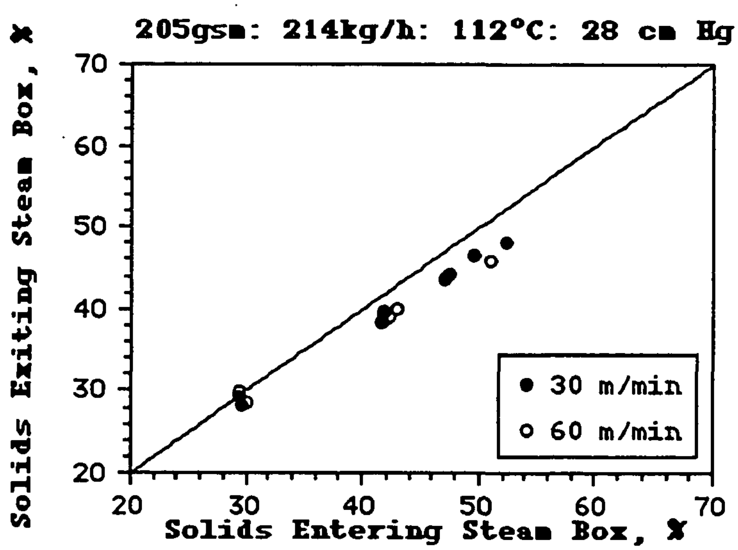

Figure 2. Increase In Sheet Moisture Resulting From Steam Preheat.

In a series of impulse drying experiments the first nip was set to a peak pressure of 6.2 MPa. Nip impressions demonstrated that the pressure distribution across the width of the prototype press roll was uniform and accurate. Based on a measured nip width of 20 mm at 6.2 MPa, a dryer speed of 60 m/min corresponded to a dwell time of 20 ms, while a dryer speed of 30 m/min corresponded to a dwell time of 40 ms.

In order to demonstrate the enhancement of impulse drying over single felted wet pressing, drying experiments were conducted over a range of ingoing roll surface temperatures from 100°C to 430°C. Experiments were conducted over a range of ingoing solids from 40% to 45% at both 20 ms and 40 ms. The rolls of wet paper were steam preheated at the conditions of Figure 2. Ingoing solids reported in all subsequent figures of this report are ingoing solids at the exit of the steam box. Figure 3 show the effect of ingoing roll surface temperature on outgoing solids for a roll of paper at an ingoing dryness of 41.5% solids. Similar results for a roll of paper at 43.5% solids are shown on Figure 4. At a nip residence time of 20 ms there was a small improvement in outgoing solids as compared to wet pressing. Increasing the nip residence time to 40 ms resulted in a dramatic improvement in outgoing solids.

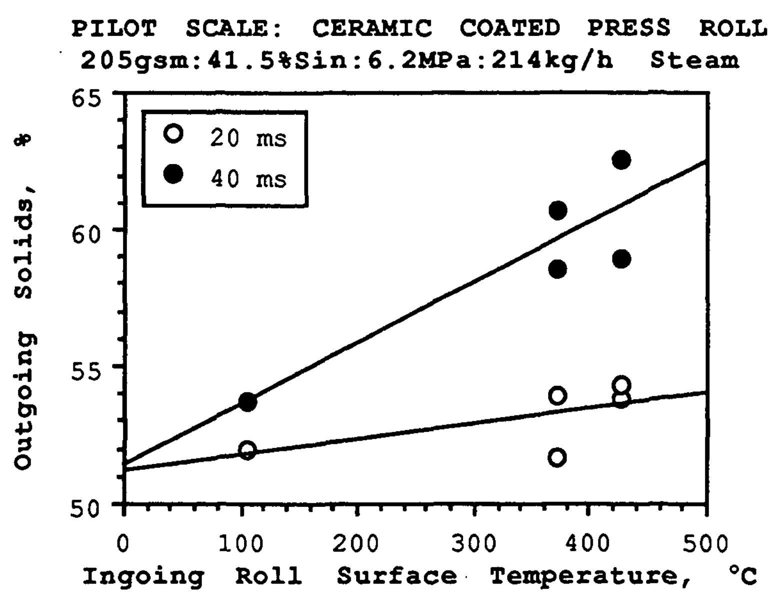

Figure 3. Outgoing Solids As A Function Of Ingoing Roll Surface Temperature At An Ingoing Solids Of 41.5%.

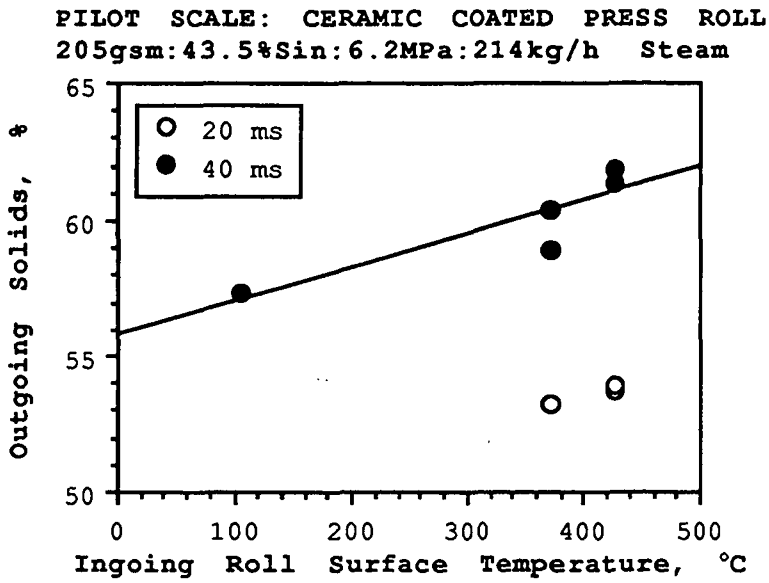

Figure 4. Outgoing Solids As A Function Of Ingoing Roll Surface Temperature At An Ingoing Solids Of 43.5%.

Our objective was to assess whether the prototype ceramic coated press roll could be used to impulse dry heavy weight grades without inducing sheet delamination. To characterize the physical properties of the paper, large samples of the wet pressed and impulse dried paper were finish dried on a drum dryer, conditioned to TAPPI standards and tested. Figure 5 shows the location of various tests performed on 22 cm x 28 cm samples. While Table 1 indicates the tests that were performed and the number of tests per location.

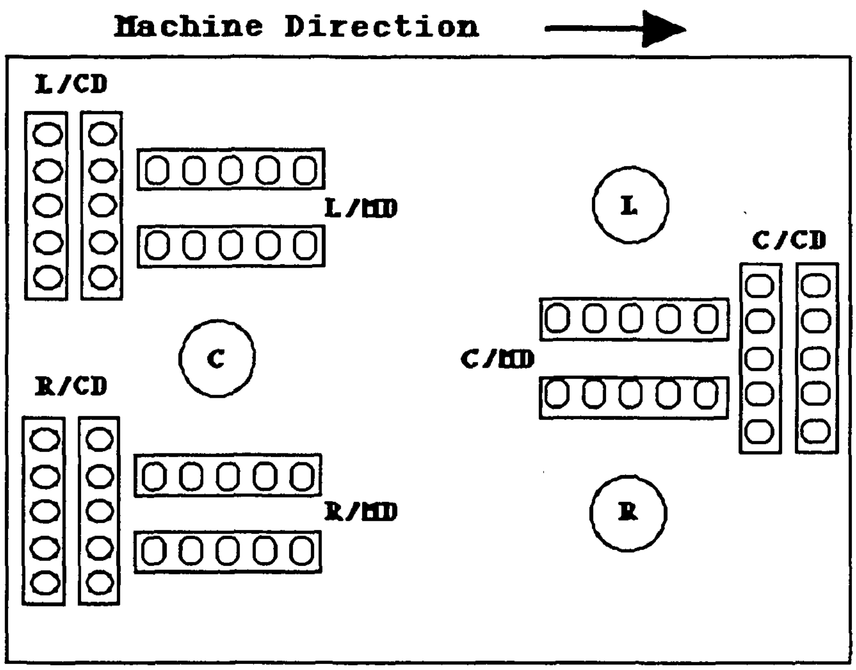

Figure 5. Schematic Of Sheet Test Locations.

TABLE 1

LOCATION	TEST PERFORMED	TESTS PER LOCATION
L/CD	Z - Ultrasound STFI Compression OD Basis Weight	10 10 2
L/MD	Z - Ultrasound STFI Compression OD Basis Weight	10 10 2
C/CD	Z - Ultrasound STFI Compression OD Basis Weight	10 10 2
C/MD	Z - Ultrasound STFI Compression OD Basis Weight	10 10 2
R/CD	Z - Ultrasound STFI Compression OD Basis Weight	10 10 2
R/MD	Z - Ultrasound STFI Compression OD Basis Weight	10 10 2
L	Burst	1
C	Burst	1
R	Burst	1

In previous laboratory scale work, we have found that delaminated regions of a sheet typically have a lower out-of-plane specific elastic modulus than surrounding non-delaminated regions of the sheet. Hence, we have used the coefficient of variation of the out-of-plane specific elastic modulus to detect the onset of sheet delamination. By comparing the coefficient of variation of an impulse dried sample with that of a wet pressed sample we can detect delamination.

Figures 6 through 9 compare the coefficient of variation of the out-of-plane specific elastic modulus for the conditions reported in Figure 3 and 4. For a nip residence time of 20 ms ingoing roll surface temperatures of as high as 426°C could be operated without inducing sheet delamination. At a nip residence time of 40 ms, delamination was not detected at an ingoing roll surface temperature of 371°C but may be present at 426°C. To further validate this observation, samples from each condition have been submitted for scanning electron microscopy cross-sections.

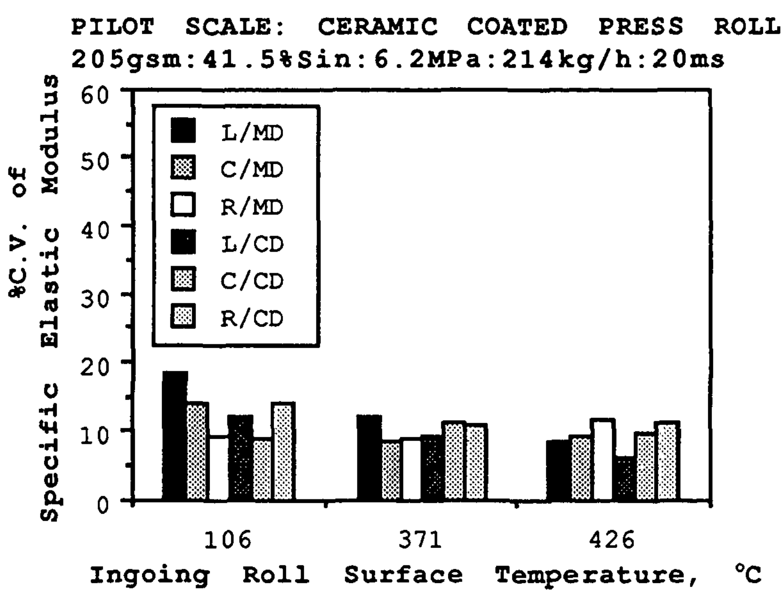

Figure 6. Coefficient Of Variation Of The Out-Of-Plane Specific Elastic Modulus At Various Ingoing Roll Surface Temperatures For An Ingoing Solids Of 41.5% At A Nip Residence Time Of 20 ms.

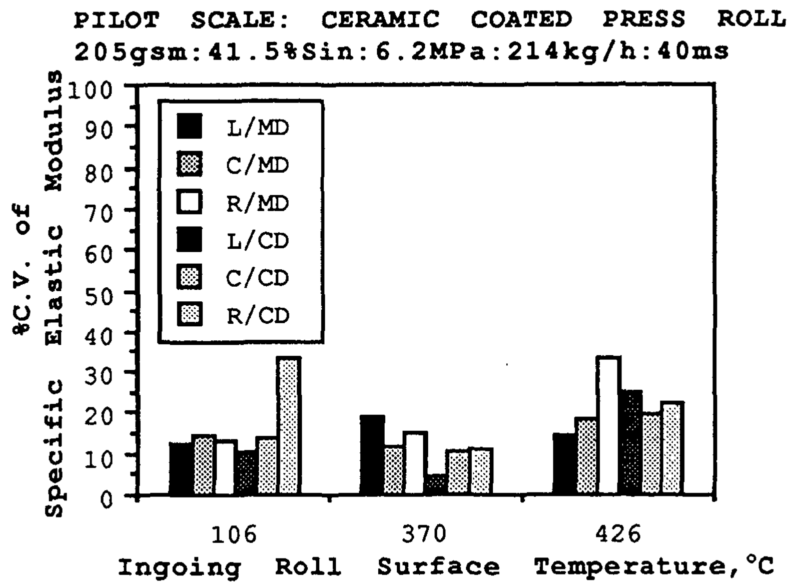

Figure 7. Coefficient Of Variation Of The Out-Of-Plane Specific Elastic Modulus At Various Ingoing Roll Surface Temperatures For An Ingoing Solids Of 41.5% At A Nip Residence Time Of 40 ms.

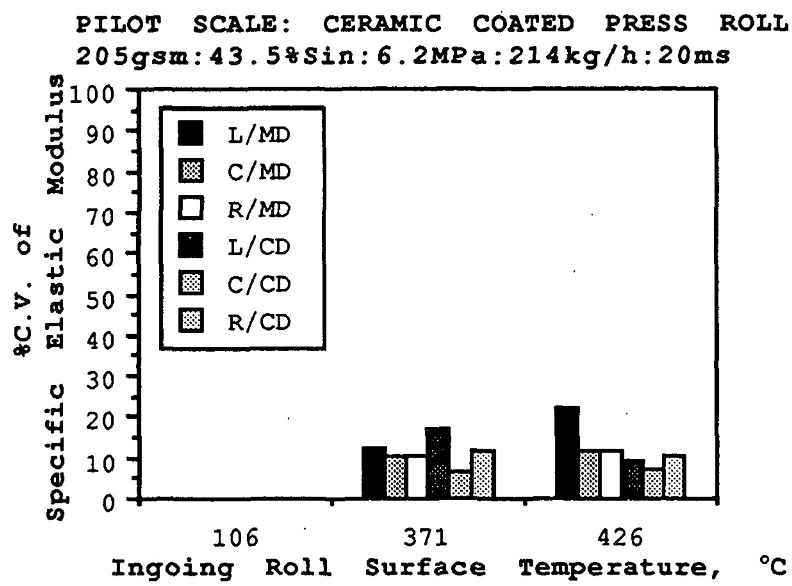

Figure 8. Coefficient Of Variation Of The Out-Of-Plane Specific Elastic Modulus At Various Ingoing Roll Surface Temperatures For An Ingoing Solids Of 43.5% At A Nip Residence Time Of 20 ms.

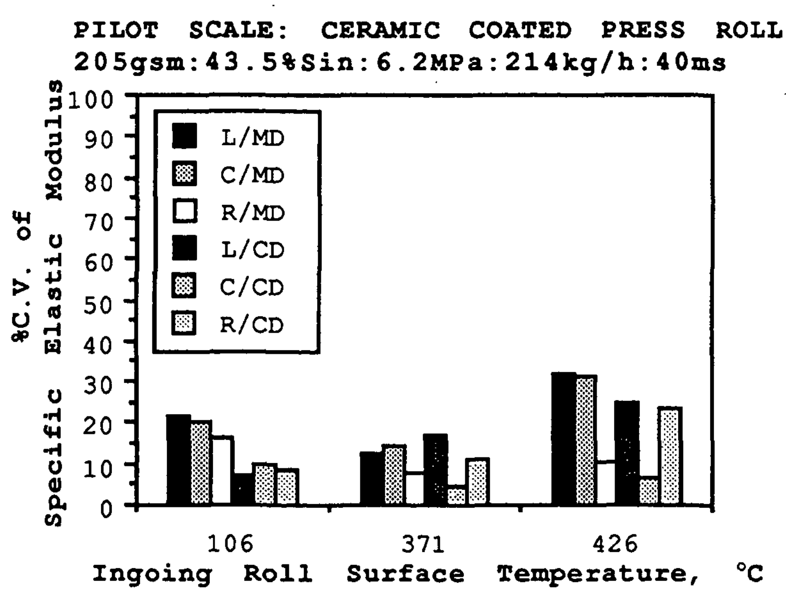

Figure 9. Coefficient Of Variation Of The Out-Of-Plane Specific Elastic Modulus At Various Ingoing Roll Surface Temperatures For An Ingoing Solids Of 43.5% At A Nip Residence Time Of 40 ms.

Out-of-plane specific elastic modulus, burst index and STFI compression index each give an indication of sheet strength. To demonstrate the improvement in physical properties achievable through impulse drying, each of these properties are shown as a function of ingoing roll surface temperature.

As shown in Figures 10 and 11, a substantial improvement in out-of-plane specific elastic modulus was achieved at a nip residence time of 40 ms.

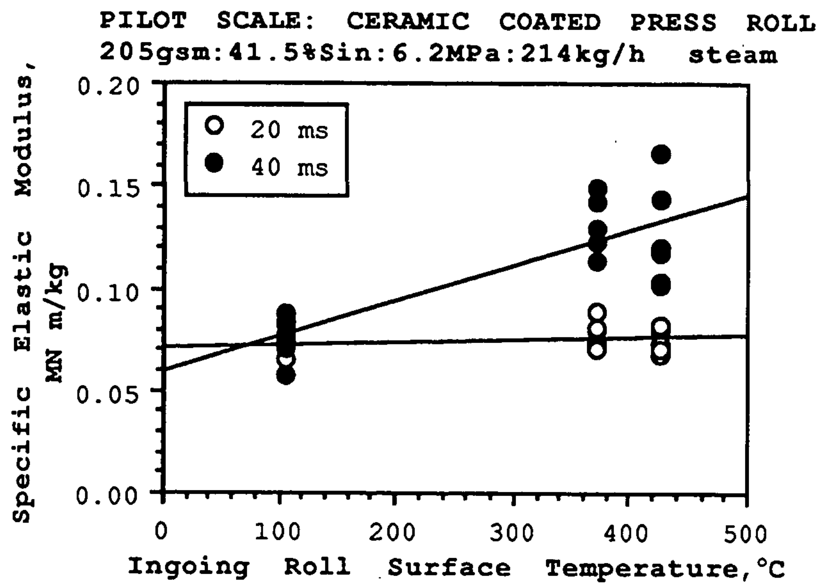

Figure 10. Out-Of-Plane Specific Elastic Modulus As A Function Of Ingoing Roll Surface Temperature For An Ingoing Solids Of 41.5%.

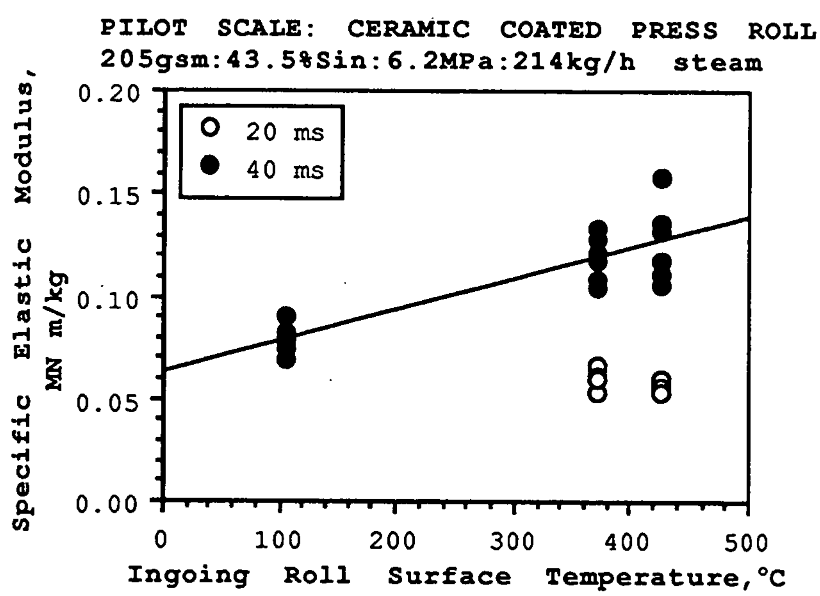

Figure 11. Out-Of-Plane Specific Elastic Modulus As A Function Of Ingoing Roll Surface Temperature For An Ingoing Solids Of 43.5%.

Soft platen density, measured during the ultrasonic testing shows a linear relationship with out-of-plane specific elastic modulus, as shown in Figure 12. Hence, strength improvements can be attributed to greater densification.

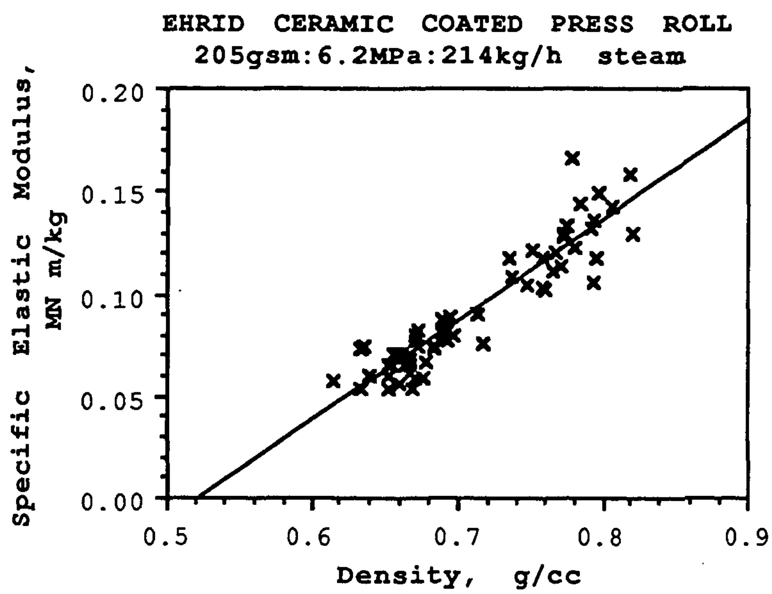

Figure 12. Out-Of-Plane Specific Elastic Modulus As A Function Of Soft Platen Density.

As shown in Figures 13 and 14, Burst index was enhanced by impulse drying at nip residence times of both 20 and 40 ms.

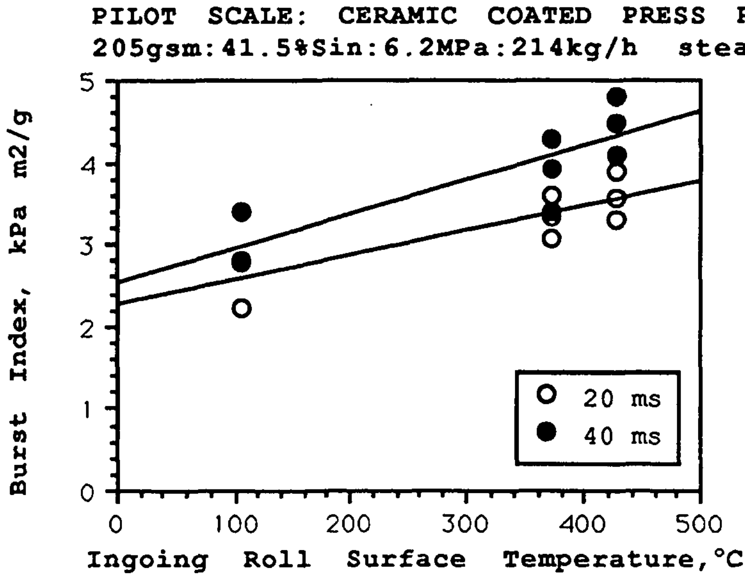

Figure 13. Burst Index As A Function Of Ingoing Roll Surface Temperature For An Ingoing Solids Of 41.5%.

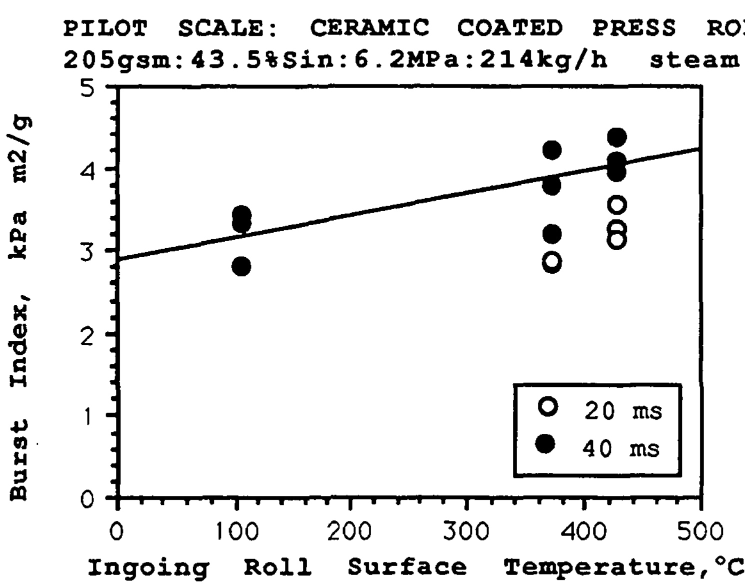

Figure 14. Burst Index As A Function Of Ingoing Roll Surface Temperature For An Ingoing Solids Of 43.5%.

Figures 15 and 16, show both machine direction (MD) and cross direction (CD) STFI index as a function of ingoing roll surface temperature. As in the case of elastic modulus, improvements to STFI index were achieved at a nip residence time of 40 ms.

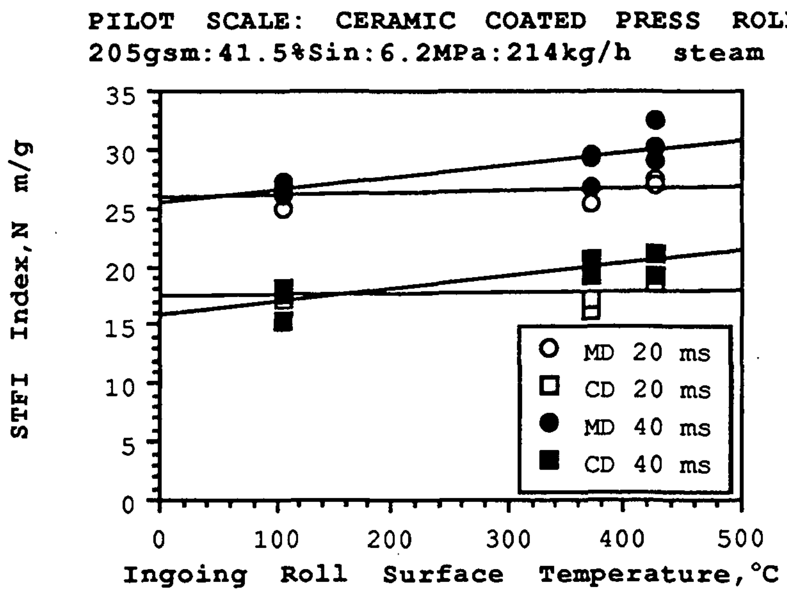

Figure 15. STFI Index As A Function Of Ingoing Roll Surface Temperature For An Ingoing Solids Of 41.5%.

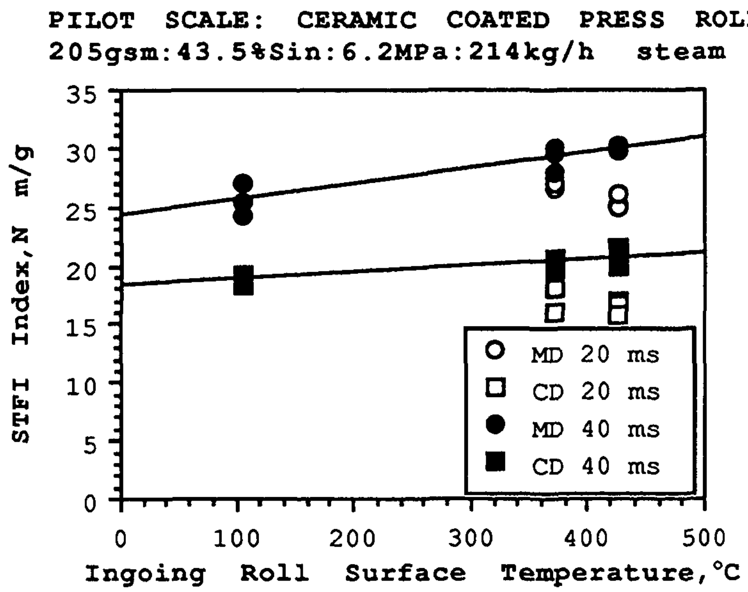

Figure 16. STFI Index As A Function Of Ingoing Roll Surface Temperature For An Ingoing Solids Of 43.5%.

Table 2 summarizes the results of these experiments in terms of maximum water removal and physical properties achieved for an ingoing solids of 41.5%. To achieve maximum benefit of impulse drying, nip residence times approaching 40 ms are required. Employing a commercially available 0.25 m long ENP, residence times of 40 ms can be obtained at machine speeds of less than 375 m/min. For higher machine speeds longer nips will be required.

TABLE 2

	WET PRESS 20ms	IMPULSE DRY 427°C 20ms	WET PRESS 40ms	IMPULSE DRY 371°C 40ms
Solids Out, %	52	54	54	60
Modulus, MN m/kg	0.07	0.07	0.07	0.12
Burst Index,kPa m^2/g	2.6	3.5	3.0	4.0
MD STFI Index,N m/g	26	26	26	29
CD STFI Index,N m/g	17	17	17	20

In conclusion, the pilot scale experiments demonstrate that the prototype ceramic coated roll can be operated at high temperatures and high pressures resulting in delamination-free paper with enhanced physical properties.

LABORATORY SCALE HEAT FLUX MEASUREMENTS:

Previously reported laboratory scale simulations have suggested the benefit of the prototype low thermal mass press roll surface. In those experiments, handsheets were steamed to a temperature of 85°C prior to impulse drying. As a result of radiation from the heated platen to the paper during steaming, significant surface moisture loss occurred during preheating. To correct for this effect, ingoing sheet solids were chosen such that after steam preheating the z-directional average ingoing solids were 30% independent of platen temperature. However, this procedure does not correct for the fact that at high platen surface temperatures extreme z-directional ingoing moisture gradients exist. To better simulate a uniform ingoing z-directional moisture gradient, the simulation equipment was modified to drastically reduce radiant heat transfer during preheat. For this purpose, a ceramic radiation shield with moisture absorbent lower layer, has been added to the equipment as shown on

Figure 17.

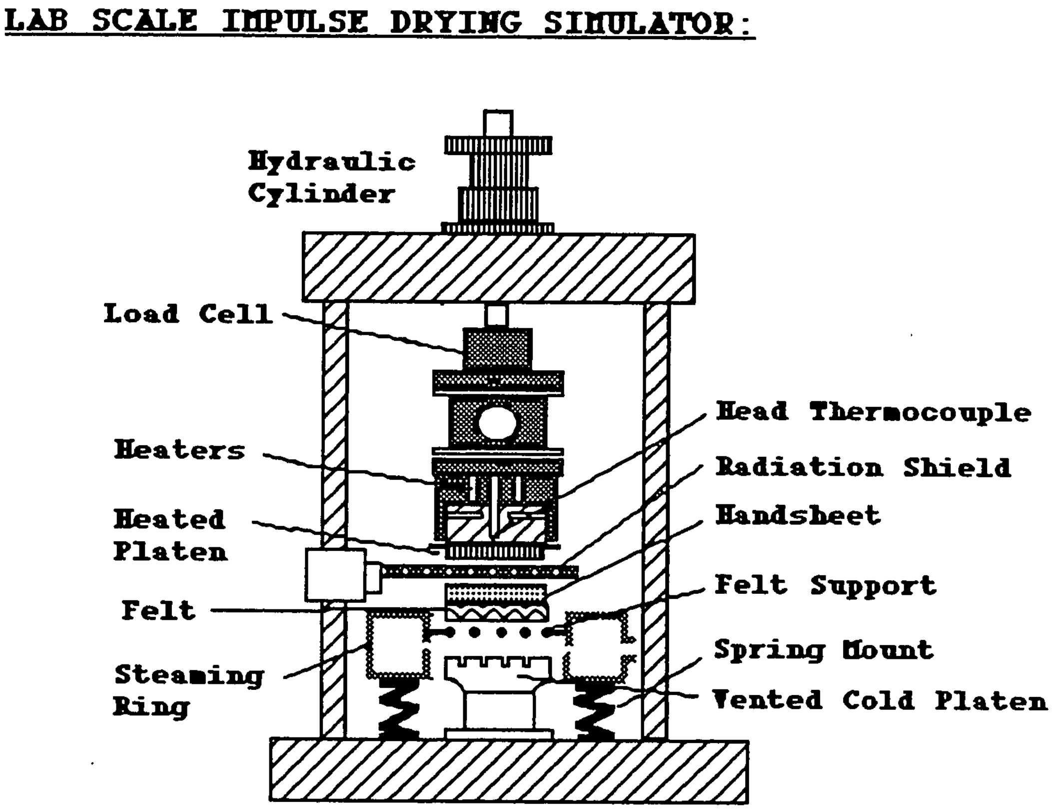

Figure 17. Laboratory Scale Impulse Drying Simulator.

The objective of recent laboratory scale impulse drying simulation experiments was to measure heat flux during impulse drying as a function of operating conditions for both steel and prototype platens. For this purpose, two types of fast response surface thermocouples have been used. For measurement of heat flux from the steel platen a NANMAC steel sheathed erodible thermocouple was used, while a NANMAC ribbon thermocouple was used with the prototype ceramic coated platen.

Figure 18 shows the operating conditions investigated in these experiments.

LABORATORY SCALE SIMULATION CONDITIONS

Basis Weight:	205 gsm
Dwell Time:	20 ms
Ingoing Solids:	30 %
Platen:	Steel and Prototype
Peak Pressure:	450 psi and 900 psi
Temperature:	190°F, 300°F, 500°F, 700°F

Figure 18. Laboratory Scale Simulation Conditions.

Water removal, delamination and heat flux results have been obtained. The following tentative conclusions have been drawn from the data, and will be discussed in more detail at the PAC meeting.

- Comparing water removal with and without the radiation shield, suggests that sheets with more water at the heated surface are more readily dried.

- At platen temperature below which sheet delamination occurred, both steel and prototype ceramic coated platens exhibit two heat flux peaks. The first peak occurs during nip compression while the second peak occurs during nip decompression. The existence of the second peak is a new and potentially significant discovery.

- Total energy transfer to the sheet during impulse drying was compared. At a given platen temperature the prototype ceramic coated platen delivered substantially less energy than the steel platen. Energy transfer from the steel platen increased with pressure, while energy transfer from the prototype platen was pressure independent.

- At a given pressure, the prototype platen could be operated at significantly higher temperatures than the steel platen without inducing sheet delamination. At these maximum operating temperatures, the prototype platen resulted in superior performance in terms of water removal. The prototype also exhibited improved energy efficiency, particularly at high pressures.

PLANS FOR THE NEXT PERIOD:

Further work is planned in order to develop and demonstrate the ceramic coated press roll concept. That work address the following goals.

- For a range of linerboard furnishes determine the impulse drying pilot scale operating conditions resulting in maximum water removal without sheet delamination.

- Investigate durability of polymer roll coating and demonstrate concept of continuous roll re-coating and/or a synthetic diamond low surface energy coatings.

- Evaluate very high internal porosity ceramic coating on laboratory scale, coat second steel roll and evaluate on pilot impulse drying press.

- Use the laboratory scale impulse drying simulator to expand the heat flux data-base to higher ingoing solids and longer dwell times. In addition, explore the influence sheet permeability and felt variables on heat flux, water removal, delamination control and the existence of the second heat flux peak.

PROPOSED PROJECT OBJECTIVES FOR NEXT FISCAL YEAR:

- Modify laboratory scale impulse drying simulator to optimize the shape of the pressure curve during impulse drying with ceramic surfaces.

- Modify pilot dryer for two nip single sided drying capability and investigate benefits of multi-nip impulse drying.

- Design, fabricate and evaluate a ceramic coated press roll on an existing pilot paper machine for a range of grades and furnishes.

FUNDAMENTALS OF WATER REMOVAL PROCESSES

STATUS REPORT

FOR

PROJECT 3480

April 4, 1991
Institute of Paper Science and Technology
Atlanta, Georgia

PROJECT SUMMARY FORM

Project Title:	Fundamentals of Water Removal Processes
Project Number:	3480
Project Staff:	Jeffrey Lindsay
Fiscal Budget:	$120,000
IPST Goal:	Assist development of water removal processes through an improved understanding of the basic physics of water flow in paper. Applications are to wet pressing, impulse drying, and displacement dewatering.

ABSTRACT

Work of the last period will be reported in terms of three separate topics: I. Measurements of Anisotropic Permeability, II. Investigation of Effective Porosity and Related Pore Properties; and III. Fundamental Physics of Vapor-Liquid Flows.

Activities in the last period have primarily focused on the issue of anisotropic permeability in paper. New measurements have been made, indicating that in-plane permeability tends to be substantially higher than z-direction permeability. The work of other researchers who are now applying these results is providing useful insights into water removal and flow processes in paper.

Measurements have indicated that values of permeability as well as anisotropy ratios may be sensitive indicators of the state and properties of paper fibers. For example, small changes in fiber state, which may be undetected in a measurement of freeness, can cause significant and easily measured changes in permeability. Because permeability is a parameter of direct physical importance in a paper machine, affecting operations such as pressing and drying, on-line permeability measurements may be useful in process control. For example, permeability measurements could be continuously made in couch trim samples to monitor fiber properties. Changes in pulping and refining are most likely to affect permeability. The utility of permeability and anisotropy ratios as tools to examine the nature of a pulp will be further explored in the coming period, with a focus on changes that occur in secondary fibers. The work on permeability is reported under Part I below.

To supplement the work on permeability, measurements of effective porosity, another fundamental property of paper sheets, are planned, as reported in Part II. Effective porosity refers to the fraction of the total void volume in a sheet which is available for flow, and is an important aspect of processes such as displacement, liquid penetration, coating and sizing. The effective porosity is expected to be anisotropic, and should be related to the effective swelling volume (specific volume) of fibers as determined from permeability data using a Kozeny-Carman approach. Equipment has been constructed which allow the moving boundaries of lateral fluid flow in a compressed sheet to be recorded photographically. Image analysis and further data reduction will be applied to then determine this parameter.

Progress has also been made in improving numerical modeling of heat transfer and displacement processes such as impulse drying. Techniques for handling the compressibility of paper have been explored, and approaches for modeling wet pressing have been reviewed. This work is discussed in Part III. A proper model of an impulse drying process must begin with a model of wet pressing, then adding on the modeling of dynamic phase-change heat transfer. A key aspect of such a model must be a proper accounting of multiphase flow, which requires information about relative permeability functions and capillary pressure functions for sheets at various degrees of compression. The required data are not available, although capillary pressure data for uncompressed sheets exist. It is proposed that Project 3480 be extended to include measurements of such parameters, with principal funding sought from the National Science Foundation. The text of a proposal (still under preparation) is included as an Appendix. Review of the proposal by members of the Project Advisory Committee is welcome.

The modeling effort is a tool to explore the fundamental physics of water removal processes such as impulse drying and displacement dewatering. Several basic aspects of impulse drying physics proposed by IPST and other researchers, and the basic physics of any displacement process in paper, were recently called into question by Back in the March 1991 Tappi Journal. These objections are discussed in some detail in Part III below. Back's work on press drying does give some insight into impulse drying, which does have a relation press drying and hot pressing than previous discussions have indicated. Concerning the importance of intense phase-change heat transfer and vapor formation in impulse drying, however, the key criticisms of Back are, regrettably, based on a typographical error in a previous publication, and on a misinterpretation of hydrodynamic pressure in a deformable porous medium.

PART I: MEASUREMENTS OF ANISOTROPIC PERMEABILITY

BACKGROUND

While flow normal to the plane of paper is of great importance in many papermaking processes, the in-plane flow of liquid through paper is receiving increasing attention. Significant in-plane flows of water during wet pressing can occur (1-4), and lateral penetration of coating colors can be important in blade coating processes (5). In the area of photography, excessive lateral penetration of developing fluids into the edge of the paper can ruin a photograph (6). In impulse drying, strong vapor pressure gradients in the machine direction may be a major cause of the delamination problem which can occur with some furnishes (7). All such flows are affected by the in-plane or lateral permeability of paper, a parameter which has been neglected in previous studies of paper permeability. While much has been published about the z-direction or transverse permeability of paper, measurements of the lateral permeability components and their relation to transverse permeability have not been available in the literature. For lack of better information, those who have dealt with two-dimensional flows in paper have thus tended to assume that the permeability of paper was uniform in all directions (1,8,9), even though paper is an obviously anisotropic material.

This lack of data is surprising, since similar measurements have been made in felts, textiles, rocks, and other porous materials. Experimental difficulties in constraining the flow to the plane of the paper, without permitting channeling along the surface of the sheet, seem to have hampered some previous efforts (see discussion in [10]).

Relevant work, however, has been done by Back (11), who examined in-plane capillary flows in paper. By observing the way in which a drop of fluid spreads out in a sheet of paper, information about anisotropy in the sheet can be obtained. He found that the capillary penetration velocity for most papers is 5-15% larger in the machine direction than in the cross-direction. Comparison of capillary wicking in the plane to that through the thickness of the sheet led him to conclude that transverse pores were as much as 90 times smaller than lateral popes (12,13). However, capillary flow is affected by both the intrinsic Darcian permeability of the sheet as well as the directional pore size distribution; relative permeability to two-phase flow is also an important and complex factor in such flows. No quantitative conclusions about permeability can be safely deduced from capillary flow experiments unless detailed information about directional pore-size distributions is available.

While no published measurements in paper are known, Peterson (14) examined the two-dimensional permeability of thick, nylon fiber mats with fibers oriented in the horizontal plane. He found the lateral permeability was 25-30% higher than the transverse permeability. Mat porosities ranged from 0.84 to 0.97. While a thick nylon mat is not an accurate model of paper, the study provides an important reference point.

To explore basic issues about the anisotropic permeability of paper, a small project was launched at the Institute of Paper Science and Technology in 1987. Results from the first phase of the study have now been published by Lindsay (15), who measured the transverse, cross-direction, and machine-direction permeability components in several paper samples. In the few samples which were examined, the ratio of average lateral to transverse permeability ranged from roughly 2 to 4, which was much larger than predicted by simple models of flow over oriented cylindrical rods (16,17), but consistent with new data from Adams (18) for textiles, in which ratios of 2 to 5 were reported.

The ratio of machine-direction to cross-direction permeability was also obtained in several paper samples in the previous study (10), with values generally in the range of 1 to 2, and frequently in the range of 1.1 to 1.3. In a related study by Horstmann et al. at IPST (19), a new experimental method to characterize edge penetration in photographic papers was used to provide information on anisotropic in-plane permeability. Measurements in 5 similar samples of uncompressed photographic paper again showed MD-CD permeability ratios in the range of 1.1 to 1.3. Transverse permeability was not measured.

In this report, we describe measurements of lateral and transverse permeability in paper using improved techniques. Our objective was to verify and expand the previously reported results, which were somewhat tentative (10). Measurements in several new paper types are reported.

EXPERIMENTAL WORK

Lateral Permeability

Apparatus. Figure 1 is a schematic of the apparatus used in this study for lateral permeability measurements. The apparatus was assembled as part of a graduate project undertaken by Wallin at IPST (20). A Carver press was modified to hold two heads which would press paper between two steel platens. The original manual hydraulic jack of the Carver press was replaced with a Firestone Airide™ air bag assembly, capable of providing loads up to about 18 kN (4000 lb). A pneumatic operating system was installed to control the air bags. The upper head, which is driven by the air bags, is a solid cylinder of aluminum, 0.13 m in diameter. A rubber disk is placed between the upper head and the upper platen to help provide uniform loads. The lower head is a thick-walled hollow cylinder through which plastic tubing can pass. The lower platen fits onto the lower head and has a fitting onto which plastic tubing can be connected. Fluid from the tubing can then pass to the upper surface of the platen, where an 0.56-cm circular

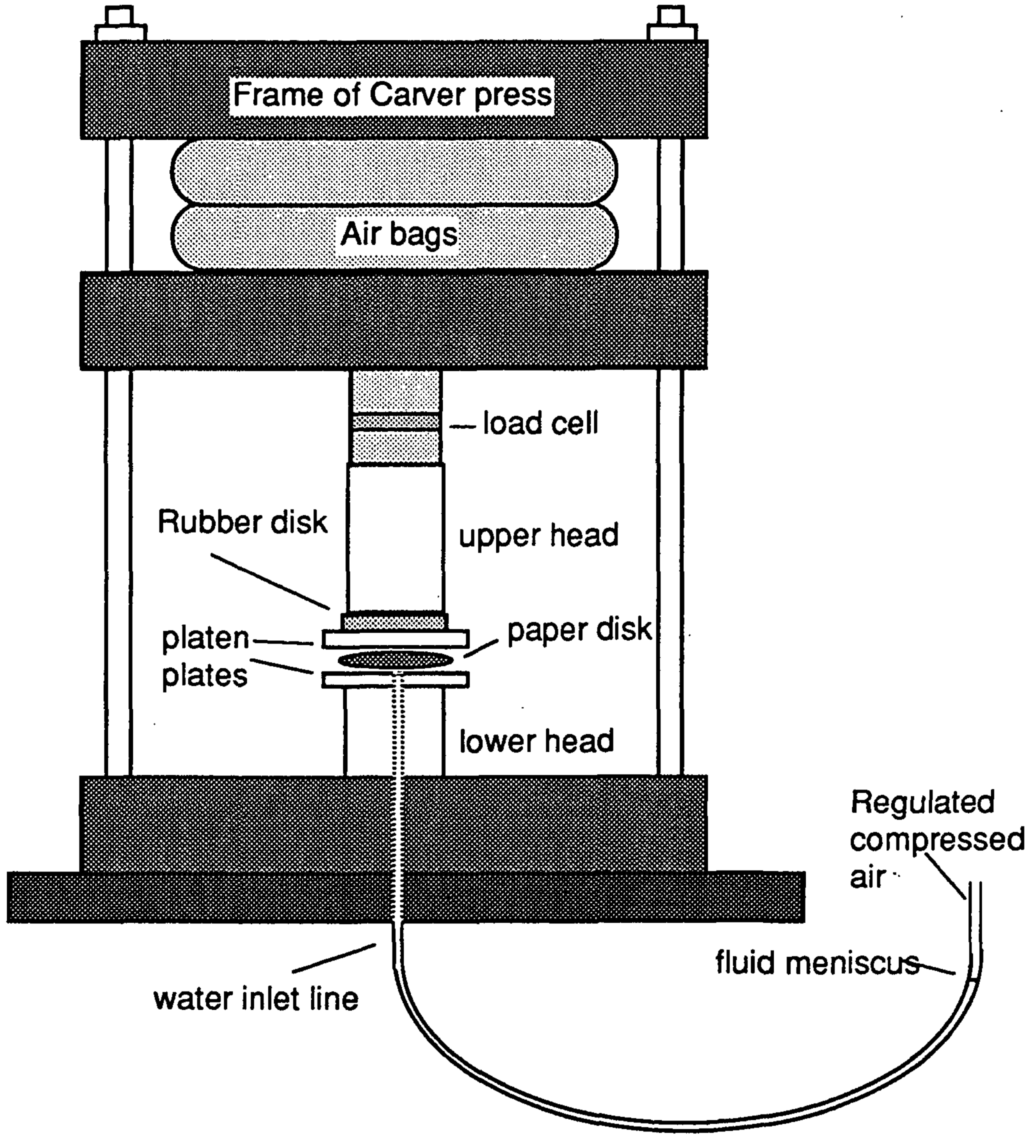

Figure 1. Schematic of the lateral permeability setup.

injection port (simply a round hole) is located. Fluid is driven into the injection port by regulated compressed air above the fluid meniscus in the line.

After a paper disk is placed between the two platens, load is applied to provide a seal between the paper surfaces and the platens. Fluid in the tubing line is then pneumatically driven into the paper. The fluid flowing into the injection port enters the paper and is forced to flow radially outward through the paper itself. If the applied load is uniform, and the sheet itself is uniform in thickness, then channel flow between the sheet and the platens is avoided. This was verified by observing the location of dyed fluid injected into sheets. The observed dye boundaries showed the expected axes of symmetry (the shape was ellipsoidal, aligned with the MD and CD axes) and was not affected by rotation of the paper disk with respect to the apparatus. (With small applied pressures, say less than 0.15 MPa [20 psi], channeling might occur.)

The thickness of the paper disk during lateral permeability measurements was measured with a set of linear variable displacement transducers (LVDT's). Three ST050 LVDT's from Schlumberger Industries were acquired, with an OD3 signal conditioner. The LVDT cores were embedded at 120° intervals around the edge of the lower platen, with sensor armatures mounted on the upper platen. The armatures induced an electronic signal in the cores, depending on the depth of penetration of the armatures.

Data Reduction. If the in-plane permeability in the machine direction, K_y, equals the permeability in the cross direction, K_x, then the in-plane permeability is easily obtained from measured parameters in the experiments:

$$K_r \equiv \frac{K_x + K_y}{2} = \frac{Q\,\mu \ln(R_o/R_i)}{2\pi\, L\, \Delta P}, \tag{1}$$

where Q is the volumetric flow rate, R_o is the outer radius of the sheet, R_i is the radius of the injection port, L is the sheet thickness, and ΔP is the pressure drop from the injection port to the edge of the sheet (the gauge pressure of the fluid in the tubing). Step-by-step details of this solution are given for a related problem in the appendix of Horstmann et al. (19). Numerical analysis has indicated that Equation 1 can be applied with reasonable accuracy even when $K_x \neq K_y$ (10).

Transverse Permeability

Apparatus. The equipment used to measure transverse permeability also uses the Carver press and is depicted in Figure 2. This equipment is similar to that used in the previous part of this study with an electrohydraulic press (10), although key parameters (hydraulic head, injection pressure, and sheet thickness) are now measured and controlled with better accuracy. A paper disk, 0.076 m (3 inches) in diameter, is compressed between two felts. The felts are in contact with finely drilled bronze plates, which provide mechanical load while allowing water to flow through. The bronze plates are drilled with 0.0023-m (0.09-

in) holes, with a center-to-center distance of 0.0032 m (0.125 in). The open surface area is 47%. The plates are thick enough (1 in or 0.0254 m) to prevent significant bowing during compression. The hydraulic head in the upper chamber is created by the height of a water reservoir above the Carver press; the reservoir is sufficiently wide to keep the hydraulic head nearly constant during a typical single measurement (if needed, additional water is added to the reservoir during a measurement). The hydraulic head, measured in centimeters above the location of the paper disk, is read from a marked column connected to the upper head. Frictional losses as water passes from the reservoir through a valve makes the measured head several centimeters of water less than the height of the reservoir surface above the paper.

Fluid passing through the paper disk exits through the lower felt and the lower drilled bronze plate. The felts were necessary to provide uniform mechanical pressure and uniform hydraulic boundary conditions. Carbon paper imprints taken under load confirmed that the felts were adequate in generating a uniform load across the paper.

To eliminate problems with leakage around the edge of the paper, only the flow through the central region (comprising 23% of the area of the paper disk) was collected and measured. This fluid entered a funnel which led the fluid through plastic tubing to a graduated cylinder below the Carver press assembly.

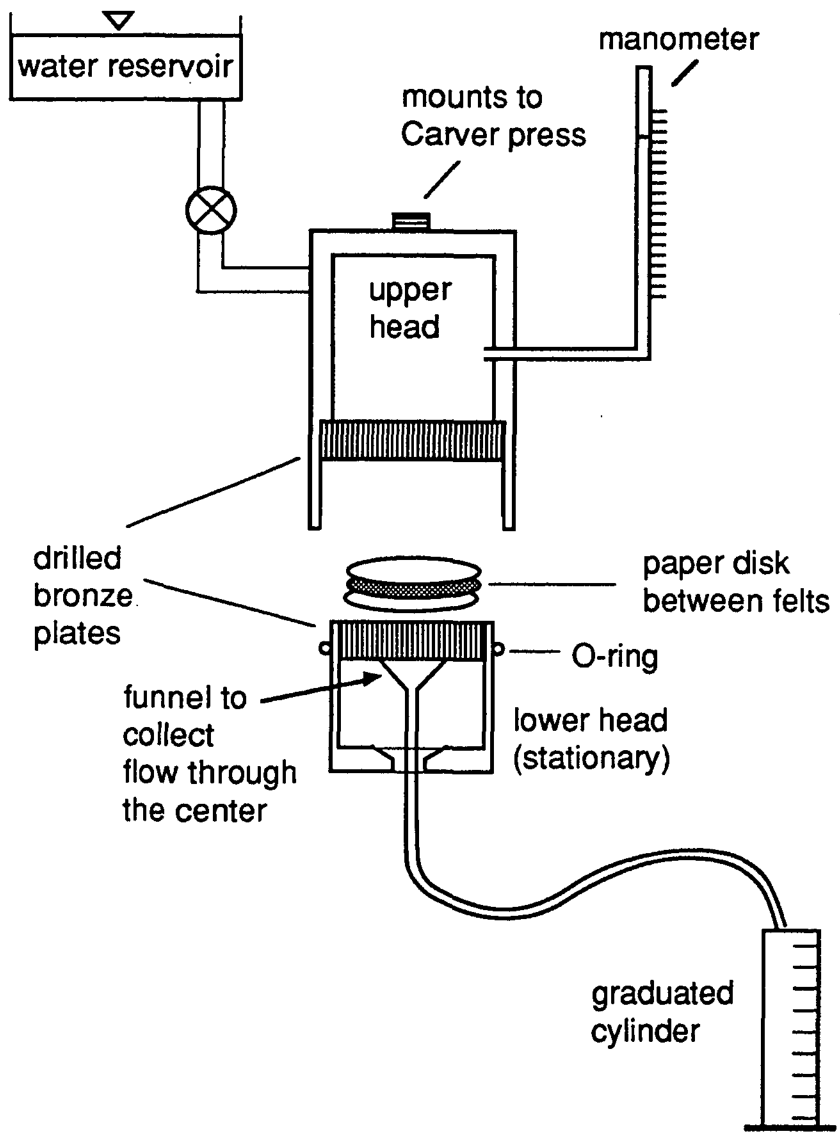

Figure 2. Schematic of the water flow system for transverse permeability measurements.

The position of the upper head in the Carver press was measured with a Kaman eddy-current transducer (ECT), and this data was applied to determine sheet thickness through a difference technique, described in (21). Data reduction procedures are also given in (21).

RESULTS

Much of the work of this portion of the study was devoted to developing the proper experimental techniques for the new equipment. Once reproducible results could be obtained, measurements were first made in sheets produced from a Southern softwood unbleached kraft (SSK) pulp. This furnish, used to produce linerboard, had a freeness of about 700 CSF. Lateral and transverse permeability measurements were made in a single 0.076-m (3-in) disk cut from a handsheet. Results are shown in Figure 3. The value of b, the ratio of average in-plane to transverse permeability, ranges from about 2 to 4 in this sample over the porosity range shown. (Again, porosity here refers to the total fraction of the volume occupied by water and is directly related to moisture ratio.) These results can be compared with previous data from linerboard handsheets made with another SSK pulp (10), reproduced in Figure 4. The previous measurements gave b values of about 1.5 to 2. They were subject to a number of possible errors, but are still consistent with the new measurements using a different pulp. However, the new data show that b increases with porosity, while previous measurements in linerboard gave the opposite trend.

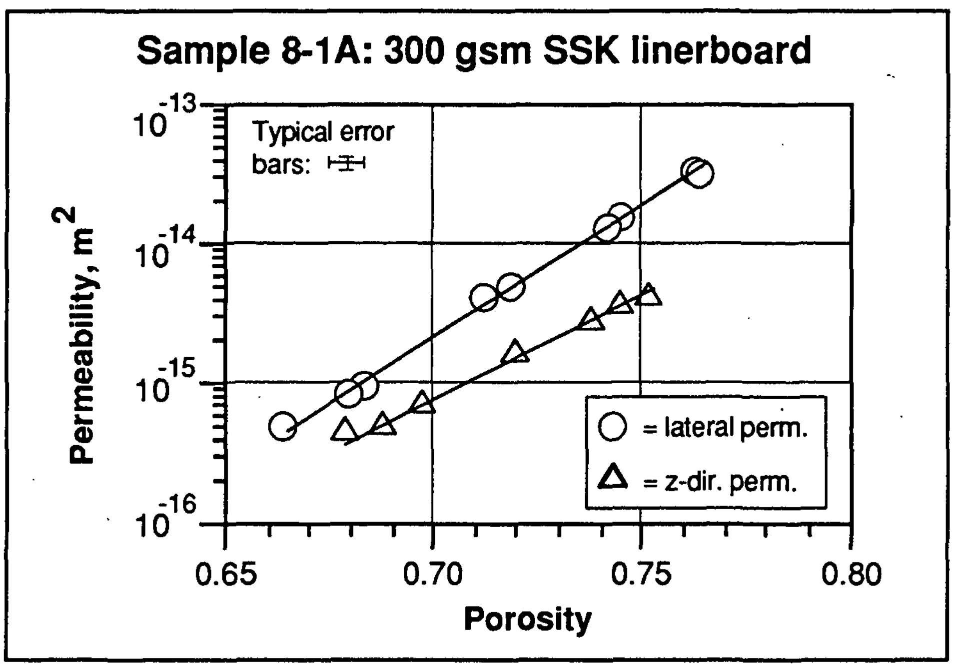

Figure 3. Lateral and transverse permeability in a linerboard handsheet.

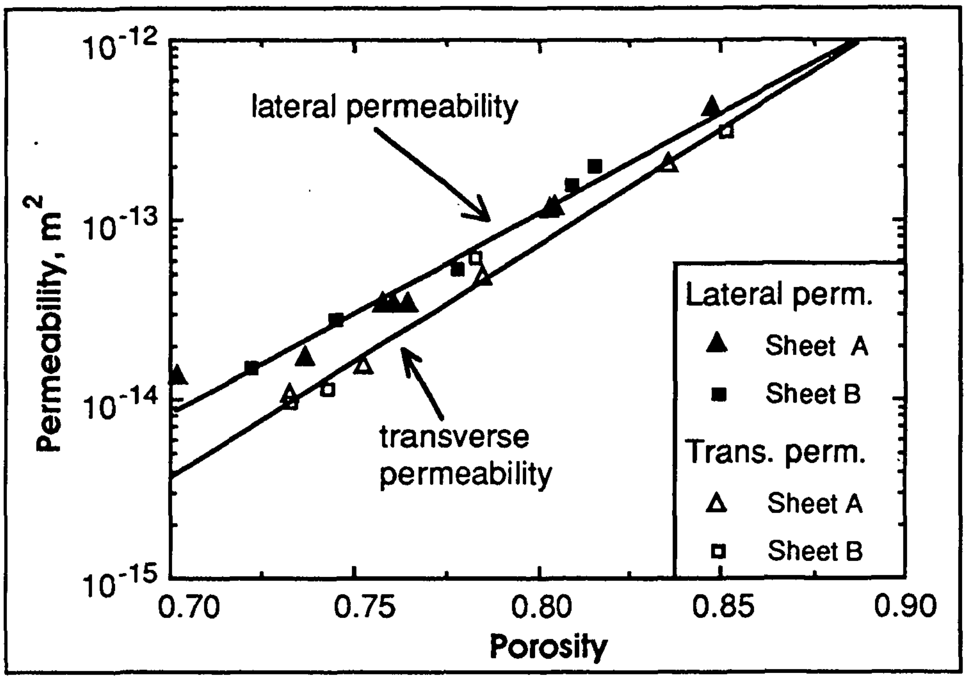

Figure 4. Previously published results for lateral and transverse permeabilities in linerboard handsheets from another SSK furnish (10).

In examining the reproducibility of permeability measurements in linerboard sheets, two clusters of data arose, depending on the history of the handsheet. Some handsheets had been made with the newly obtained fresh pulp for use in early trials with the present equipment. In addition, some couch trim had been taken from a commercial linerboard machine running the SSK furnish. Sheets from this early part of the current study were stored under refrigeration and measurements were made in them several weeks later, once the experimental techniques had been fully developed. In addition, new handsheets were then made from the pulp slurry which had also been stored under refrigeration. Interestingly, the sheets from the stored pulp had lower permeabilities than the handsheets and couch trim which came from the fresh pulp and were then stored. The difference in permeability is shown by transverse permeability data in Figure 5.

Physical changes in the pulp slurry may have occurred, even though the freeness did not change significantly. On the other hand, the pulp was washed and screened and handsheets were formed by a different person for the two cases, and the difference may be partially due to a difference in fines level or handsheet formation technique. Fiber analysis has been planned to better understand why the two sets of samples are so different.

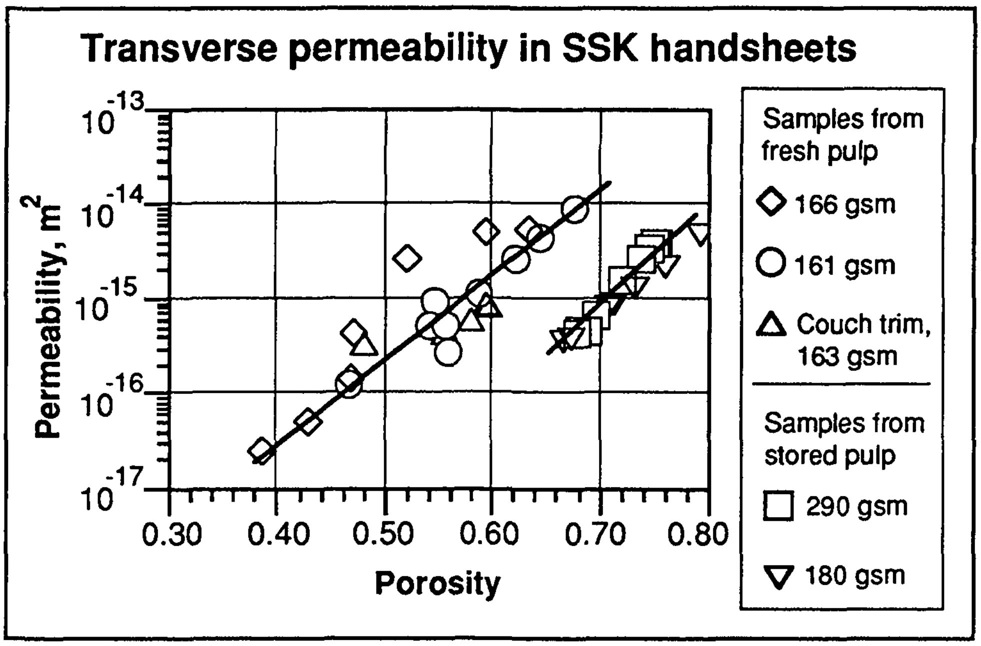

Figure 5. Comparison of transverse permeability measurements in two sets of samples from SSK linerboard pulp.

In the lower permeability line in Figure 5, two basis weights give the same permeability results. This held true in other samples examined. Ideally, permeability should be independent of basis weight in a uniform, homogeneous porous medium. In very thin sheets, however, nonuniformities may lead to apparent differences in permeability. The difficulty in defining a sheet thickness in very thin sheets would also affect the permeability as a function of porosity.

Measurements were also made in an unbleached thermomechanical pulp (TMP) with a freeness of about 100 CSF. Lateral and transverse permeability results are shown in Figure 6, where separate data for two 200 gsm handsheets are included. The reproducibility of the measurement techniques appears satisfactory. Note, however, that large differences between the lateral and transverse permeability values exist. Values of b range from about 5 at low porosities to nearly 10 at the higher porosities measured. This is larger than the range reported in the previous study, where the highest b values seen were about 4-5 (12).

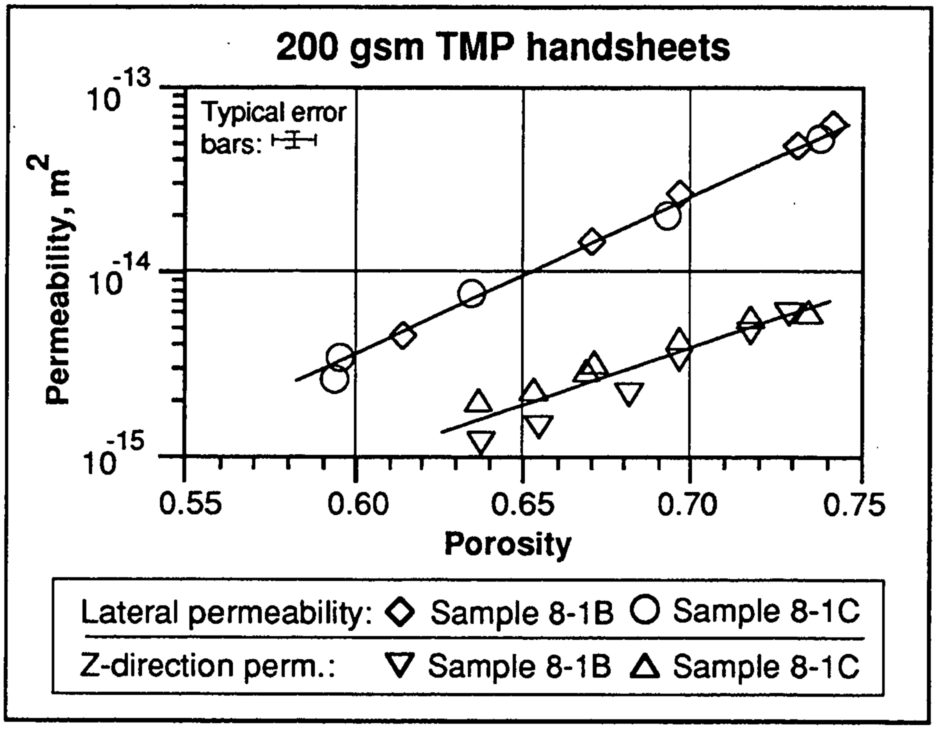

Figure 6. Lateral and transverse permeabilities in two 200-gsm TMP handsheets.

Further lateral and transverse permeability measurements with TMP are shown in Figure 7, where an 87 gsm handsheet was used. Transverse permeability measurements were repeated using a different set of felts and a different operator (a lab technician) as a check on the experimental method. The agreement between the two runs is excellent, and the deviation at the lower porosity can be explained by a minor error in the felt thickness calibration procedure used during the second run. In these samples the lateral-to-transverse permeability ratio, b, is virtually constant over the porosity range examined, with a value near 10.

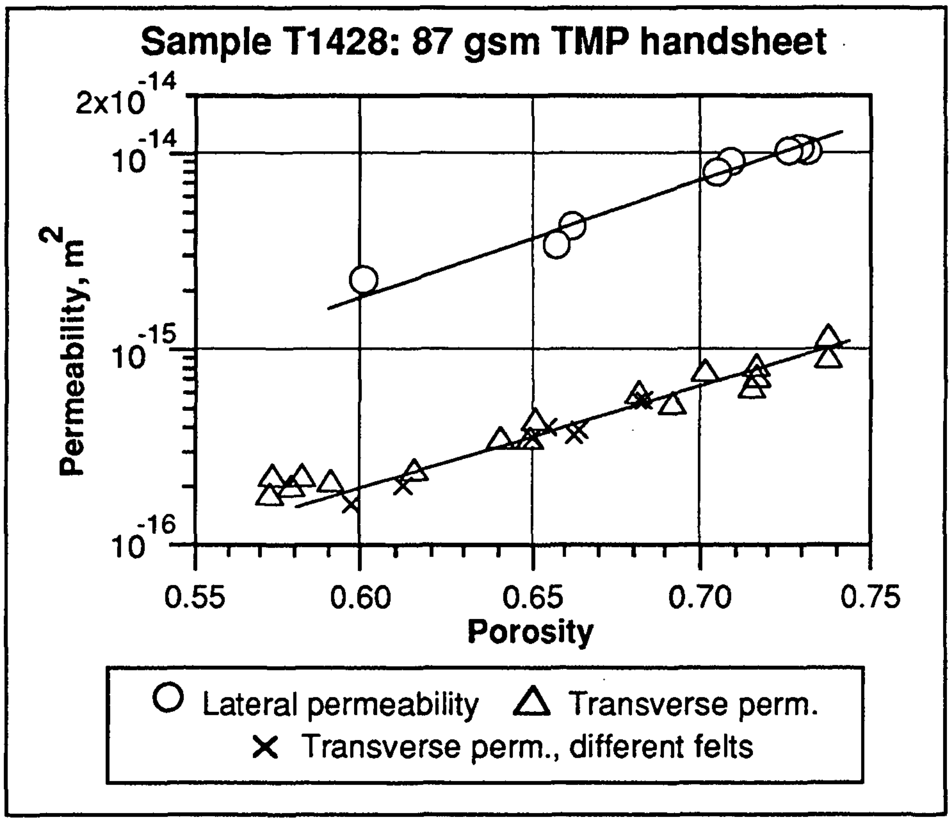

Figure 7. Lateral and transverse permeability measurements in an 87 gsm TMP handsheet.

As with the linerboard sample, two clusters of permeability data were found in the TMP samples. This is shown in Figure 8. (Similar clusters appeared in the lateral permeability data curves). Sheets from one batch, all prepared during one week by one of the authors, had a lower permeability than sheets prepared from the same pulp but made several weeks later by a laboratory technician. Perhaps the washing and screening done for the second batch removed more fines from the pulp and increased the permeability. These results are still perplexing since just the opposite trend was seen in the linerboard, where the handsheets made by a technician from the stored pulp had lower permeabilities. In this case, however, the pulp was not fresh for either set of data, but had been in storage at IPST for about one year. Physical degradation of the pulp over time may thus account for the changes in permeability shown in Figure 5, while washing of fines from already stabilized pulp may explain the changes in Figure 8. Again, fiber and sheet analysis is needed to elucidate these phenomena.

The results in Figure 8 also show that the measured transverse permeability was not a function of sheet thickness for the range of basis weights examined.

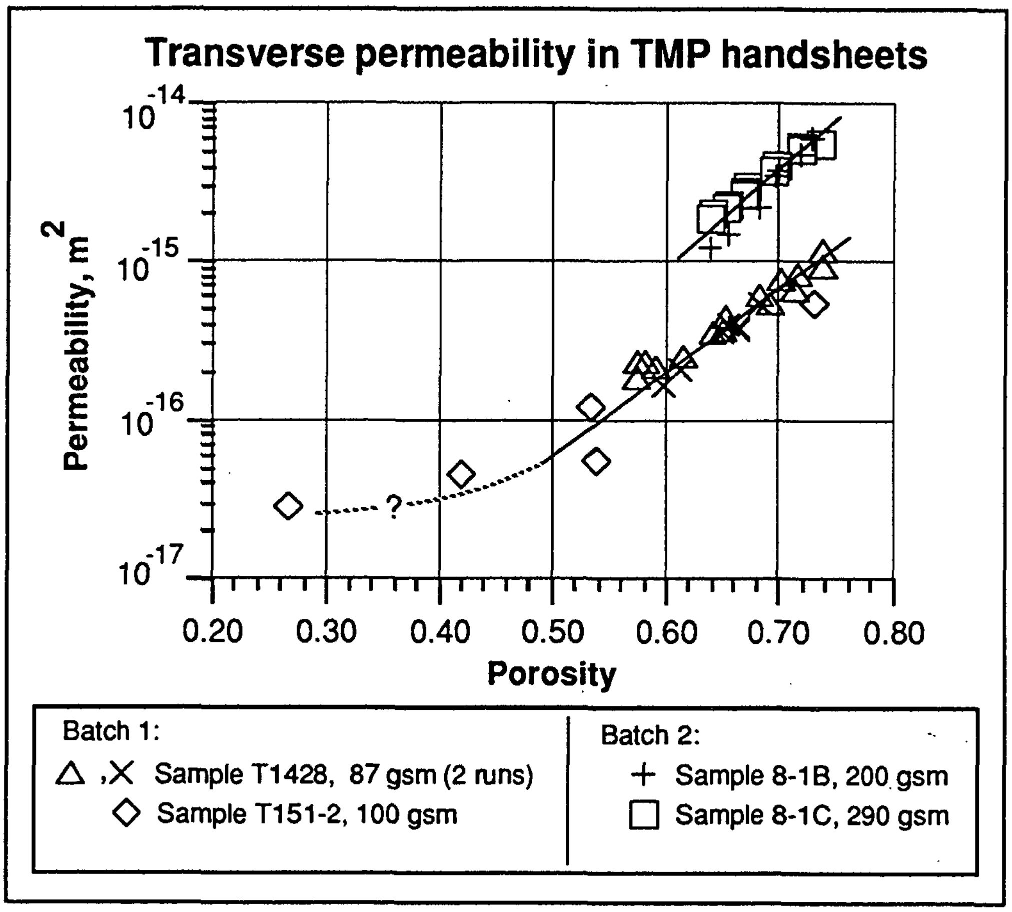

Figure 8. Comparison of transverse permeability measurements in two batches of TMP sheets prepared at different times and by different people.

Several other sets of either lateral or transverse permeability data alone were collected, but are not included here. Lateral permeability measurements were also attempted in the couch trim from a linerboard machine, but the uniformity of the couch trim was very poor (50% variation in thickness across the width of a sample), resulting in measurements that were impossible to interpret. (Transverse permeability measurements in couch trim could be made with more confidence because a smaller cross-section of uniform thickness is needed in those measurements.)

DISCUSSION AND APPLICATIONS

Physically Plausible Results?

Where an accurate comparison of lateral and transverse permeabilities in a single sheet was possible, b values (ratio of lateral to in-plane permeability) greater than 1 have again been found in this study, confirming previous findings (10). While our earlier work found values between 2 and 5, values as high as 10 have now been found. We must first consider whether such findings are physically plausible, and, if so, what implications there might be for the paper industry.

Previous authors have considered the flow of liquid over oriented arrays of cylinders, and concluded that the resistance for flow normal to the cylinders would be roughly twice that of the resistance for parallel flow (16,17,22). If paper could be approximated by such a flow system, then z-direction flow would correspond to flow normal to the cylinders, and in-plane flow would represent a combination of normal and parallel flow, depending on the fiber orientation distribution. The ratio of lateral to transverse permeability (inverse of the resistance ratio) should then be less than 2 and greater than 1.

Closer approximations to paper may be possible if flattened elliptical rods are considered instead of cylindrical rods. Epstein and Masliyah (23) modeled flow normal to infinite elliptical rods and found that the permeability was a strong function of axis aspect ratio and orientation of the rod. Their results suggest that for rods of aspect ratio 5 with the minor axis aligned with the flow, the transverse permeability could be on the order of 60% less than would be predicted from the Happel model. Applying this result to paper, the expected upper limit for b in paper may be on the order of 3 instead of 2, depending on the shape and orientation of the fibers.

Brown (24) found analytical solutions for flow normal and parallel to infinitely long elliptical fibers. For axis aspect ratios of 3 or less, he found that the predictions of models based on cylindrical fibers were accurate. For aspect ratios above 5, however, b values much greater than 2 are possible, with a value of 8 predicted for an aspect ratio of about 10. Brown cites an unpublished study (25) indicating that wet wood fibers generally have aspect ratios less than 3.5, but upon drying the lumens collapse and the ratio can become as large as 10.

Based on Brown's work, therefore, the high b values observed here may be physically plausible. Note also that Adams (18, p. 94) reported b values ranging from 2 to 5 in a Ph.D. thesis dealing with in-plane flow in textiles. These measurements were incidental to his study and only a few were made, but they do strengthen the claim of plausibility for b values well above 2 in paper.

Applications

If high b values do exist in paper, several ramifications arise. Attempts to understand the fundamentals of pressing through analysis or computational techniques must reckon with the high lateral permeabilities which have previously been overlooked. Issues such as crushing and the back flow of water away from the nip must be reconsidered in terms of the anisotropic flow properties of paper. This was recently done by Roux and Vincent (26) in an advanced numerical model of two-dimensional flow in wet pressing. Using our recently published data for anisotropic permeability ratios, the found that increasing values of b lead to a reduction in water removal in the nip. For b values as high as 5, the exiting solids level was reduced by approximately one percentage point compared to the isotropic case (b=1). This sounds reasonable, for a higher in-plane permeability means that more of the flow in the nip will be driven laterally, back into the sheet, instead of being driven into the felt.

Results from this study also have application to the fundamental fluid dynamics of blade coating, where high in-plane pressure gradients can exist in paper near the blade which will affect the penetration and flow of coating (27). The concept of high lateral permeability is also influencing thinking concerning the problem of delamination in impulse drying, where the lateral flow of steam in a nip may be part of the problem but also may be used to help provide novel solutions (28).

One further ramification of this study comes from the observation that significant changes in permeability could occur in handsheets from a given pulp, possibly depending on either the storage time of the pulp or the details of the washing, screening, and handsheet formation processes. This suggests that small changes in the furnish (refining, screening, fines, additives, etc.) or in the formation process may have strong effects on true sheet permeability, even though the measured freeness of the pulp may not change significantly. Occasional monitoring of web permeability, perhaps even in couch trim samples or broke, might be informative in understanding the behavior of a paper machine and the effects of parameters at the wet end.

While further research is needed to relate fiber properties to observed values of anisotropy, one interesting development comes through the work of Cush Hamlen (29), a Ph.D. student under L. E. Scriven at the University of Minnesota. Hamlen is currently using a supercomputer to model the detailed three-dimensional structure of a sheet formed by elliptical rods. Once the sheet is formed in computer memory, information about the anisotropic pore structure is computed. Among the many fundamental properties which can be predicted is the anisotropic permeability of the sheet, where our data are used for comparison. Since the model uses nonswollen, uniform fibers, it is not surprising that his anisotropy ratios are in the range of 1 to 2, closer to theoretical predictions, but the trends Hamlen observes in terms of fiber properties are most interesting. Hamlen's model permits a fiber stiffness parameter which determines how much a fiber can bend over other fibers as it is placed on the sheet. Increasing fiber stiffness increases the anisotropy (the b value increases). The explanation is that a more flexible fiber can more easily fill in the large in-plane pores that form in the sheet, and thus help decrease the in-plane permeability. Our results are consistent with this, for the highest anisotropy values seen (b= 5-10) have been in TMP sheets, where the fibers tend to be stiff. Kraft pulps, which should have relatively flexible fibers, show less anisotropy (b=1.5-4). Further work is needed in this area.

CONCLUSIONS

We have further confirmed a prior, tentative observation that lateral or in-plane permeability in paper is greater than the transverse or z-direction permeability. Ratios as high as 10 were observed in this study. Combined with the previous results, we can now say that, to date, all observations of this ratio, b, lie in the range of 1.5 to 10. This observation appears to be physically plausible, although simple attempts to predict b using arrays of cylinders as a model for paper give values less than 2. The relation between lateral and transverse permeability needs to be considered in future work dealing with wet pressing, blade coating, and any other system where two-dimensional flow in paper may be important.

It appears that permeability values and anisotropy ratios could be used as sensitive indicators of fiber state, with possible applications to process control. Further work in this area is needed.

PLANS FOR WORK INVOLVING ANISOTROPIC PERMEABILITY

1. Begin measurements of permeability changes induced by recycling.
2. Investigate the relation between fiber properties and measured anisotropy ratios. Measure fiber properties such as stiffness for several pulp types and compare results with anisotropy ratios.
3. Investigate the utility of permeability measurements as a quality control tool. Examine available techniques for rapid and simple estimates of permeability.

LITERATURE CITED

1. Vincent, J. P. and Roux, J. C., "A Simulation Tool for the Press Section of the PM," Paper Tech. Ind. 29(5): 236(1988).

2. MacGregor, M. A., "Wet Pressing Research in 1989–An Historic Perspective, Analysis and Commentary," Transactions of the Ninth Fundamental Research Symposium Held at Cambridge, ed. C. F. Baker, Mechanical Engineering Publications, Ltd., London, 1989.

3. Gudehus, T., "Stoffentwässerung im Walzenpreßspalt," Das Papier, 42(4): 174-184 (1988).

4. Mukhopadhyay, A. and Kingsbury, H. B., "A Study of Two-dimensional Flow in the Press Nip," Tappi J., 63(7): 87-90 (1980).

5. Windle, W., Beazley, K. M., and Climpson, M., "Liquid Migration from Coating Colors. II. The Mechanism of Migration," Tappi J., 53(12): 2232-2236 (1970).

6. Crouse, B. W., and Warner, C. L., "Mechanistic Aspects of Edge Wicking," 1986 Papermakers Conference, p. 7, Tappi Press, Atlanta, GA, 1986.

7. Crouse, J. W., Woo, Y. D. and Sprague, C. H., "Delamination — a Stumbling Block to Implementing Impulse Drying Technology for Linerboard," Tappi J., 72(10): 211-215 (Oct. 1989).

8. Mukhopadhyay, A., and Kingsbury, H. B., "A Study of Two Dimensional Flow in the Press Nip," Tappi J., 63(7): 87-90 (1980).

9. Roux, J.-C., "Modélisation et Optimisation du Fonctionnement d'une Section de Presse (S) de Machine a Papier," Ph.D. Dissertation, Grenoble National Polytechnic Institute, Grenoble, France (1986).

10. Lindsay, J. D., "The Anisotropic Permeability of Paper: Theory, Measurements, and Analytical Tools," IPST Technical Paper Series #289, The Institute of Paper Science and Technology, Atlanta, Georgia, 1988.

11. Back, E. L., "Capillary Suction Method for Evaluating the Water Resistance of Insulating Board," Svensk Papperstidning 68: 173-178 (1965).

12. Back, E. L., "The Pore Anisotropy of Paper Products and Fibre Building Boards," Svensk Papperstidning, 69: 219 (1966).

13. Didriksson, E. I. E., and Back, E. L., "The Effect of Density on the Pore Size and Anisotropy of Fibre Building Boards," Svensk Papperstidning, 69: 769 (1966).

14. Peterson, R. M., "Two-Dimensional Flow of Incompressible Fluids Through Deformable Porous Media," Tappi J., 53(1): 71-77 (1970).

15. Lindsay, J. D., "The Anisotropic Permeability of Paper," Tappi J., 73(5): 223-229 (May 1990).

16 Happel, J., "Viscous Flow Relative to Arrays of Cylinders," AIChE J., 5(2):174-177 (1959).

17. Sparrow, E. M. and Loeffler, A. L., "Longitudinal Laminar Flow Between Cylinders Arranged in Regular Arrays," AIChE J., 5(3): 325-330 (1959).

18. Adams, K. L., "Permeability Characterization of Engineering Fabrics," Ph. D. Dissertation, Chemical Engineering Department, Princeton University (Jan. 1989).

19. Horstmann, D. H., Lindsay, J. D., and Stratton, R. A., "Using Edge-Flow Tests to Examine the In-Plane Anisotropic Permeability of Paper," Tappi J. (in press, 1991).

20. Wallin, J. R., "Determination of In-plane Permeability of Paper," A190 Report, The Institute of Paper Science and Technology, Atlanta, Georgia, 1990.

21. Lindsay, J. D., and Wallin, J. R., "Characterization of In-plane Flow in Paper," IPST Technical Paper Series #367, The Institute of Paper Science and Technology, Atlanta, GA, 1990.

22. Jackson, G. W. and James, D. F., "The Permeability of Fibrous Porous Media," Can. J. Chem. Eng., 64: 364-374 (1986).

23. Epstein, N. and Masliyah, J. H., "Creeping Flow through Clusters of Spheroid and Elliptical Cylinders," Chem. Eng. J., 3(2): 169-175 (1972).

24. Brown, G. R., "Creeping Flow of Fluids Through Assemblages of Elliptic Cylinders and its Application to the Permeability of Fiber Mats," Ph.D. Thesis, The Institute of Paper Chemistry, Appleton, Wisconsin (now The Institute of Paper Science and Technology, Atlanta, Georgia), 1975.

25. Farrar, N. O, unpublished work, The Institute of Paper Chemistry. Appleton, Wisconsin, 1964, as cited by Brown, G. R., "Creeping Flow of Fluids Through Assemblages of Elliptic Cylinders and its Application to the Permeability of Fiber Mats," Ph.D. Thesis, The Institute of Paper Chemistry, Appleton, Wisconsin, 1975, p. 24.

26. Roux, J. C., and Vincent, J. P., "A Proposed Model in the Analysis of Wet Pressing," Tappi J., 74(2): 189 (Feb. 1991).

27. Chen, K. S. A, and Scriven, L. E., "Liquid Penetration into a Deformable Porous Substance," Tappi J., 73(1): 151-161 (Jan. 1990).

28. Orloff, D. I., personal communication, The Institute of Paper Science and Technology, Atlanta, Georgia, 1990.

29. Hamlen, C., Chem. Eng. Dept. and Minnesota Supercomputer Inst., Univ. of Minnesota, Minneapolis, MN, personal communication, 1991.

PART II: INVESTIGATION OF EFFECTIVE POROSITY AND RELATED PORE PROPERTIES

BACKGROUND

The essence of water removal is the flow of water through pores in paper. A fundamental issue is where the water flows, and how much of the pore space is available to flow. The fraction of pore space available to flow is defined as the effective porosity. It is especially important when two phases are involved, as when gas displaces liquid, for it governs the speed of the phase boundary. In other words, the penetrating phase can only move through the open, interconnected pores. If the effective porosity of this pore space is small, the penetrating fluid boundary may advance rapidly, yet the amount of penetrating fluid will be small.

Many factors determine the nature of the interconnected pores. In paper, the pore structure of paper is complicated by the anisotropic orientation of fibers, diverse fiber forms, the presence of fines and fibrils, the presence of pores and micropores in the fiber itself, and by the complex interactions of cellulose and water (1,2). Some of the water is trapped in micropores or large dead-end pores, or is associated with the cellulose, and hence cannot flow under a hydraulic pressure gradient. When immiscible fluids are present, capillary forces between the two phases affect the distributions of the phases and limit the fraction of the pore space through which flow can occur.

A variety of studies have been conducted to understand where the water is in the sheet and how much might be available for removal. Lindström (3) provides an excellent review of this topic. Useful information can be obtained from water retention values, solute exclusion measurements (4,5), and from values of specific volume (a better term would be "associated volume") of fibers from permeability measurements (6). The distribution of water in swollen fibers is affected by mechanical loading, which forces some of the trapped or bound water out of the fiber into the interfiber volume (7).

An example of an application of such information to water removal is the recent study of Roux and Vincent (8), who numerically modeled wet pressing. Part of the model must deals with the interfiber porosity and its decrease with compression. For a given dry solids volumetric fraction, e_S (= 1– the absolute porosity), the interfiber porosity is modeled as

$$\varepsilon_{eff} = 1 - \varepsilon_s\left[1 + WRR(\rho_s/\rho_l)\right], \tag{1}$$

where e_{eff} is the effective porosity, WRR is the water retention ratio, r_s is the density of cellulose and η is the density of water. WRR is assumed to be constant, although it must decrease under compression as water is squeezed from the fibers and as water removal causes irreversible physical changes in the fiber (9). The approach used in Equation 1 may give plausible results in a computer model, but the relation between water retention values and the physics of flow between the fibers is not well founded. It is well known, however, that for a given fiber type, a higher water retention value is correlated with decreased water removal in pressing.

Measurements of fiber specific surface and specific volume using permeability data are more closely tied to the physics of flow, but still are based on a capillary flow model which is not firmly rooted in physical reality, at least not when one deals with a swollen, anisotropic medium like wet paper. This approach also requires the assumption that the specific surface area and the specific volume of the fibers do not change with compression, an assumption not likely to be accurate except over a small range of compression.

Particular questions arise in dealing with anisotropy. For instance, using recent data for the anisotropic permeability of paper, the calculated specific volume of paper proves to be an anisotropic parameter, whereas physically, the volume should be a scalar, independent of direction. An example is shown in Figure 1. The analysis is done by plotting $(Kc^2)^{1/3}$ versus c, where c is the solids concentration and K is permeability. The slope and intercepts of the resulting lines can then be used to obtain the specific surface area (m^2/g fiber) and the specific volume (cm^3/g fiber). Two different lines are obtained using lateral and transverse permeability data. The analysis gives specific surface areas of 14.4 and 85.7 m^2/g for the lateral and transverse flow cases, respectively, and specific volumes of 1.88 and 1.31 cm^3/g for the lateral and transverse flow cases, respectively. Of course, what is measured is not the swollen volume of fiber, but an estimate of the hydrodynamic volume seen by the fluid. Fluid flowing in different directions faces different pore structures and may thus experience different hydrodynamic fiber volumes or effective porosities. True effective porosities are probably related to estimates of specific volume from the permeability method or from water retention values, but the relationships may be imprecise.

Improved techniques for estimating effective porosity would be helpful in advancing our understanding of fluid flow and water removal processes in paper.

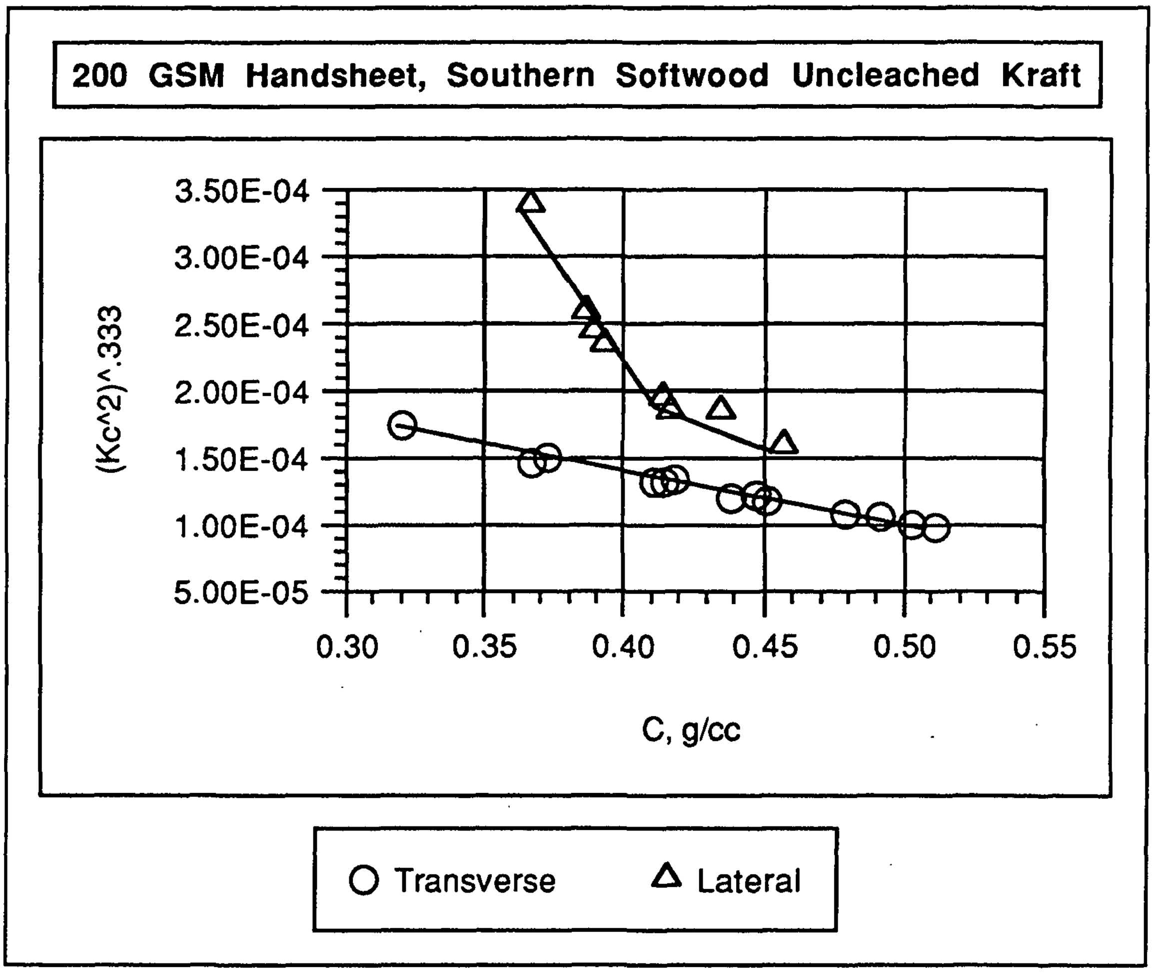

Figure 1. Comparison of lateral and transverse permeability curves in obtaining specific surface area and specific volume of fibers for a linerboard furnish.

EXPERIMENTAL APPROACH

One way of evaluating effective porosity would be to track the flow of a penetrating fluid in the plane of a sheet, comparing the apparent volume penetrated with the total pore volume. Total pore volume is obtained from a knowledge of fiber density and sheet volume. To avoid capillary effects and interface instabilities (viscous fingering), there should be relatively small capillary forces between the two phases, and the displacing phase must not have a lower viscosity than the phase being displaced. Displacing liquid water with colored water is likely to succeed in such a measurement.

The lateral permeability apparatus already in use (see Part I above) allows a fluid to be injected into the center of a disk of paper under compression. In order to observe the growth of a dyed region during such an experiment, a replacement for the upper metal platen of that equipment has been constructed which permits optical access to the compressed sheet. The platen replacement is a large cube of clear, rigid plastic which will transmit force from the Carver press assembly to the paper, as shown in Figure 2. A metallic mirror oriented at 45° was cast into the plastic cube. The mirror allows a viewer or a camera standing in front of the cube to observe the paper while it is under compression between the plastic cube and the lower platen. The growth of a dyed zone, formed by injected of colored water through the lower platen, can be viewed and recorded dynamically.

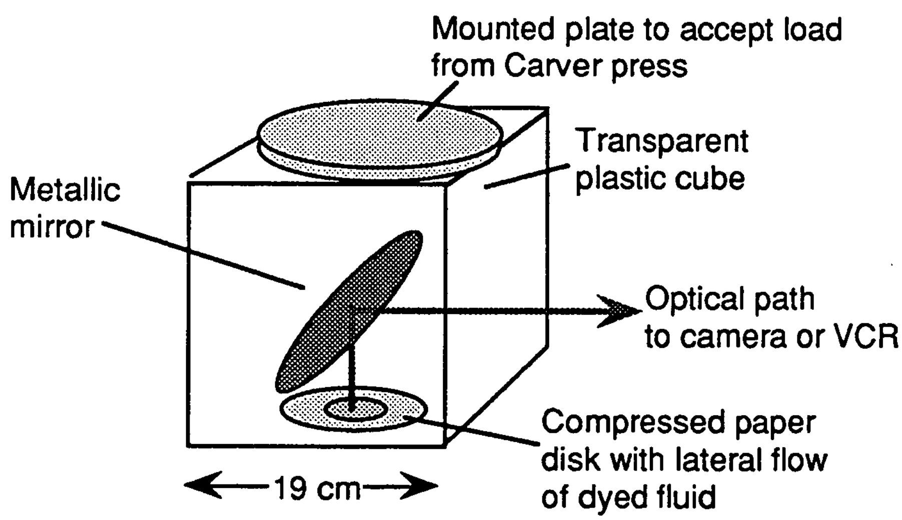

Figure 2. Plastic pressing block with mirror for optical access to a compressed sheet.

The shape of the boundaries of the dyed region will give information about the in-plane anisotropy. However, anisotropy (non-circularity) in the mean boundary shape will be influenced by both anisotropic permeability and anisotropic effective porosity. Decoupling the two parameters can be done by measuring the distribution of moisture in the sheet, possibly by quickly cutting the sheet into small sections and separately weighing each section to determine its moisture content. Capacitance probes, gamma-radiation absorbance, and beta-radiography are other methods which may be used. If the moisture distribution shows no directionality, then the anisotropy of the moving boundaries can be attributed solely to anisotropic permeability. The precision needed to detect anisotropic effective porosities for in-plane flow may hinder this phase of the work, but the average value alone will be of fundamental importance.

APPLICATIONS

Effective porosity controls the motion of interfaces in displacement and penetration processes. In displacement dewatering, for example, the effective porosity at a given compression is proportional to the amount of water which can be displaced by vapor, in addition to water removal by pressing. Effective porosity, or extra-fiber porosity, is also a primary variable in wet pressing and is required for use in advanced wet-pressing models.

PLANS FOR THE COMING PERIOD

1. Measure effective porosities in several paper types as a function of compression using in-plane flow visualization.
2. Compare measured effective porosities to values based on specific surface estimates from permeability measurements and to values based on water retention (Equation 1 above).
3. Determine if in-plane anisotropy in effective porosity can be detected.

LITERATURE CITED

1. Caulfield, D. F., "The effect of cellulose on the structure of water: View 2," Fibre-Water Interactions in Paper-making, Transactions of the Symposium at Oxford, Sept. 1977 , British Paper and Board Ind. Fed., London, 1977.

2. Etzler, Frank, "A Comparison of the Properties of Vicinal Water in Silica, Clays, Wood, Cellulose and Other Polymeric Materials," Water Relations in Food, ed. H. Levine, L. Slade, Plenum, 1991.

3. Lindström, T., "The Concept and Measurement of Fiber Swelling," Paper - Structure and Properties, ed. J. A. Bristow and P. Kolseth, pp. 75-97, Marcel Dekker, Inc., New York, NY, 1986.

4 Carlsson, G., Lindström, T., and Scöremark, C., "Expression of Water from Cellulosic Fibres Under Compressive Loading," Fibre-Water Interactions in Paper-making, Transactions of the Symposium at Oxford, Sept. 1977 , British Paper and Board Ind. Fed., London, 1977.

5. Stone, J. E., and Scallan, A. M., "The Effect of Component Removal upon the Porous Structure of the Cell Wall of Wood. Part III. A Comparison Between the Sulphite and Kraft Processes," Pulp and Paper Canada, 69(12): 69/T288 (June 21, 1968).

6. Carroll, M., and Mason, S. G., "The Measurement of Fiber Swelling by the Liquid Permeability Method," Can. J. Tech., 30: 321 (1950).

7. Carlsson, G., "Some Fundamental Aspects of the Wet Pressing of Paper," Ph.D. Dissertation, Dept. of Paper Technology, The Royal Institute of Technology, Stockholm, Sweden, 1983.

8. Roux, J. C., and Vincent, J. P., "A Proposed Model in the Analysis of Wet Pressing," Tappi J., 74(2): 189 (Feb. 1991).

9. Carlsson, G. and Lindström, T., "Hornification of Cellulose Fibers During Wet Pressing," Paper III in "Some Fundamental Aspects of the Wet Pressing of Paper," Ph.D. Dissertation, Dept. of Paper Technology , The Royal Institute of Technology, Stockholm, Sweden, 1983.

PART III: FUNDAMENTAL PHYSICS OF VAPOR-LIQUID FLOWS

OVERVIEW

Vapor-liquid flow in paper is important in several processes. Water removal processes such as displacement dewatering, impulse drying, through drying, conventional cylinder drying, and even wet pressing are affected by the simultaneous flow of vapor and liquid. Work done under Project 3480 has dealt with several aspects of such flows during the last period. Specific progress has been made in the modeling of impulse drying and displacement dewatering, where routines for handling paper compressibility are being developed. In connection with student research, a fundamental study of steam-water flow during boiling in fibrous media is underway and will be briefly discussed here. A critical need, common to all work in this area, is accurate information on relative permeabilities in paper. Relative permeability refers to the reduction in permeability for the flow of one phase caused by the presence of another immiscible phase; typical relative permeability curves for gas and liquid phases are depicted in Figure 1. It is a complex and important phenomenon which ultimately requires experimental data to be handled properly. As an appendix, we include the main body of text from a draft of a proposal to the NSF for funding to measure relative permeabilities in paper ad other fibrous systems.

Before reviewing research progress, we will briefly review the possible role of vapor-liquid flows in the physics of impulse drying and displacement dewatering. We do this in response to a recent publication in the *Tappi Journal* by Back, who denies that vapor formation or vapor injection can enhance water removal, and who states that impulse drying offers nothing new over other commercial water removal processes. These claims will be shown to be inaccurate.

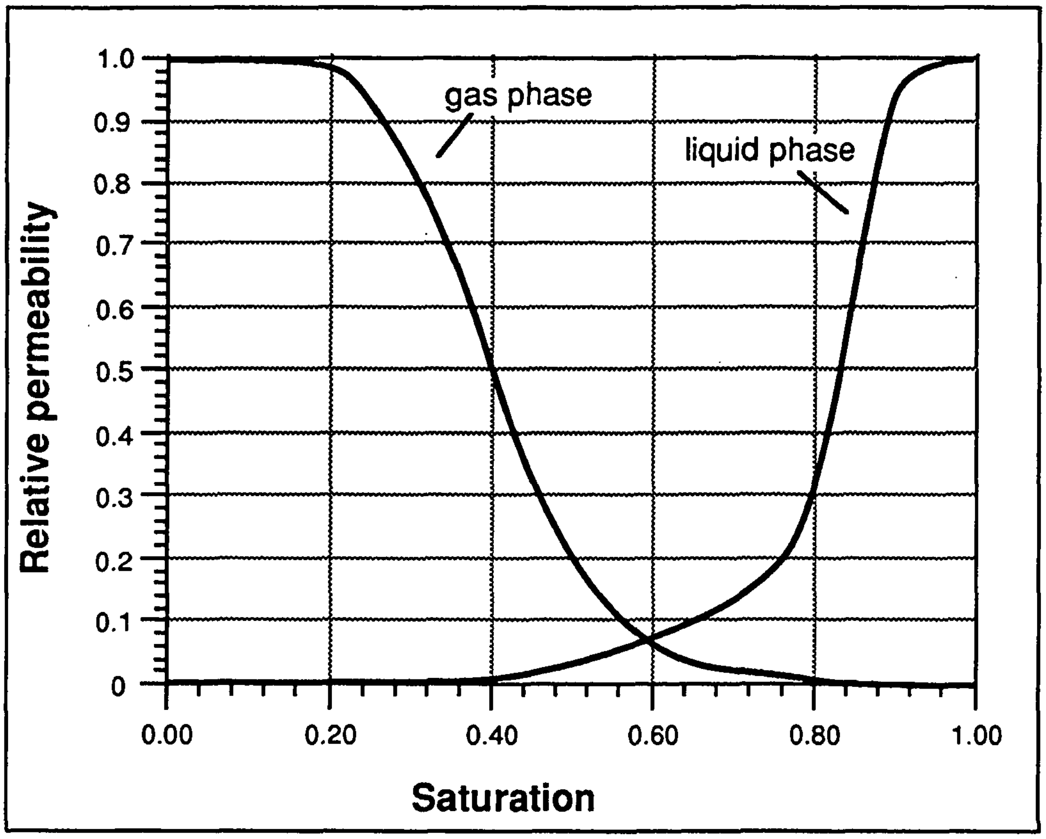

Figure 1. Representative relative permeability functions for gas and liquid in a porous medium.

DISCUSSION OF IMPULSE DRYING PHYSICS: COMMENTS ON AN ARTICLE BY E. L. BACK

In the March 1991 *Tappi Journal*, E. L. Back (1) presents a critical review of impulse drying in which he challenges current theories of impulse drying physics, as proposed by researchers at the IPST (2-9). The possibility of vapor formation playing a role in water removal is expressly denied. Impulse drying is said to be a combination of "superhot wet pressing" with some evaporative drying. The feature of intense heat transfer is downplayed, and impulse drying heat transfer is said to be comparable to hot pressing or even convective drying as found in Yankee dryers. While Back's discussion of the relation of impulse drying to hot pressing and press drying raises several valid points, his analysis of hydrodynamic pressure is subject to a serious error. Furthermore, his discussion of impulse drying heat fluxes is affected by an unfortunate typographical error in one publication, and perhaps a misreading of data in others.

Hydrodynamic Pressure: The Effect of a Vapor Phase

A variety of studies at the IPST have concluded that phase-change heat transfer plays a critical role in impulse drying (4-6,10). While viscosity reduction and thermal softening of fibers clearly play important roles in impulse drying, the formation of a pressurized steam zone at some point in the nip has received attention as a mechanism which can displace additional liquid water or at least resist rewet in impulse drying (7). Back, however, claims that formation a vapor phase cannot increase water removal. If it forms, Back argues, it simply "replaces" the water that was there, staying at equilibrium with the water pressure that was there or in the adjacent layer in the sheet, unable to act separately on the liquid water (pp. 142-143 of (1)). In other words, the vapor phase cannot increase the hydraulic pressure gradient across the sheet, and thus cannot help move liquid water out of the web. This is a serious thermodynamic fallacy. True, the vapor phase must be in equilibrium with whatever liquid it contacts, so, neglecting the secondary effect of capillary pressure, the vapor and liquid phases must be at the same pressure where they share a boundary. However, as heat is added to the system, water and steam can reach a new equilibrium at a higher pressure and temperature (e.g., think of a typical pressure cooker).

To clarify this, think of a wet sheet being pressed by a cold surface onto a felt. After a short period of time, equilibrium is reached (neglecting slow creep effects), the hydraulic pressure in the sheet drops to zero, and the total applied pressure is taken up entirely by the solid network. The sheet is still saturated, but without further compression, there is no driving force to move it into the felt (let's neglect capillary forces again).

Consider what would happen if the cold platen were now instantly heated to, say, 200°C (equilibrium vapor pressure = 1 .56 MPa or 226 psi). Heat transfer would rapidly take place between the hot surface and the moist upper layer of the sheet. The metal surface would begin to cool and the upper layers of the sheet would become hot. Within microseconds, some of the water would reach temperatures exceeding 100°C, with vapor pressures in excess of the atmospheric pressure. Vapor slightly above atmospheric pressure will begin to form, but there is very little space for the vapor to expand into, so the vapor zone may be extremely small. Heat continues flowing into the system, the water temperature continues to rise, and the pressure of the vapor zone follows, staying in equilibrium with the water.

If there had been no viscous or inertial resistance to flow, the water could not sustain a pressure above atmospheric, and the steam zone would quickly expand, displacing and perhaps moving past the water until it vented to the atmosphere. But there is flow resistance due to the permeability of the paper and the viscosity of the water. As soon as the water temperature exceeds 100°C, vapor pressure begins to induce flow. This can happen long before thermal softening of the fibers plays any significant role in water removal. Viscous resistance limits the flow velocity of the water, so the vapor pressure can continue to climb, and the hydraulic pressure gradient across the fluid also continues to climb. As the hydraulic pressure gradient increases, the discharge velocity of the water also increases.

The vapor zone can definitely drive liquid water out of the sheet. As it does so, the heat flux into the water can drop as it moves away from the hot surface, and the vapor pressure may also drop after passing through a maximum. But the fundamental principles of thermodynamic equilibrium, mass and energy conservation, and fluid flow all interact to create a system in which the formation of a vapor zone can help remove water from a sheet by increasing the hydraulic pressure gradient. The analysis of such a system, with idealized physical properties, has been done numerically (7,11).

Note that thermodynamic equilibrium does not mean that the temperature of the vapor zone is determined by the previously prevailing liquid pressure, rather that the pressure of the vapor zone is fixed by the local temperature of the system, which in turn is controlled by heat flux into the system. As the vapor pressure or liquid pressure increases, the mechanical pressure at that point decreases. Of course, if that vapor pressure exceeds the applied mechanical pressure, "lift off" takes place.

Related criticism can be applied to Back's proposed pressure gradients presented in Figure 15 of his article, where he speculates on the distribution of hydraulic and network pressures are distributed across a sheet during pressing with cold and hot surfaces. The sketches indicate that a dry, steam-filled zone could be at a substantially lower hydraulic pressure than is found in the middle of the sheet. The solid network takes up more of the total pressure, he argues in the caption, because "the compressed network can withstand a higher pressure."

It is true that heating of the web next to the hot surface causes a softening of the fibers and increases the densification of the solid. The densification may be so great that very high network pressures would be required at room temperature, but not at high temperatures. As the fibers soften, they can densify further under a constant or even a decreasing load. The key question is not what the density of the fibers are, but what the network and hydraulic pressures are.

I can conceive of no scenario in which heating a pressing surface could lead to a fluid pressure distribution as Back has sketched, with a high hydraulic pressure in the middle of the sheet and a lower hydraulic pressure at the pressing surface. Instead, the fluid pressure in a non-expanding nip should be highest at the pressing surface and drop continuously towards the felt, whether the fluid is steam or liquid water. The figure in question depicts a thermodynamic error, with a vapor-liquid region at a pressure well below that of the adjacent fluid.

While a pressurized vapor zone can enhance the hydraulic pressure gradient in water and thus assist water removal and resist rewet, it is not clear how significant this effect is. Even if vapor zones are important, most of the water removal occurs through standard pressing mechanisms, and separating the effects of vapor action from fiber softening, viscosity reduction, and evaporation is difficult under the extreme conditions of impulse drying. Experimental evidence with flash x-ray radiography indicates that vapor can displace liquid water in impulse drying (8), but this study left many questions unanswered. Back cites Macklem and Pulkowski (12) for evidence that vapor plays no role in water removal. The latter study, however, does not present a proper assessment of the issue. For example, the authors' claim that impulse drying removes about as much water as expected for super-hot wet pressing is based on an inappropriate extrapolation of a crude rule-of-thumb. Back also claims that a vapor pressure effect in impulse drying is contradicted by data showing improved water removal with higher mechanical pressures. This does not follow, however. Increased compression of a sheet almost always increases water removal. Indeed, the proposed physical model of impulse drying predicts that higher vapor pressures should occur in a higher pressure nip, although it may take longer for the hydraulic pressure to drop enough for vapor to form.

While further work is needed to ascribe a quantitative significance to the vapor displacement mechanism in impulse drying, one piece of evidence clearly indicates that vapor formation is important: sheet delamination. If post-nip vapor pressures in the sheet can be great enough to blow the sheet apart, vapor pressures in the nip should also be available to assist water removal or to at least resist rewet as the sheet begins to expand. The problem of delamination, incidentally, appears to have been brought under control through the recent work of Orloff (13), who is now obtaining remarkable dryness levels and sheet properties in a 40-ms nip using novel press rolls fabricated with plasma-sprayed ceramic coatings.

The Issue of Heat Flux

The intense heat transfer applied in impulse drying has long been touted as a feature which distinguishes it from other conventional pressing and drying processes. Sprague (14), for example, offers a paradigm for comparing water removal processes on a plot of process temperature versus energy demand per mass of water removed. Such a comparison suggests that impulse drying lies in a unique regime, with an exceedingly high operating temperature (much greater than is found in hot pressing) but with a surprisingly economical energy demand (for moist sheets, typically well below that of press drying or other evaporative processes). The heat transfer mechanism is then of pivotal importance in discussing impulse drying as a novel technology.

Back claims that the heat flux in impulse drying is not unusual for paper drying processes. Unfortunately, a misreading of data in one publication, combined with an unfortunate typographical error in another, have led to this incorrect conclusion. From our numerical modeling of an idealized impulse drying process (7), he cites a peak heat flux value of 0.8 kW/m^2, and compares it to a value of 0.08MW/m^2 from press drying. However, the numerical results in the cited publication clearly show peak fluxes on the order of 5 MW/m^2, not 0.8 kW/m^2. I do not know where the extremely low cited value came from. Back also compares data from Sprague (14) for peak heat fluxes to those from a Yankee dryer, finding the impulse drying fluxes to be of the same order (Figure 16 of (1)). Unfortunately, the graph from Sprague suffers from an obvious typographical error in the axis labeling, with unreasonable values as high as 400,000 kW/m^2 listed. Back realized that an error was made, but the "corrected" labeling in the reproduced figure still show peak heat flux values that are an order of magnitude below the values commonly cited elsewhere in the literature (5,6,7,9). Typical measured values of peak heat flux range from about 2 to

8 MW/m^2, and more recent measurements by Orloff (15) show some values higher than 10 MW/m^2. Such values are much beyond those reported for press dryers (0.08 MW/m^2) or Yankee dryers (< 0.15 MW/m^2).

Summary

Back's contributions to water removal processes have been substantial, and the information he presents about press drying and other technologies raises several valid points and challenges with respect to impulse drying . His comments on sheet compressibility, thermal softening and viscosity reduction emphasize areas that have not received sufficient attention in past work on impulse drying. However, his elimination of vapor displacement as a potential dewatering mechanism, whether for impulse drying or for direct displacement dewatering (16), is unfounded. Likewise the claim that no new mechanisms are involved in impulse drying cannot be substantiated by an appeal to heat flux data. This is not to say that vapor displacement is proven to be significant, nor that impulse drying is dominated by any new mechanisms. But the intense phase-change heat transfer that occurs, coupled with the possibility of vapor action in removing liquid water, makes impulse drying a truly interesting process which cannot justifiably be treated as just another variant of press drying, hot pressing, wet pressing, or tissue drying.

MODELING OF IMPULSE DRYING AND DISPLACEMENT PROCESSES

The history of numerical modeling of impulse drying at the IPST begins with the work of Pounder and Ahrens (11), which was an ambitious attempt to include many of the complexities of pressing and heat transfer, often in the absence of adequate empirical information for use in the model. The complexity of the model, coupled with problems in the numerical methods, made it a difficult tool to use and interpret in studying the basic physics of impulse drying. Later, Lindsay (7,9) took a different approach, developing a true moving boundary model of a greatly simplified, idealized version of impulse drying in order to understand some of the key proposed mechanisms such as vapor formation and heat pipe effects. The most severe simplification imposed was the treatment of the paper as a rigid porous medium. A motivation for this was the realization that even state-of-the-art models of pure wet pressing are based on many crude simplifications and approximations, giving results of questionable accuracy at great computational expense. To double the complexity and uncertainty of such a model by adding the mechanisms of impulse drying would probably be of little fundamental value. The object of the modeling effort was not to exactly model the impulse drying process, but to examine several aspects of the proposed heat transfer mechanisms in an approximate manner.

Members of the IPST Project Advisory Committee have requested modifications in the model to deal with deformable media, and efforts have thus been made to determine a proper approach for modeling idealized impulse drying or displacement dewatering systems in a non-rigid sheet. The motivation for this improvement recently increased after reviewing recent heat flux data from Orloff (15), which show the possibility of unusual heat transfer mechanisms that are intimately linked to the compression - and decompression - of the paper. In particular, a second peak in the heat flux curve has been reported at low nip residence times (ca. 20 ms). The second peak occurs as the mechanical pressure is dropping rapidly, but is still finite. Of several theories which have been discussed, the best candidate for an explanation is an increase in moisture content in part of the sheet upon decompression. This may be related to a rewetting phenomenon. To explore this puzzling phenomenon with numerical computations, the model, MIPPS, must be modified to handle compressible media.

After review a number of works on modeling flows in deformable media, an approach to the problem at hand has been devised. A moving grid scheme will be used, in which the physical locations of computational nodes continuously changes as the medium compresses. Nodes will be spaced uniformly in terms of basis weight layers. The model will solve equations of continuity for solid and fluid phases and will determine the relative fluid velocity (velocity of the fluid phase with respect to the solid matrix) using Darcy's law with empirical expressions for permeability as a function of compression. Effective porosity, the portion of the total void fraction contained in interconnected pores available for flow, will be estimated crudely pending actual measurements of effective porosity, as discussed in Part II of this report. The transfer of heat and the development of vapor and two-phase zones will proceed much as is now done in MIPPS-II, with the exception that capillary wicking (heat pipe effects) will be modeled using crudely estimated values for relative permeability and empirical estimates of capillary pressure functions.

Some experience in solving the equations to predict compression and hydraulic pressure development has been acquired in the last period. Figure 2 below shows the results from a sample computation of compression in a sheet of paper which was initially saturated and at atmospheric pressure.

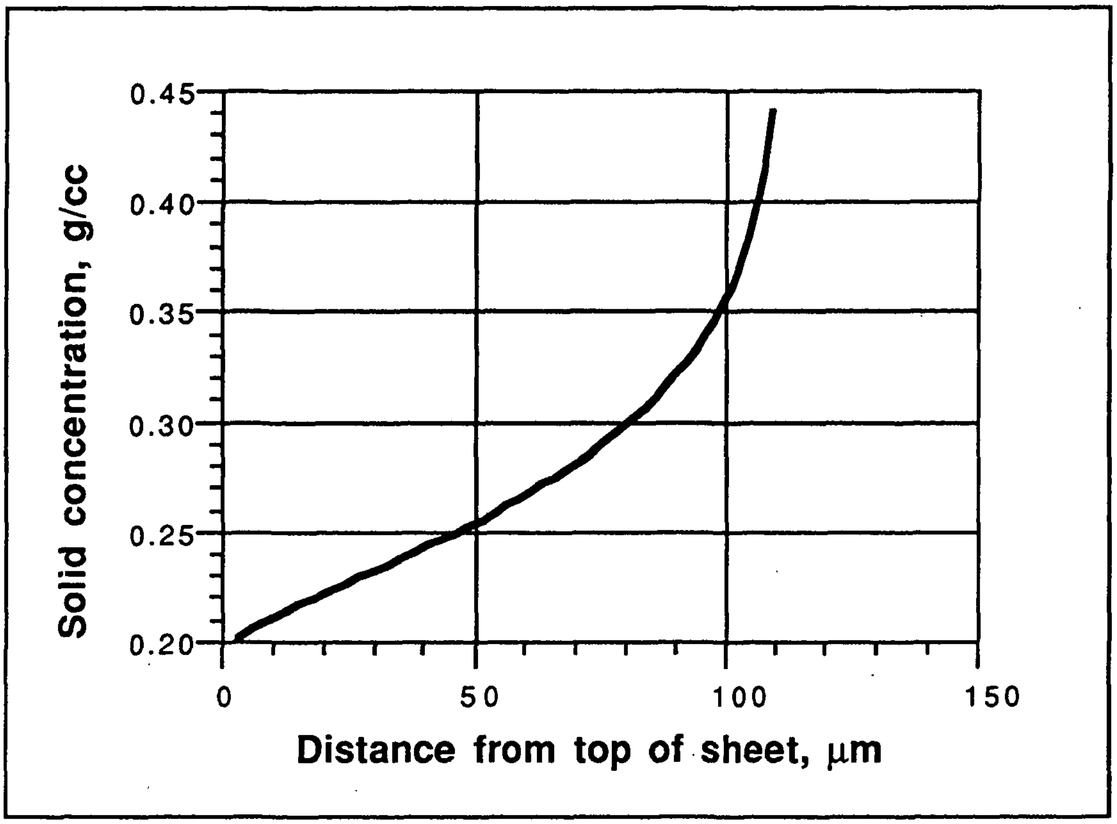

Figure 2. Sample prediction of consolidation in an initially uniform, saturated sheet during pressing.

Given time demands, development of the model will proceed slowly, and may require a full year before full computations can be reported.

STUDIES OF BOILING IN FIBROUS MEDIA

To gain a better understanding of the phase-change heat transfer which can occur in processes like impulse drying, a study of boiling in fibrous media was conducted through the student research of Rudemiller (17,18,19). Rudemiller investigated the effects of a fibrous medium in modifying boiling behavior, and made fundamental contributions to the heat transfer literature. The study opened many further avenues for research. This work is now being continued with the help of Marty Hoskins, an A190 student who will begin his Ph.D. research shortly. Hoskins has reinstalled the apparatus of Rudemiller at the new IPST location and is using gamma-radiography to measure of vapor-liquid distributions in a fibrous bed with boiling.

In the last period, some of the results of Rudemiller were evaluated in terms of a simple model of two-phase flow. Rudemiller's data for boiling heat flux as a function of surface temperature revealed a nucleate boiling regime followed by a sudden transition to a constant heat flux regime at higher superheats (superheat is the difference between surface temperature of the boiling cell and the saturation temperature of the liquid). While the boiling results in fibrous media show different features than are reported in boiling studies in other porous media (typically large particles or isotropic sand), the constant heat flux regime appears to be analogous to the dryout regimes commonly observed by others, in which the upward vapor flow is rapid enough to impede the downward liquid flow which supplies fluid for vaporization.

A rigorous analysis of the flows in the constant heat flux regime requires information about relative permeability functions and capillary pressure functions, if one makes the usual assumption that the countercurrent flows of liquid and steam are sufficiently dispersed across the fibrous bed that the whole system can be treated as uniform and homogeneous. However, some researchers report formation of steam chimneys during boiling, meaning that macroscopic, separate channels for gas and liquid flow occur. There was some evidence of fixed vapor pathways forming in Rudemiller's experiments, at least in the upper part of the fibrous bed.

Straightforward analysis is possible if we assume that the upward steam flow is completely segregated into dry chimneys occupying a fraction X of the cross-section of the bed. Downward liquid flow likewise is assumed to take place in purely saturated zones occupying a fraction (1-X) of the cross-sectional area of the fibrous bed. The competing upward and downward flows are a function of the vapor pressure at the boiling surface, which cannot be specified *a priori*. Depending on the flow state, the gauge pressure which can exist at the boiling surface must lie between 0 and the hydraulic head of the initial liquid column, ηgH. Assume that the pressure at the boiling surface is ηgHC, where C lies between 0 and 1. For a given value of C, the forces for steam and liquid flow are specified and flow proceeds according to Darcy's law for each phase. Conservation of mass (gas and liquid must have equal absolute mass flow rates) then establishes the relationship between X and C:

$$X = \frac{\dfrac{\rho_l^2 (1\text{-}C)}{\mu_l}}{\dfrac{\rho_v}{\mu_v}[\rho_l(1\text{-}C) + (\rho_v\text{-}\rho_l)] + \dfrac{\rho_l^2(1\text{-}C)}{\mu_l}}, \qquad (1)$$

where r is density, m is viscosity, and the subscripts l and v refer to the liquid and gas phases, respectively. The heat flux is then the heat of vaporization times the mass flux of vapor (or water), giving

$$Q = \frac{\rho_v X K h_{vap}}{\mu_v}\left(\rho_l g(1\text{-}C) + (\rho_v\text{-}\rho_l)g\right), \qquad (2)$$

where K is the permeability, h_{vap} is the heat of vaporization, and Q is the heat flux per unit area. With two equations and three unknowns, Q, X, and C, we can plot Q against either of the other variables. A plot of Q versus C is shown in Figure 3; the plot appears identical for Q versus X because of the relationship between X and C. A maximum value of heat flux is thus obtained, corresponding to the critical flux for our system.

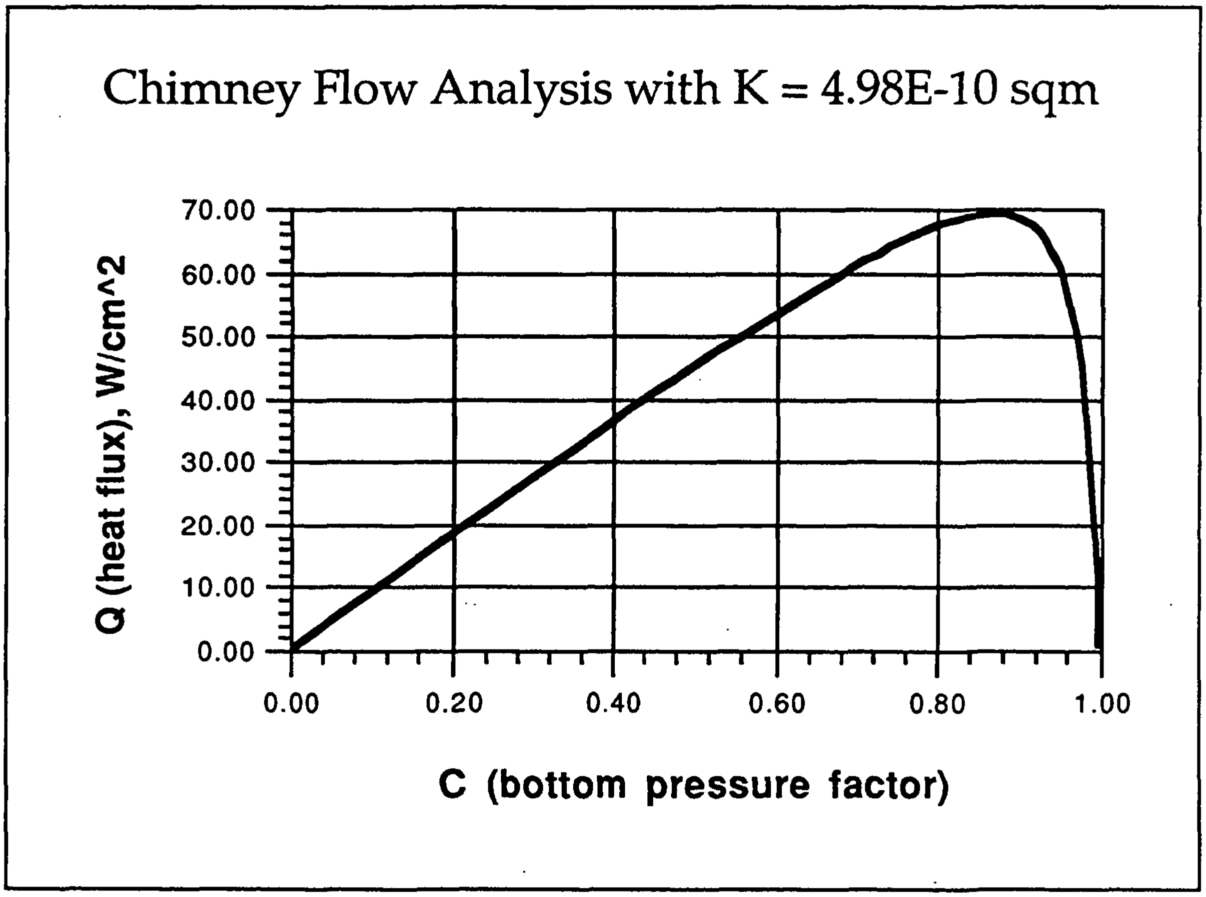

Figure 3. Predicted critical heat flux versus bottom pressure factor using a measured permeability value from Rudemiller (17). Measured critical heat flux was 16 W/cm^2.

Because the above "chimney model" totally neglects the increased flow resistance caused by surface tension forces between gas and liquid as they compete for the same flow space, the predicted flow rates and thus the predicted heat flux values should represent an absolute maximum for the system. Rudemiller's critical heat flux values are substantially lower (about 16 W/cm^2 for the case corresponding to Figure 3) than those predicted with Equations 1 and 2, which suggests that gas and liquid flows are not totally segregated, and that relative permeability effects are important.

The chimney model approach turns out to give the same results as a zero-dimensional model of Bau and Torrance (20), who treated countercurrent vapor-liquid flow as homogeneous but with linear relative permeability functions, $k_{rl} = S$ and $k_{rv} = (1-S)$. The difference between the predicted and observed critical heat fluxes can be taken as a qualitative measure of the nonlinearity of the relative permeability functions for the fibrous system.

Gamma-radiography measurements of vapor-liquid distributions during boiling will be used to see if steam chimneys form and if other nonhomogeneities exist. Lehtinen, in a study of microscopic flows during drying of paper, found visual evidence of strong heterogeneous flows for steam and liquid water (21). Some thermocouple measurements during impulse drying have suggested that the motions of liquid and steam are not smoothly distributed across the sheet. AN improved understanding of vapor-liquid flows during phase-change heat transfer may ultimately be applied to impulse drying.

PLANS FOR THE COMING PERIOD:

1. Develop Fortran code for one-dimensional consolidation of a moist sheet and begin incorporation into MIPPS.
2. Investigate vapor-liquid flows during boiling in porous media with gamma-densitometry. Relate results to impulse drying, where possible.

LITERATURE CITED

1. Back, E. L., "Why is Press Drying/Impulse Drying Delayed?," Tappi J., 74(3): 135 (March 1991).

2. Orloff, D. I., High Intensity Drying Processes – Impulse Drying, Report 4 prepared for the U.S. DOE, Office of Industrial Programs, under contract DE-FG02-85CE40738, The Institute of Paper Science and Technology, Atlanta, Georgia, May 1990.

3. Orloff, D. I., High-Intensity Drying Processes – Impulse Drying, Annual report prepared for the U.S. DOE, Office of Industrial Programs, under contract No. DE-FG02-85CE40738, The Institute of Paper Science and Technology, Atlanta, Georgia, Sept. 1990.

4. Burton, S. W., and Sprague, C. H., "The Instantaneous Measurement of Density Profile Development During Web Consolidation," J. Pulp Paper Science, 13 (5): J145 (1987).

5. Burton, S. W., Ph.D. Dissertation, The Institute of Paper Chemistry, Appleton, WI, 1986.

6. Lavery, H. P., High Intensity Drying Processes - Impulse Drying, Second Annual Report for U.S. DOE under Contract No. DE-FG02-85CE40738, The Institute of Paper Science and Technology, Atlanta, Georgia, Feb. 1988.

7. Lindsay, J. D., "The Physics of Impulse Drying: New Insights from Numerical Modeling," in Fundamentals of Papermaking, Trans. of the Ninth Fund. Res. Symp., Cambridge, UK, Sept. 1989, ed. C. F. Baker and V. W. Punton, vol. 2, pp. 679-729, Mechanical Engineering Publications, London, 1989.

8. Zavaglia, J. C. and Lindsay, J. D., "Flash X-ray Visualization of Multiphase Flow During Impulse Drying," Tappi J., 72(9): 79-85 (1989).

9. Lindsay, J. D. and Sprague, C. H., "MIPPS: A Numerical Moving Boundary Model for Impulse Drying," J. Pulp Paper Sci., 15(4): J135-141 (1989).

10. Lindsay, J. D., "New Drying and Dewatering Processes in Papermaking," Oji International Seminar on Advanced Heat Transfer in Manufacturing and Processing of New Materials, Fujihara Sci. Found., Tomakomai, Japan, Oct. 28-Nov. 1, 1990.

11. Pounder, J. R., and Ahrens, F. W., "A Mathematical Model of High Intensity Paper Drying," Drying Technology, 5(2): 213-243 (1987).

12. Macklem, E. A., and Pulkowski, J. H., "Impulse Drying – A Pressing/Flashing Drying Phenomena," 1988 Engineering Conference, Chicago, Illinois, Sept. 19-22, 1988.

13. Orloff, D. I., High-Intensity Drying Processes – Impulse Drying, Annual report prepared for the U.S. DOE, Office of Industrial Programs, under contract No. DE-FG02-85CE40738, The Institute of Paper Science and Technology, Atlanta, Georgia, Sept. 1990.

14. Sprague, C. H., "An Integrated View of Web Consolidation Processes," in Fundamentals of Papermaking, Trans. of the Ninth Fund. Res. Symp., Cambridge, UK, Sept. 1989, ed.

C. F. Baker and V. W. Punton, vol. 2, Mechanical Engineering Publications, London, 1989.

15. Orloff, D. I., The Institute of Paper Science and Technology, personal communication, 1991.

16. Lindsay, J. D., Experimental Evaluation of Displacement Dewatering, AIChE Annual Meeting, Chicago, Illinois, Nov. 11-16, 1990.

17. Rudemiller, G. R., "A Fundamental Study of Boiling Heat Transfer Mechanisms Related to Impulse Drying," Ph.D. Dissertation, The Institute of Paper Chemistry, Appleton, WI, 1989.

18. Rudemiller, G. R. and J. D. Lindsay, "An Investigation of Boiling Heat Transfer in Fibrous Porous Media," Heat Transfer 1990, vol. 5, Proc. of the Ninth International Heat Transfer Conference,Jerusalem, Israel, July 1990, ed. G. Hestroni, Hemisphere Publ. Corp., New York, 1990.

19. Rudemiller, G. R. and Lindsay, J. D., "Apparatus for Investigating Boiling Phenomena in a Fibrous Porous Medium," Int. Commun. Heat Mass Transfer, 16(6): 785-794 (1989).

20. Bau, H. M., and Torrance, K. E., "Boiling in Low-Permeability Porous Materials," Int. J. Heat Mass Transfer, 25(1): 45-55 (1982).

21. Lehtinen, J., "Some Theoretical Aspects Regarding the Basic Processes and the Energy Economics of the Convac Drying Process for Paper and Board," Proc. of the Third Intl. Drying Symposium, Birmingham, Sept. 13-16 (1982).

EXTENSION TO PROJECT 3480: —FUNDAMENTALS OF MULTIPHASE FLOW IN FIBROUS MEDIA— A PROPOSAL TO THE NATIONAL SCIENCE FOUNDATION

A proposal is under preparation to NSF for a two-year project to extend the research which is currently funded under Project 3480. Feedback from the Project Advisory Committee on the proposed work is solicited. IPST cost sharing for the proposed work will be on the order of 30-50%. Below is the main body of the proposal as it currently stands.

PROJECT OBJECTIVES

The proposed project seeks to provide fundamental yet practical information about vapor-liquid flow in anisotropic fibrous media, with an emphasis on measurements of relative permeability functions at various degrees of compression. The practical application is to water removal processes in the pulp and paper industries. An improved understanding of vapor-liquid flow processes in fibrous media such as paper could be used to enhance conventional drying processes, and could be used to improve emerging water removal technologies such as impulse drying and displacement dewatering, which are described below.

The proposed work includes original measurements of the following: anisotropic permeability and relative permeability in paper and other fibrous media, gas-liquid (saturation) distributions during isothermal two-phase flow and boiling systems in fibrous media; and capillary pressure functions in which the effect of compression and temperature on sheet structure is considered. These measurements are unified by the thrust to understand how the consolidated, fibrous structure of paper affects multiphase flow, with and without heat transfer.

RATIONALE

Multiphase flow in fibrous media is of substantial importance in the pulp and paper industries. Many water removal and drying technologies bring about the simultaneous flow of steam and liquid water through paper and felts. The flow of air and water in fibrous mats also plays an important role in wet pressing operations, in which roll presses are used to remove water form a partially saturated sheet. Information about multiphase flow in paper is scanty, and researchers therefore often rely on inappropriate correlations for key parameters in investigations of industrially important processes.

The importance of considering anisotropy must be stressed. Paper is a highly anisotropic medium, and multidimensional flows are increasingly being recognized as important, although many practical flows are primarily in the thickness direction of the sheet.

In describing multiphase flows through porous media where inertial effects are minor, a modification of Darcy's law is typically used:

$$q_\alpha = \frac{-k_{r\alpha}\mathbf{K}\bullet\nabla P_\alpha}{\mu_\alpha} \tag{1}$$

where a denotes a phase, **q** is the superficial velocity vector, k_{ra} is a relative permeability with a value between 0 and 1, **K** is the second-order permeability tensor (a diagonalizable matrix), P_a is the hydraulic pressure in the a phase, and μ_a is the viscosity of phase a. While k_{ra} is almost always assumed to be a scalar (1), in an anisotropic medium with directional pore structures, it is difficult to believe that relative permeability should be isotropic, for relative permeability is affected by pore structure. Indeed, recent experimental work has shown that relative permeability can be anisotropic (2,3), with the anisotropy increasing with decreasing saturation. If the concept of anisotropic relative permeability is introduced, the proper tensor form of Equation (1) should be

$$q_\alpha = \frac{-\mathbf{k}_{r\alpha}:\mathbf{K}\cdot\nabla P_\alpha}{\mu_\alpha} \tag{2}$$

where $\mathbf{k}_{ra}$ is now a fourth-order tensor, whose dyad product with **K** gives the new apparent permeability tensor, **K'**:

$$\mathbf{K}' = \mathbf{k}_{r\alpha}:\mathbf{K}. \tag{3}$$

The 81 possible terms in the relative permeability tensor can be reduced to three parameters if we assume that the principal axis frame of **K'** (formed by its eigenvectors) is the same as that of **K** (consistent with the observations of McCord and Stephens (2)), and that **K'**, like any typical permeability tensor (4), is symmetric. The diagonalized (principal axis frame) form of **K'** can then be written as

$$\mathbf{K'} = \begin{bmatrix} k_{r\alpha,1}K_1 & 0 & 0 \\ 0 & k_{r\alpha,2}K_2 & 0 \\ 0 & 0 & k_{r\alpha,3}K_3 \end{bmatrix}, \qquad (4)$$

where $k_{ra,i}$ is the relative permeability in principal direction x_i, and K_i is the intrinsic permeability in that direction. To understand the behavior of multiphase flow in a deformable, anisotropic medium such as paper, the three components of **K** must be measured as functions of porosity, and the three relative permeability factors must be measured as functions of saturation, porosity, and possibly other factors.

Capillary pressure, the difference in equilibrium pressures across the phase-boundary of two immiscible fluids, also plays an important role in dealing with multiphase flow. It is at least a function of saturation, surface tension, and pore structure, and is subject to hysteresis.

Permeability, relative permeability and capillary pressures represent primary parameters that must be measured in order to begin a fundamental understanding of the behavior of multiphase flows in porous media. Because these parameters are intimately tied to the complex pore structure of the medium, attempts to generalize these functions or to apply data from one class of porous media to another are generally not successful. Once these parameters are available, fundamental analysis of the flows is possible, and numerical predictions of saturation distributions and flow rates can be compared to measured values to obtain further insight into the physical behaviors of dynamic and steady-state systems.

INDUSTRIAL NEED FOR FUNDAMENTAL DATA FOR FIBROUS SYSTEMS

Water removal from a wet fibrous web is a critical operation in papermaking. Over 300,000 liters of water typically enter the paper machine for each ton of paper produced. Most of this water is removed by drainage and mechanical pressing. Only the final 0.5% or less of this water must be removed by evaporation, but doing so uses most of the energy needed for papermaking and requires a vast amount of equipment. There is definitely an economic incentive for improved water removal techniques.

In the critical areas of pressing and drying, a number of recent innovations in the paper industry may result in improved performance, including energy savings and paper property improvements (5). Multiphase flow takes place in many of these technologies. Two examples are impulse drying and displacement dewatering, emerging technologies which are under development at the The Institute of Paper Science and Technology with funding from industry (6,7) and the Department of Energy (8,9). Conventional pressing and drying operations also involve multiphase flow. As noted below, there is relatively little useful information about multiphase flow in paper or related fibrous media, yet a great need exists for fundamental information to guide the development of processes in which multiphase flow occurs.

Impulse Drying

Impulse drying is a novel water removal process which was first developed at The Institute of Paper Chemistry (currently The Institute of Paper Science and Technology). At a superficial level, impulse drying can be described as a variation of long-nip wet pressing, with one roll heated to 250-375°C (Figure 1). In impulse drying, intense heat transfer drives a process that gives significantly higher dryness than wet pressing. Most of the additional water removed in impulse drying is liquid, meaning that the total amount of water that needs to be evaporated to dry a sheet may be reduced in impulse drying. Impulse drying not only offers the potential for energy and capital savings over traditional water removal methods, but can give significantly improved paper properties as well (10,11). It has generated a good deal of industrial interest, with current emphasis on its potential in the production of newsprint (12) and linerboard for corrugated containers.

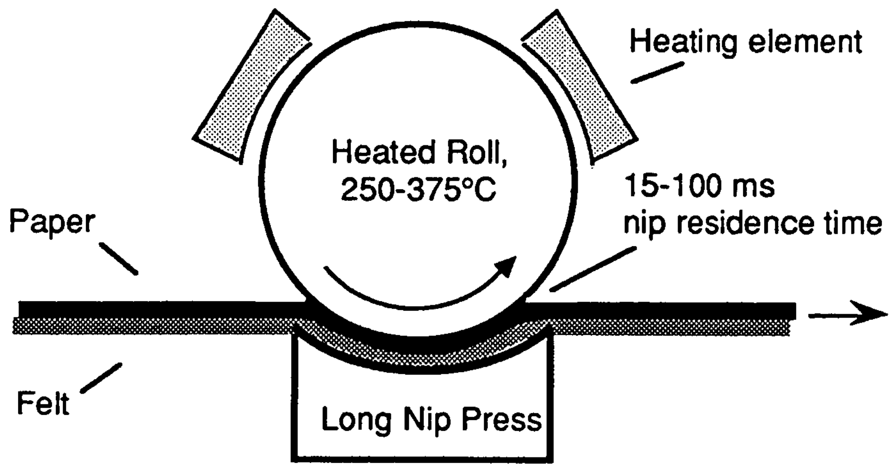

Figure 1. Possible implementation of impulse drying.

Based on a variety of studies into the physics of the impulse drying process (5,10,13), it appears that vapor formation in the nip is a key factor in impulse drying physics. Generation of a vapor phase within the sheet which may lead to vapor-liquid displacement, pushing additional water from the paper into a felt. Sustained vapor pressures at the nip exit may also increase water removal by resisting the rewetting which may occur as suction forces and capillary pressure pull some water from the felt back into the sheet (14,15). Dynamics of flow and heat transfer in the paper remain elusive, however, due to the general lack of measured values for parameters relevant to two-phase flow. The details of multiphase flow in consolidating paper are thus poorly understood.

Although impulse drying has received much attention and has been the focus of many studies over the past several years, the process has not yet been commercialized. The main roadblock to commercialization has been delamination, a problem directly related to multiphase flow (16). Delamination refers to the catastrophic disruption of the sheet that can occur when the internal vapor pressure generates sufficient force to overcome the bond strength of the sheet as it leaves the mechanical restraint of the nip. Two-dimensional flow of vapor is likely as the sheet leaves the narrow nip region, thus information on anisotropic relative permeabilities could be of value in this application. While progress has been made in understanding some aspects of delamination (17) and even in controlling it with novel heat transfer surfaces (18), our fundamental understanding of delamination and of the general physics of impulse drying is still immature.

Displacement Dewatering

Displacement dewatering denotes a process in which a pressurized gas phase is used to increase liquid water removal from a mechanically compressed sheet. Water is removed by both a pressing effect and a vapor-liquid displacement mechanism. This process is similar to what may occur in impulse drying, although in impulse drying the gas phase is generated internally by heat transfer. In the theory of displacement dewatering, high dryness levels may be achieved without the high densification required in pressing alone. The potential to decouple dryness and density has lead to recent investigations of displacement dewatering at IPST (19,20).

If true displacement dewatering is achieved, relatively little vapor would be required to pass through the sheet – ideally only enough to uniformly displace the free water in the interconnected pores of a compressed sheet (1 MPa or more of applied pressure may be required). The objective is to avoid significant vapor flow in contrast to through-drying, in which the sheet is dried evaporatively by passing through large quantities of heated air (21) 22,23). In practice, however, the gas in a displacement dewatering process is likely to break through some pores in the sheet and also remove water by entrainment and evaporation. This undesired effect is an intrinsic instability in gas-liquid displacement in porous media, and is known as viscous fingering (24).

Several approaches can be taken to reduce viscous fingering and thus improve the efficiency of a displacement process. For example, if the in-plane permeability is much higher than the transverse permeability, viscous fingers penetrating in the transverse direction may have a tendency to spread laterally and be less severe. This possibility lead to the first published measurements of the anisotropic permeability tensor in paper by Lindsay (25,26,27), who found that in-plane permeabilities exceed transverse permeabilities by factors as high as 2-10, a result consistent with related measurements in textiles (28). Heat transfer particular can also play a role in decreasing instabilities (29). As a hot viscous finger penetrates into cooler liquid, the gas begins to cool and contract, thus decreasing the growth rate of the viscous finger. The most promising strategy, however, may be to use a condensible vapor as the displacing phase, as when steam displaces water. As fingers of steam penetrate into the sheet and contact cooler liquid, they will condense. The viscous fingers become self-sealing to a degree. The combined effects of heat transfer and condensation are believed to make superheated steam a good candidate for displacement dewatering.

The analysis of displacement dewatering, which involves multidimensional, multiphase flow in paper, would benefit from information on the fundamentals of air-water and steam-water flows in fibrous media.

Conventional Pressing and Drying

Conventional wet pressing, in which liquid water is squeezed out of a wet sheet into an absorbent felt, is now known to involve multiphase flow (30, 31). During the pressing process, a sheet is squeezed to a minimum thickness, and then re-expands as the mechanical pressure is relived. During the re-expansion processes, vacuum pressure can be generated in the sheet which can induce air flow into the sheet and possibly cause cavitation (32,33,34), as well as causing some of the already-removed water to flow back into the sheet (the poorly understood phenomenon of rewetting). Proper understanding of the water removal processes in pressing requires information about relative permeabilities. Without such information, crude approximations are being used. Roux and Vincent (30), for example, in a recent numerical model of wet pressing, rely on crude estimates of relative permeability based on an assumed pore size distribution. Their model, incidentally, predicted that two-dimensional flow does play an important role in wet pressing. By considering anisotropic permeabilities ratios from Lindsay (25), they found that higher in-plane permeabilities contribute to a reduction in water removal in pressing.

Jewett (31) likewise developed a fairly comprehensive numerical model of pressing which comprised a large body of experimental data. The model was intended to be of direct value to the industry in designing and improving wet pressing operations. A critical aspect of the model was the treatment of two-phase flow in the expansion phase of the pressing event, but due to the absence of data, Jewett borrowed a questionable theoretical derivation of Wilder (35) for relative permeability as a function of saturation. Wilder's function was claimed to be universally applicable to any porous medium and any pair of immiscible fluids since no information about pore structure or fluid properties was required in its derivation (such an expression, unfortunately, is likely to be universally *inapplicable*). However, due to the lack of basic data, the use of inapplicable expressions for relative permeability is all that can be done short of actually making measurements.

The analysis of paper drying, which is of tremendous industrial significance, also requires information about relative permeability. Analysis of the gas phase is often done in terms of

Fickian diffusion, but the motion of the liquid phase is treated as Darcian flow through a partially saturated medium. Current efforts to analyze and model paper drying, such as the work of Seyed-Yagoobi at Texas A&M and others in the Texas Drying Consortium, requires information such as relative permeabilities and capillary pressures as functions of saturation and porosity (36). Adequate measurements are lacking in these areas, especially for relative permeability. Data on diffusion coefficients in paper are also needed, but are beyond the scope of the proposed study.

PRESENT STATE OF KNOWLEDGE

Studies of Multiphase Flow in Fibrous Media

The fundamentals of multiphase flow in porous media have been studied extensively in several contexts. Much of the focus has been in geologic systems, where oil recovery (37), nuclear waste disposal (38,39), and groundwater management (40,41) have been the major applications. Cooling systems for nuclear power plants have also been the focus of numerous investigations (42,43). Chemical separation processes involving bubble columns or adsorption towers comprise a related area, in which countercurrent (less commonly sometimes cocurrent) flow of gas and liquid through a solid packing has been extensively studied and correlated (44). None of these systems relate directly to the problem of multiphase flow in paper, which is a consolidated, swollen, highly anisotropic fibrous medium. Even the generic topic of multiphase flow in oriented fibrous mats has received little attention in the literature. The most relevant contribution is the work of Parker (45,46), who measured relative permeability in mats of moist glass fibers. Unfortunately, the effect of saturation gradients across the mat (end effects) are not considered, so relative permeabilities are only obtained for averaged saturations, which can be a serious source of error.

Novel dewatering processes for paper have motivated several relevant studies. Zavaglia and Lindsay (47) applied flash x-ray radiography to investigate the dynamic steam-water flow that occurs in impulse drying. The flow visualization study confirmed that a steam front can form and apparently displace liquid water that was initially near the surface of the sheet, as evidenced by the motion of a drop of aqueous silver nitrate tracer solution. No evidence of viscous fingering was observed. Lindsay (14,48) and Pounder and Ahrens (49) have taken several different approaches in numerically modeling the two-phase flow and phase-change heat transfer that occurs during impulse drying. Lindsay (50) concluded that a heat-pipe mechanism probably plays an important role in impulse drying. Fundamental information about relative permeabilities and capillary pressures is needed to extend this work.

The question of boiling heat transfer in a fibrous medium has been addressed by Rudemiller and Lindsay (51,52), who sought basic information on the physics of impulse drying. At low superheats, a nucleate-boiling regime is observed with lower heat fluxes than occur in open water. At higher superheats, a transition to a constant heat flux regime occurs, apparently coinciding with dryout at the heater surface. An unusual instability accompanies the transition between the two regimes, with a momentary rapid escalation of heat flux before stabilization at a lower value. Boiling has also been studied in a variety of non-fibrous porous media such as sand (53, 54,55), large glass particles (56,57), or packed beds simulating reactor debris (58). The study of boiling in fibrous media is being continued by Hoskins and Lindsay (59), who are applying neutron radiography to examine local saturation gradients and to investigate the transition instability mentioned above. The lack of fundamental information about relative permeabilities in a fibrous medium remains a roadblock. Once such data are available, however, analytical approaches such as those of Udell (54), Tung and Dhir (60), or Lipinski (61) will be helpful.

The performance of displacement dewatering has been studied by Lindsay (62), who concluded that viscous fingering probably plays an important role. While the phenomenon of viscous fingering decreases the importance of relative permeabilities in describing such a displacement process, basic information on gas-liquid flows is still needed to explore the limits of the process.

Several authors have explored the flow of air through thin, moist sheets of paper. The drying of paper by blowing hot air through a web is a commercial technology known as through-drying, and is commonly applied to lightweight, highly porous grades. Measurements of true permeability and relative permeability have generally not been reported because the process uses uncompressed sheets whose thickness is difficult to measure. Lampinen (63), for example, measured gas flow rates through moist paper and reported the results as K_{app}/L, the apparent permeability divided by the (unknown) thickness. With a number of assumptions, such data could be converted to rough estimates of relative permeability for gas flow, but the effect of strong, unmeasured saturation gradients in the drying sheet may seriously distort the results.

Data for the relative permeability of the liquid phase as a function of saturation is not known to be available for paper. However, in a study of capillary wicking in highly porous filter paper, Gillespie (64,65) applied a relative permeability function for water flow, $k_{rw} = (S/S_{max})^3$, based on results of Wyckoff and Botset (66) for gas-water systems in sand. The predictions of a simple analytical model then gave reasonable agreement with the experimental data. The sensitivity of his results to the assumed form of k_{rw} was not discussed, and the analysis introduced several sources of error which may have offset each other. Nevertheless, the possibility that results from sand may apply to paper is intriguing.

The Anisotropy of Paper

Important flow processes in paper can be multidimensional in a number of cases (67,68,69). To date, however, virtually the entire focus of experimental measurements has been in the transverse direction, with very little information available about in-plane flows. Recently the first published measurements of the anisotropic permeability of paper were made by Lindsay (25,26), and supplemented by Lindsay and Wallin (27) and Horstmann et al. (70). In-plane permeabilities exceed transverse permeabilities by factors of roughly 2-10, depending on fiber type and degree of compression. Machine direction in-plane permeability is generally 10-30% greater than in the cross-direction (fibers and thus pores tend to be preferentially aligned in the machine direction of a paper machine). Hamlen at the Univ. of Minnesota is currently predicting anisotropic permeabilities in a 3-D computer simulation of a thin fiber network (71). His results are helping to explain the differences in anisotropy observed in papers made from different fiber types (27).

Anisotropic capillary flows have been studied by Back (72), who found that in-plane capillary flows are faster than transverse capillary flows. Back's work does not permit evaluation of permeabilities, since capillary flow involves a coupling of permeability and local pore size distributions, which need not be simply related. Fundamental information about the anisotropic pore size distribution in paper might be obtained by measuring anisotropic capillary flows in a paper for which the intrinsic permeability is already known. Since capillary flow involves the coupling of permeability and effective pore size, a deconvolution procedure could allow effective pore size in various directions to be extracted. Such a procedure has not yet been attempted.

In contrast to studies of intrinsic, single-phase permeability, we have been unable to find any published studies of anisotropic relative permeabilities in paper or similar fibrous media.

Measurement of Relative Permeability

Relative permeability has been studied in many contexts. Experimental work has been extensive for applications related to the petroleum industry, where oil-water systems are of interest (73). Traditionally, authors have sought to express relative permeability solely as a function of saturation, but other factors can play a role. In some cases, the distribution of the two phases in a porous network can be affected by the viscosity ratio and the capillary number, rather than just the amounts of the two phases. Hysteresis in relative permeabilities has been reported, indicating that that details of the phase distributions depends on the flow history; hysteresis in contact angles has also been reported. Of importance to steam-water systems is Verma's (74) finding that phase-change can enhance the apparent relative permeability of steam, for some steam can condense before a restrictive throat and pass through as water, to re-evaporate on the other side of the throat. The lower kinematic viscosity of water compared to steam result in an increase in steam conductivity.

Measurement of relative permeability poses a number of pitfalls, which may account for the divergent results sometimes seen in the literature. Typical measurement techniques involve measuring the pressure drop across a fixed length of a porous medium through which two phases are flowing, and relating the flow resistance to apparent relative permeabilities at the average saturation occurring between the points of measurement. The major experimental difficulty involves capillary end-effects (73,74), which induce saturation gradients that can extend into the measurement zone. Since relative permeability functions are highly nonlinear, use of an averaged saturation value for a given pressure drop may lead to large errors unless the saturation is nearly constant in the measurement zone. If saturation and phase pressures can be measured at multiple points in the measurement zone, the presence of saturation gradients need not interfere significantly with the measurement.

The difficulties of direct measurements have led to an increasing application of an indirect method for estimating relative permeability. If a pore structure is assumed, and if it is assumed that nonwetting fluid is restricted to the largest pore only, and the wetting fluid to the smallest pores, then capillary pressure data can be used to estimate relative permeability:

$$k_{rw}(S_r) = S_r^2 \int_0^{S_r} \frac{dS_r'}{P_c^2(S_r')} \Big/ \int_0^1 \frac{dS_r'}{P_c^2(S_r')}, \tag{5}$$

where S_r is the reduced saturation. This approach cannot be expected to consistently give useful results. Even if the assumptions in this approach were correct, inaccuracies in the capillary pressure curve can lead to serious errors in relative permeability calculations (75). Direct measurement of k_r must be preferred, when possible.

PROPOSED RESEARCH

The ultimate aim of this study will be to obtain relative permeability data for air-water and steam-water flows in several types of paper as functions of saturation and compression (porosity). Complimentary data on capillary pressure will also be obtained. The results will be applied to the analysis of impulse drying and displacement dewatering, and will be made available to those studying paper drying and wet pressing. The experimental work will proceed in several phases, beginning with less difficult aspects in order to build confidence with the experimental approach and to make corrections and improvements in the approach where needed.

Relative permeability experiments

In-plane Components in Model Fibrous Systems

Measurements of relative permeability will begin with model fibrous systems, composed of non-swelling fibers such as ceramic or glass. Uniform fibrous beds will be formed according to the procedures of Rudemiller (76). The two components of in-plane relative permeability will first be sought. The in-plane permeability apparatus developed by Lindsay (26,27) will be used. In this apparatus, a disk of fibrous medium (5-10 cm diameter) is evenly compressed between two parallel platens. A small injection port in the lower platen serves as an inlet for flow of a pressurized fluid. The thickness of the sheet is continually monitored by three LVDT's mounted around the outer edge of the platens. For the case of single-phase injection, Lindsay (25) outlines how measurement of flow rates, injection pressure, viscosity and sheet thickness is used to obtain the average in-plane permeability. The radial flow problem in an anisotropic medium was solved numerically to check the accuracy of the approximate methods used. By injecting a dyed fluid and observing the eccentricity of the elliptical dyed zone which grows about the injection port, the ratio of the orthogonal in-plane permeability components can also be obtained. The latter procedure is similar to that reported by Adams et al. (77) for textiles, although less tedious analytical methods of analysis can be used with high accuracy instead of an iterative least-squares approach(25).

In adapting this apparatus for measurements in two-phase flow, several modifications are required. Minor modifications to the injection assembly are needed to allow injection of controlled flow rates of gas and liquid phases. More important is the need to monitor saturation and pressure at various points in the sample, for it is possible that capillary end effects may lead to saturation gradients that persist through the radius of the sample. Use of an extremely wide fibrous mat is unlikely to succeed, for the high pressure drops required to get measurable flow across a very wide mat might cause enough deformation in the r-direction to create porosity and intrinsic permeability gradients. Radiographic techniques that could be applied to saturation measurement are available at the IPST, but are not likely to be accurate enough in measuring saturation changes in a thin mat. These techniques include flash x-ray radiography and gamma-densitometry. The first two probably require several centimeters of sample to accurately distinguish saturation levels. Personal experience with flash x-ray radiography, for example, indicates that there is relatively little resolution when absorption is through a thin volume, such as a sheet of paper. Verma (74) discusses requirements of gamma-densitometry techniques, and similar conclusions can be drawn. It is proposed that measurements of capacitance and conductance across various points of the platens could be used to monitor saturation. In particular, pairs of small capacitance probes will be installed at various points flush with the surfaces of incompressible, dielectric platens (e.g., made of polycarbonate). Capacitance measurements were used by Kuo (78) to successfully monitor moisture levels in paper of 0 to 1.8 kg water/kg dry fiber during through-drying experiments. The circuitry employed will borrow features from Kuo's design as well as those from more recent capacitance probes used for studies of two-phase flow (79). Extensive calibration will be required, and a lack of sensitivity near full saturation may be a problem. Limited spatial resolution due to edge effects may also be encountered.

Thick mats for which gamma-densitometry will work also may be tried, but the problem of stratification in the vertical direction may hinder the effort.

When steam-water flow is studied, elevated temperatures will be needed. The platens and the loads elements inducing compression will require a temperature-controlled environment and monitoring of local temperatures through thermocouples installed on the platens. Radial temperature gradients may be deliberately imposed to examine their effect on flow behavior, but that problem is outside the scope of the present proposal.

In addition to knowing the injection pressure and ambient pressure, it is necessary to have information about the pressure gradient throughout the sheet. Small capillary tubes will be inserted through the platen at various points to transmit pressure to sensitive transducers. With care, it is possible to distinguish between pressure in the liquid and gas phases. For example, liquid pressures can be measured with a fluid-filled tubed which communicates with the porous medium through a porous wick of smaller mean pore size than the medium (80). Air-filled tubes are likely to transmit gas pressure, especially if a minute amount of air is injected through the tube before the measurement is taken to clear a fluid meniscus from the tube opening. In a steam-water system, Verma (74) used a tube that was 2°C hotter than the medium to prevent liquid condensation at the tube. Time and experimentation will be required to implement the pressure monitoring system properly.

For the various probes to be installed around the platens, connections to transducers or meters must be done in such a way to still permit a uniform compressive load to be applied to pair of platens. A tentative design for the system is shown in Figure 2; details of miniature pressure transducer placement are not shown. Once the apparatus has been tested and improved, wiring and transducers can be molded into rigid plastic sections to assist in applying a uniform compressive load to the sheet.

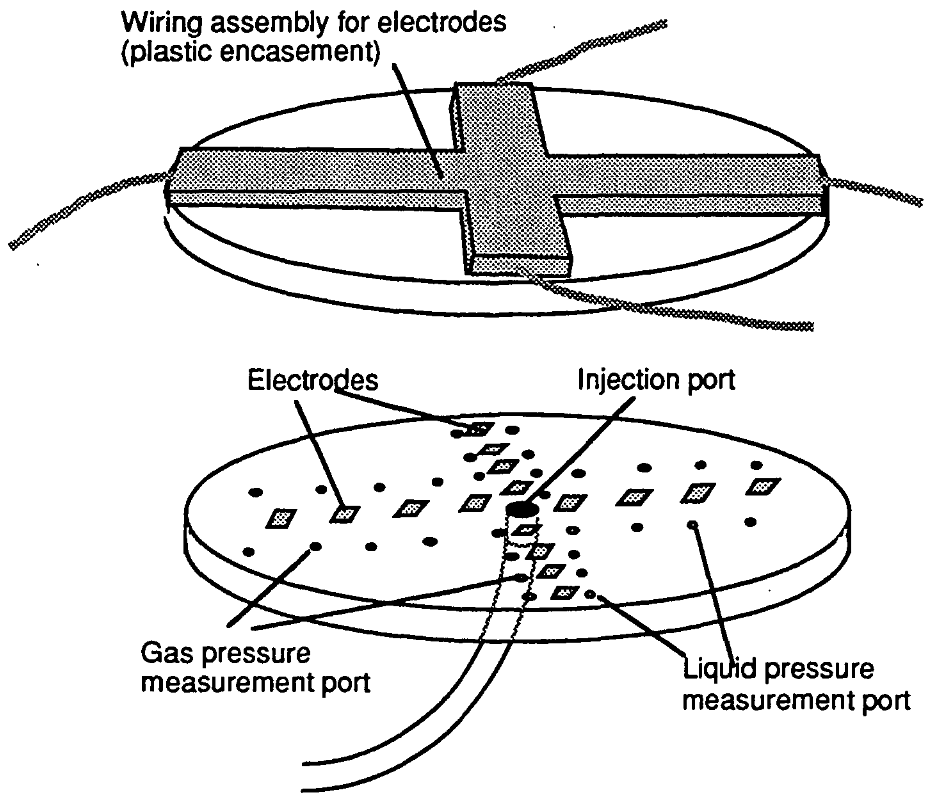

Figure 2. Possible design of platen assembly for measurement of saturations and pressures in a sheet with lateral flow.

Transverse Relative Permeability in Model Fibrous Systems

Measurement of relative permeability in the transverse direction can be done with a technique similar to the Penn State method. A fibrous bed is formed in a cylinder with the plane of deposition normal to the cylinder axis. A dispersed flow of gas and liquid enter one end, and leaves the other end. Both ends are restrained by a porous structure which can withstand the compressive load to be applied (e.g., highly porous sintered metal plates). Pressure and saturation are monitored at several locations, as discussed above, with the difference that the sample thickness will now be sufficient for accurate measurements with gamma-densitometry and flash x-ray radiography. The gamma-densitometry technique will be used primarily, for the flash x-ray apparatus tends to be heavily committed to other work and requires that the flow apparatus be installed in a special lead-shielded room. If possible, however, flash x-ray techniques will be used to supplement the gamma-densitometry measurements. While the flash x-ray procedure is more difficult to use for quantitative analysis, even with image analysis techniques, it does allow a large section of the flow to be examined simultaneously and instantaneously, in contrast to the several minutes of averaging per measurement required of gamma-densitometry.

Relative Permeability in Paper

Once the measurement techniques have been developed and tested for model fibrous media, which tend to have much higher porosities and permeabilities than paper, the more difficult case of measurements in paper can be tackled. The measurements of relative permeability in all three principal directions for model fibrous mats should indicate whether relative permeability can be treated as a scalar in fibrous media. If not, which is probably the case, then measurements in all three principal directions will be sought in paper. If anisotropic permeability appears to be a scalar in the model systems, all three components will be measured at least once in paper to confirm that observation, but progress could be more rapid if measurements in one direction alone were sufficient.

Several papers will be explored. It is proposed that at least three distinct, industrially significant pulp types be examined: kraft pulps, chemithermomechanical (CTMP) pulps, and recycled newsprint. If the low permeability of recycled newsprint seriously impedes measurements, a more porous recycled pulp will be considered.

Capillary Pressure Measurements

Systems of equations for multiphase flow that require relative permeability data also typically require information about capillary pressure as a function of saturation. While measurements of capillary pressure have been made in paper and fibrous mats (Rudemiller, others), the influence of compression and temperature does not seem to have been considered. The reported measurements seem to be for at room temperature and without significant mechanical compression, yet compression changes the pore structure of the sheet, and temperature affects the physics of sheet compression through its influence on fiber stiffness. Even were such measurements available for some papers or fibrous media, they are unlikely to apply exactly to the particular media that will be studied here.

Equipment for capillary pressure measurement has been developed at the IPST (76). It is proposed that a version of the 'pressure plate' method (81) be used, which is similar to standard drainage or suction measurements. In addition to compressed gas acting as the driving force, the device will permit a compressive load to be applied through a mechanical plate driven by a simple screw assembly. A temperature bath will be installed around the apparatus to allow temperature effects to be explored. Measurements will be made in model fiber systems as well as in paper.

Application of Results

Experimental results will also be applied to assist the numerical modeling efforts for impulse drying and displacement dewatering. Proper modeling of heat pipe effects, in particular, requires both relative permeabilities and capillary pressure data. Such information as function of compression will be especially important. Of particular importance is the issue of delamination in impulse drying. Information about the resistance of vapor flow in the plane and in the thickness direction of a moist paper sheet may clarify thinking and suggest new approaches. For example, if high in-plane steam flows occur near the nip exit, perhaps modified sheet structures with altered in-plane permeabilities would increase the operating window of impulse drying.

The resulting data from model fibrous systems will be applied to the on-going study of boiling in fibrous media, which is directed at understanding heat transfer processes in impulse drying. Once relative permeability functions and capillary pressure functions are established, a model of countercurrent steam-liquid flow can be developed to predict saturation gradients which will be measured by Hoskins (59) and the dryout heat flux (constant heat value) measured by Rudemiller and Lindsay (51). The theoretical approach will follow that of Tung and Dhir (60), but modified for significant capillary forces; the analysis of Udell (54) will also be applied.

Information about relative permeabilities will probably be of most value to other researchers dealing with conventional evaporative drying; those studying wet pressing may also benefit. A better understanding of two-phase flow processes will not only allow numerical models to be more realistic, but may be of help in in assisting innovations in water removal systems.

TECHNOLOGY TRANSFER

The IPST is a central source of fundamental information to the pulp and paper industries. Results of the research will be broadly disseminated through pulp and paper journals, general engineering symposia and publications (TAPPI, AIChE, and ASME), and IPST publications. The principle investigator also serves on the advisory board to the Texas Drying Consortium, where advanced computational modeling of drying is being pursued. The PI is also in contact with several others who are pursuing studies of drying in paper, and will seek to assist their work through the timely sharing of information. Relative permeability values and other information of use to the modeling work would be made directly available to those pursuing the modeling of drying.

LITERATURE CITED

1. Collins, R. E., "Flow of Fluids through Porous Materials," Reinhold Publ. Co., New York (1961), pp. 64, 177.

2. McCord, J. T.; Stephens, D. B., "Comment on 'Effective and Relative Permeabilities of Anisotropic Porous Media' by Bear, Braester, and Meiner," Transport in Porous Media., 3: 207-210 (1988).

3. Bear, J., Braseter, C., and Menier, P., "Effective and Relative Permeabilities of Anisotropic Porous Media," Transport in Porous Media, 2: 301-316 (1987).

4. Guin, J. A., Kessler, D. P., and Greenkorn, R. A., "The Permeability Pensor for Anisotropic Nonuniform Porous Media," Chem. Eng. Sci., 26: 1475-1478 (1971).

5. Lindsay, J. D., "New Drying and Dewatering Processes in Papermaking," Oji International Seminar on Advanced Heat Transfer in Manufacturing and Processing of New Materials, Fujihara Sci. Found., Tomakomai, Japan, Oct. 28-Nov. 1, 1990.

6. Orloff, D. I., Project 3470 Status Report, Fundamentals of Drying, report to member companies of The Institute of Paper Science and Technology, March 22, 1990, Atlanta, Georgia.

7. Lindsay, J. D., Project 3480 Status Report, Fundamentals of Water Removal Processes, report to member companies of The Institute of Paper Science and Technology, March 22, 1990, Atlanta, Georgia.

8. Orloff, D. I., High Intensity Drying Processes – Impulse Drying, Report 4 prepared for the U.S. DOE, Office of Industrial Programs, under contract DE-FG02-85CE40738, The Institute of Paper Science and Technology, Atlanta, Georgia, May 1990.

9. Orloff, D. I., High-Intensity Drying Processes – Impulse Drying, Annual report prepared for the U.S. DOE, Office of Industrial Programs, under contract No. DE-FG02-85CE40738, The Institute of Paper Science and Technology, Atlanta, Georgia, Sept. 1990.

10. Burton, S. W., and Sprague, C. H., "The Instantaneous Measurement of Density Profile Development During Web Consolidation," J. Pulp Paper Science, 13 (5): J145 (1987).

11. Ellis, R. L., Impulse Drying Shows Promise in Reducing Energy Costs, American Papermaker, 53(10): 35-36 (1990).

12. Sparkes, D. G., and Poirier, D., "Impulse Drying at Paprican," Pulp Paper Can., 91(4): T147-T150 (1990).

13. Lavery, H. P., High Intensity Drying Processes - Impulse Drying, Second Annual Report for U.S. DOE under Contract No. DE-FG02-85CE40738, The Institute of Paper Science and Technology, Atlanta, Georgia, Feb. 1988.

14. Lindsay, J. D., "The Physics of Impulse Drying: New Insights from Numerical Modeling, in "Fundamentals of Papermaking,"," Trans. of the Ninth Fund. Res. Symp., Cambridge, UK, Sept. 1989, ed. C. F. Baker and V. W. Punton, vol. 2, pp. 679-729, Mechanical Engineering Publications, London, 1989.

15. Beck, D. A., "Re-examining Wet Pressing Fundamentals: A Look Inside the Nip Using Dynamic Measurement," Tappi. , 70(4): 129-133 (April 1987).

16. Crouse, J. W., Woo, Y. D., and Sprague, C. H., "Delamination — a stumbling block to implementing impulse drying technology for linerboard," Tappi J., 72(10): 211-215 (Oct. 1989).

17. Orloff, D. I., High Intensity Drying Processes – Impulse Drying, Report 4 prepared for the U.S. DOE, Office of Industrial Programs, under contract DE-FG02-85CE40738, The Institute of Paper Science and Technology, Atlanta, Georgia, May 1990.

18. Orloff, D. I., High-Intensity Drying Processes – Impulse Drying, Annual report prepared for the U.S. DOE, Office of Industrial Programs, under contract No. DE-FG02-85CE40738, The Institute of Paper Science and Technology, Atlanta, Georgia, Sept. 1990.

19. Sprague, C. H., New Concepts in Wet Pressing, Final report prepared for the US DOE under contract AC02-84CE40685, U.S. Dept. of Energy, Office of Industrial Programs, Washington, D.C., March 1986.

20. Lindsay, J. D., Experimental Evaluation of Displacement Dewatering, AIChE Annual Meeting, Chicago, Illinois, Nov. 11-16, 1990.

21. Holden, G. R., Apparatus for Dewatering of Fibrous Webs in Papermaking and Similar Machines, U. S. Patent 3 284 285, Nov. 8, 1966.

22. Kawka, W., Theoretical and Experimental Analysis of the Blow-Through Process of Fibrous Web Dewatering, trans., Przeglad Papier., vol. 39, no. 11/12, pp. 403-407, 1983.

23. Kawka, W., and Ingielewicz, H., A New Technology for Producing Porous Papers Using Through Dryers, trans., Przeglad Papier., vol. 30, no. 1, pp. 10-18, 1974.

24. Homsy, G. M., "Viscous Fingering in Porous Media," Ann. Rev. Fluid Mechanics, 19: 271-311 (1987).

25. Lindsay, J. D., "The Anisotropic Permeability of Paper: Theory, Measurements, and Analytical Tools," IPC Technical Paper Series #289, The Institute of Paper Chemistry, Appleton, Wisconsin, 1988.

26. Lindsay, J. D., "The Anisotropic Permeability of Paper," Tappi J., 73(5): 223-229 (May 1990).

27. Lindsay, J. D., and Wallin,J. R., "Characterization of In-Plane Flow in Paper," AIChE Annual Meeting, Chicago, Nov. 1990.

28. Adams, K. L., "Permeability Characterization of Engineering Fabrics," Ph.D. Dissertation, Dept. of Chem. Eng., Princeton University, Princeton, New Jersey, 1989, p. 94.

29. Miller, C. A., "Stability of Moving Surfaces in Fluid Systems with Heat and Mass Transport," AIChE J., 19(5): 909-915 (1973).

30. Roux, J. C., and Vincent, J. P., "A Proposed Model in the Analysis of Wet Pressing," Tappi J., 74(2): 189 (Feb. 1991).

31. Jewett, K. B, "The Application of a Model for Two Phase Flow Through a Compressible Porous Media to the Wetpressing of Paper," Ph. D. Thesis, Chem. Eng. Dept., University of Maine at Orono, Orono, Maine, Dec. 1984.

32. Carlsson, G., "Some Fundamental Aspects of the Wet Pressing of Paper," Ph.D. Dissertation, Dept. of Paper Technology, The Royal Institute of Technology, Stockholm, Sweden, 1983.

33. Beck, D. A., "Re-examining Wet Pressing Fundamentals: A Look Inside the Nip Using Dynamic Measurement," Tappi J., 70(4): 129-133 (April 1987).

34. Thorne, J. T., "The Effect of Capillary Rewet on Wet Pressing Operations," Master's Thesis, Chem. Eng. Dept., University of Maine at Orono, Orono, Maine, May 1981.

35. Wilder, J. E., "Paper Drying: Capillary Transfer Between Porous Compressible Materials," Ph.D. Dissertation, Dept. of Mech. Eng., Massachusetts Institute of Technology, Cambridge, MA, 1967.

36. Seyed-Yagoobi, J., Mech. Eng. Dept., Texas A&M university, personal communication, 1990.

37. Patel, K. and Greaves, M., "Role of Capillary and Viscous Forces in Mobilization of Residual Oil," Can. J. Chem. Eng., 65: 676-679 (1987).

38. Doughty, C., and Pruess, K., "A Seminanalytical Solution for Heat-pipe Effects Near High-level Nuclear Waste Packages Buried in Partially Saturated Geologic Media," Int. J. Heat Mass Transfer, 31(1): 79-90 (1988).

39. Pollock, D. W., "Simulation of Fluid Flow and Energy Transport Processes Associated with High-level Radioactive Waste Disposal in Unsaturated Alluvium," Water Resources Research, 22: 765-775 (1986).

40. Huyakorn, P. S.; Springer, E. P., "A Three-Dimensional Finite-Element Model for Simulating Water Flow in Variably Saturated Porous Media," Water Resources Res., 22(13): 1790-1808 (1986).

41. Cooley, R. L., "A Finite difference Method for Unsteady Flow in Variably Saturated Porous Media: Application to a Single Pumping Well," Water Resources Research., 7(6): 1607-1625 (1971).

42. Tsai, T. P. and Catton, I., "The Effect of Flow From Below on Dryout Heat Flux," J. Heat Transfer, 109: 491 (May 1987).

43. Macbeth, R. V., "Boiling on Surfaces Overlayed with a Porous Deposit: Heat Transfer Rates Obtainable by Capillary Action," United Kingdom Atomic Energy Authority, Reactor Group, Report AEEW-R.711, June 1971.

44. Treybal, R. E., "Mass-transfer Operations," McGraw-Hill, New York, NY, 1980, pp. 194-209.

45. Parker, Joseph D., "Permeability of Water to Partially Saturated Glass Fiber Beds," Industrial and Engineering Chemistry, 52(3): 247 (1960).

46. Parker, J. D., "An Investigation of the Permeability to Water of Partially Saturated Beds of Glass Fibers," Ph.D. Dissertation, The Institute of Paper Chemistry, Appleton, WI, (currently the IPST, Atlanta, GA), 1958.

47. Zavaglia, J. C. and Lindsay, J. D., "Flash X-ray Visualization of Multiphase Flow During Impulse Drying," Tappi J., 72(9): 79-85 (1989).

48. Lindsay, J. D. and Sprague, C. H., "MIPPS: A Numerical Moving Boundary Model for Impulse Drying," J. Pulp Paper Sci., 15(4): J135-141 (1989).

49. Pounder, J. R., and Ahrens, F. W., "A Mathematical Model of High Intensity Paper Drying," Drying Technology, 5(2): 213-243 (1987).

50. Lindsay, J. D., "Advances in the Numerical Modeling of Impulse Drying," 1989 TAPPI Engineering Conference, Atlanta, Sept. 1989.

51. Rudemiller, G. R. and J. D. Lindsay, "An Investigation of Boiling Heat Transfer in Fibrous Porous Media," Heat Transfer 1990, vol. 5, Proc. of the Ninth International Heat Transfer Conference,Jerusalem, Israel, July 1990, ed. G. Hestroni, Hemisphere Publ. Corp., New York, 1990.

52. Rudemiller, G. R. and Lindsay, J. D., "Apparatus for Investigating Boiling Phenomena in a Fibrous Porous Medium," Int. Commun. Heat Mass Transfer, 16(6): 785-794 (1989).

53. Bau, H. H., and Torrance, K. E., "Thermal Convection and Boiling in a Porous Medium," Letters in Heat and Mass Transfer, 9: 431-441 (1982).

54. Udell, K. S., "Heat Transfer in Porous Media Considering Phase Change and Capillarity — the Heat Pipe Effect," Int. J. Heat Mass Transfer., 28(2): 485-495 (1985).

55. Bau, H. M.; Torrance, K. E., "Boiling in Low-Permeability Porous Materials," Int. J. Heat Mass Transfer, 25(1): 45-55 (1982).

56. Dhir, V. K., and Barleon, L., "Dryout Heat Flux in a Bottom-Heated Porous Layer," Trans. Amer. Nucl. Soc., 38: 385-386 (June 1981).

57. Fukusako, S., and Hotta, N., "Water-Injection Effect on Boiling Heat Transfer in a Water-Saturated Porous Bed," J. Heat Transfer, 111: 207-210 (1989).

58. Tsai, T. P., and Catton, I., "The Effect of Flow From Below on Dryout Heat Flux," J. Heat Transfer, 109: 491 (May 1987).

59. Hoskins, M., and Lindsay, J. D., "Gamma-densitometry Measurements of Saturation Gradients During Boiling in Fibrous Media," A190 Project, The Institute of Paper Science and Technology, Atlanta, Georgia (in progress, 1991).

60. Tung, V. X., and Dhir, V. K., "A Hydrodynamic Model for Two-phase Flow Through Porous Media," Int. J. Multiphase Flow, 14(1): 47-65 (1988).

61. Lipinski, R. J., "A Model for Boiling and Dryout in Particle Beds," NUREG/CR-2646, Sandia National Laboratories, Albuquerque, NM, June 1982.

62. Lindsay, J. D., "Experimental Evaluation of Displacement Dewatering," AIChE Annual Meeting, Chicago, Nov. 1990.

63. Lampinen, M. J., "Mechanics and Thermodynamics of Drying," Drying '80, ed. A. S. Mujumdar, Hemisphere, Washington, D. C., 1980.

64. Gillespie, T., "The Spreading of Low Vapor Pressure Liquids in Paper," J. Colloid Science, 13: 32-50 (1958).

65. Gillespie, T., "The Capillary Rise of a Liquid in a Vertical Strip of Filter Paper," J. Colloid Science, 14: 123-130 (1959).

66. Wyckoff, R. D., and Botset, H. G., J. Appl. Phys., 7: 325 (1936).

67. MacGregor, M. A., "Wet Pressing Research in 1989–An Historic Perspective, Analysis and Commentary," Transactions of the Ninth Fundamental Research Symposium Held at Cambridge: Sept. 1989, ed. C. F. Baker, Mechanical Engineering Publications, Ltd., London, 1989.

68. Crouse, B. W., and Warner, C. L., "Mechanistic Aspects of Edge Wicking," 1986 Papermakers Conference, Tappi Press, Atlanta, GA, 1986.

69. Windle, W., Beazley, K. M., and Climpson, M., "Liquid Migration from Coating Colors. II. The Mechanism of Migration," Tappi J., 53(12): 2232-2236 (1970).

70. D. H. Horstmann, J. D. Lindsay, and R. A. Stratton, "Using Edge-Flow Tests to Examine the In-Plane Anisotropic Permeability of Paper," Tappi J. (in press, 1991).

71. Hamlen, C., Chem. Eng. Dept. and Minnesota Supercomputer Inst., Univ. of Minnesota, Minneapolis, MN, personal communication, 1991.

72. Back, E. L., "The Pore Anisotropy of Paper Products and Fibre Building Boards," Svensk Papperstidning, 69: 219 (1966).

73. Dullien, F. A. L., "Porous Media: Fluid Transport and Pore Structure," Academic Press, New York, 1979, chapter 6.

74. Verma, A. K., "Effects of Phase-Transformation on Steam-water Relative Permeabilities," Ph.D. Dissertation, Univ. of California, Berkeley, CA, 1986.

75. Vogel, T., and Cislerova, M., "On the Reliability of Unsaturated Hydraulic Conductivity Calculated from the Moisture Retention Curve," Trans. Porous Media, 3: 1-15 (1988).

76. Rudemiller, G.R., "A Fundamental Study of Boiling Heat Transfer Mechanisms Related to Impulse Drying," Doctoral Dissertation, The Institute of Paper Science and Technology, Atlanta, GA (1989).

77. Adams, K. L., Russel, W. B., and Rebenfeld, L., "Radial Penetration of a Viscous Liquid into a Planar Anisotropic Porous Medium," Int. J. Multiphase Flow, 14(2): 203-215 (1988).

78. Kuo, Wen-Ling, "The Kinetics of Normal-Through Drying of Paper with Air," Ph.D. Thesis, Chem. Eng. Dept., Polytechnic Institute of Brooklyn, 1965.

79. Geraets, J. J. M. and Borst, J. C., "A Capacitance Sensor for Two-Phase Void Fraction Measurement and Flow Pattern Identification," Int. J. Multiphase Flow, 14(3): 305-320 (1988).

80. Bear, J., "Dynamics of Fluids in Porous Media.," American Elsevier, New York, NY, 1972, p. 477.

81. Robertson, A. A., "Investigation of the Cellulose-Water Relationship by the Pressure Plate Method," Tappi J., 48(10): 568 (Oct. 1965).

Project Title: X-Ray Studies of Web Consolidation
Project Number: 3480
Project Staff: Cyrus K. Aidun
IPST Goal: Develop a novel technique for direct visualization and measurement of web consolidation.

OBJECTIVES:

Investigate the feasibility of using the flash x-ray technique for measurement of sheet deformation in a roll press.

SUMMARY OF RECENT PROGRESS:

- The final report for this project, including the final conclusions, is presented below.
- The results have been published at the Annual AIChE Forest Products Meeting [1].

CONTENTS

I. INTRODUCTION

Web consolidation theories currently available are mainly based on indirect measurements and speculation. In this project, we use the flash x-ray imaging in conjunction with image analysis techniques to generate direct results on the fluid flow and property development in wet pressing and impulse drying. An image analyzer at the Institute will be used to obtain quantitative results on local sheet deformation, densification, and dewatering.

Wet pressing, impulse drying, or any other process which involves fluid flow in a deformable porous media share a common feature -- coupling between the fluid flow and the deformation of the medium. The technique we are using in this study allows direct measurement and analysis of this behavior. Detailed analysis of the relation between the sheet deformation (strain gradient in normal as well as lateral directions) and the fluid flow is the key to understanding and controlling the property development and dewatering behavior in web consolidation.

II. BACKGROUND:

When an inhomogeneous medium is exposed to x-ray radiation, components with different x-ray absorption coefficients will produce a contrast image. For example, a sheet of paper will absorb less radiation than a metallic sheet.

By placing small solid x-ray tracers (particles, fibers, or continuous wires) in a sheet of paper, we are able to capture their displacement before and after pressing. An exaggerated example is shown in Figure 3, where spherical metallic particles are sandwiched between several sheets. Because of reproduction of the image, the particles cannot be seen in Figure 3b; however, they can be seen in the original x-ray radiograph. A more realistic image is shown in Figure 4. Using the image analyzer, we then label each particle and measure its relative displacement in all directions. This information gives a direct measure of the local strain gradient tensor (i.e., local deformation in all directions). The local strain tensor and local hydraulic pressure can then be calculated. These results would be useful in understanding the dewatering mechanisms in wet pressing and web consolidation processes in general.

An experimental roll press has been designed and constructed for the flash x-ray studies. It consists of 6" diameter, 1" thick rolls with maximum operating speed of 300 ft/min. The value of the nip pressure is dependent on the thickness of the sheet and the felt. The relative positions of the x-ray unit with the rolls and the x-ray film cartridge are shown in Figures 1 and 2. The x-ray radiation source is a Hewlett-Packard Model 43733A flash x-ray unit.

a)

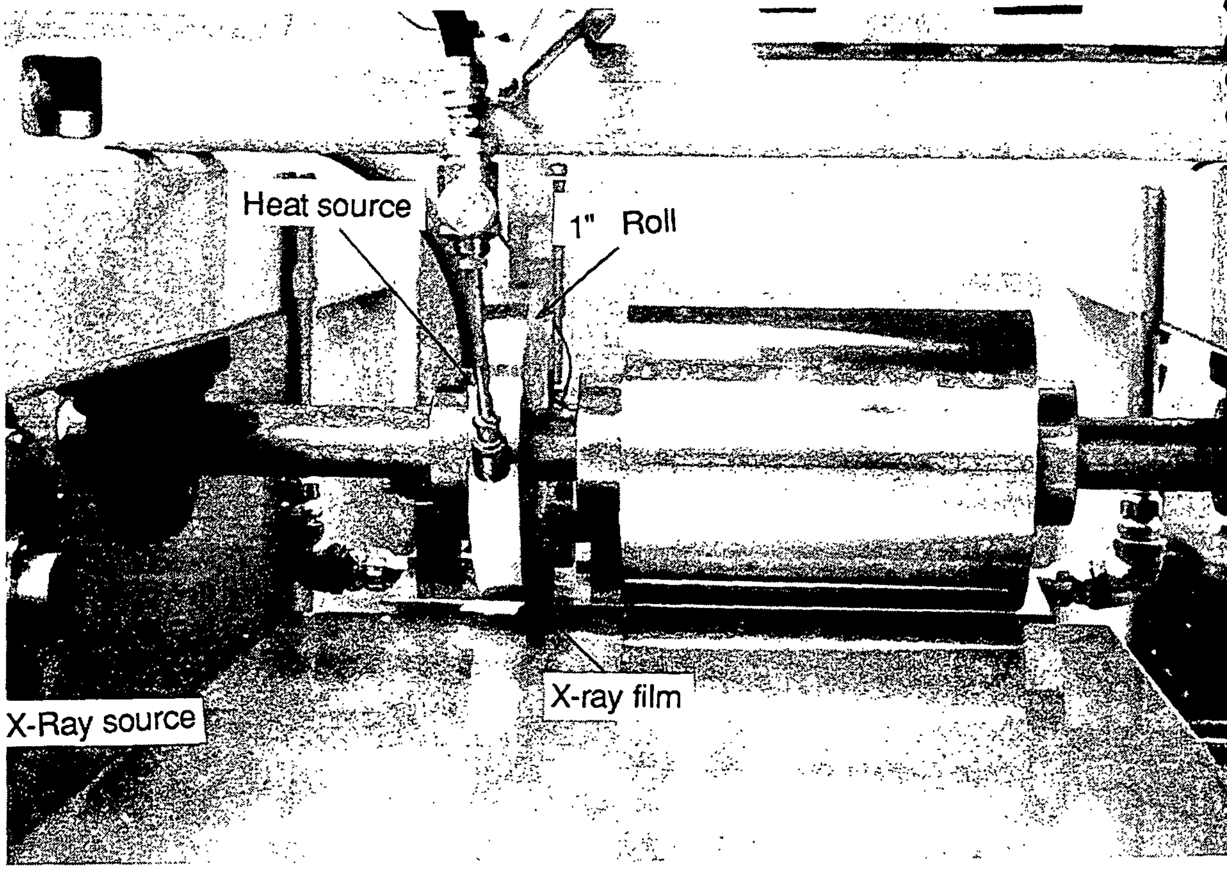

b)

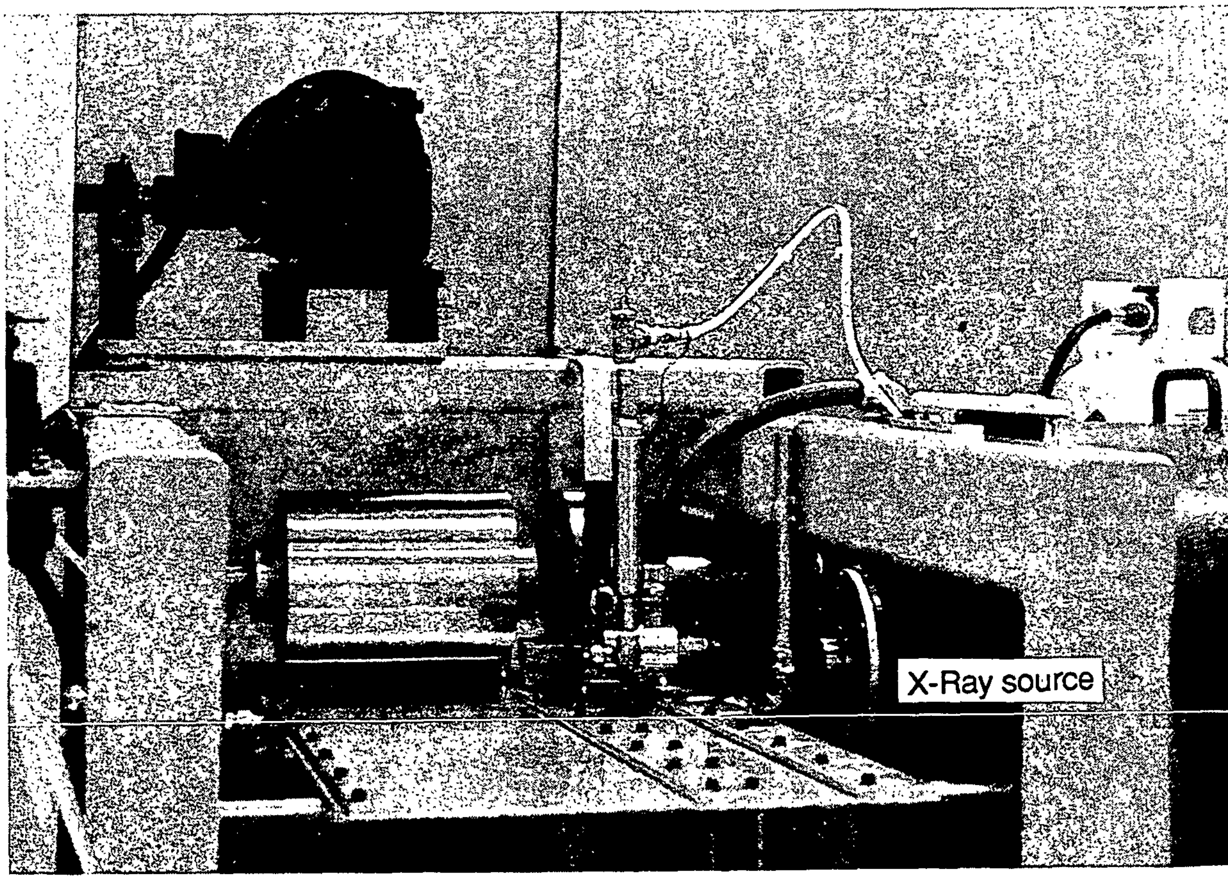

Figure 1. X-Ray Roll Press a) exit side b) entering side

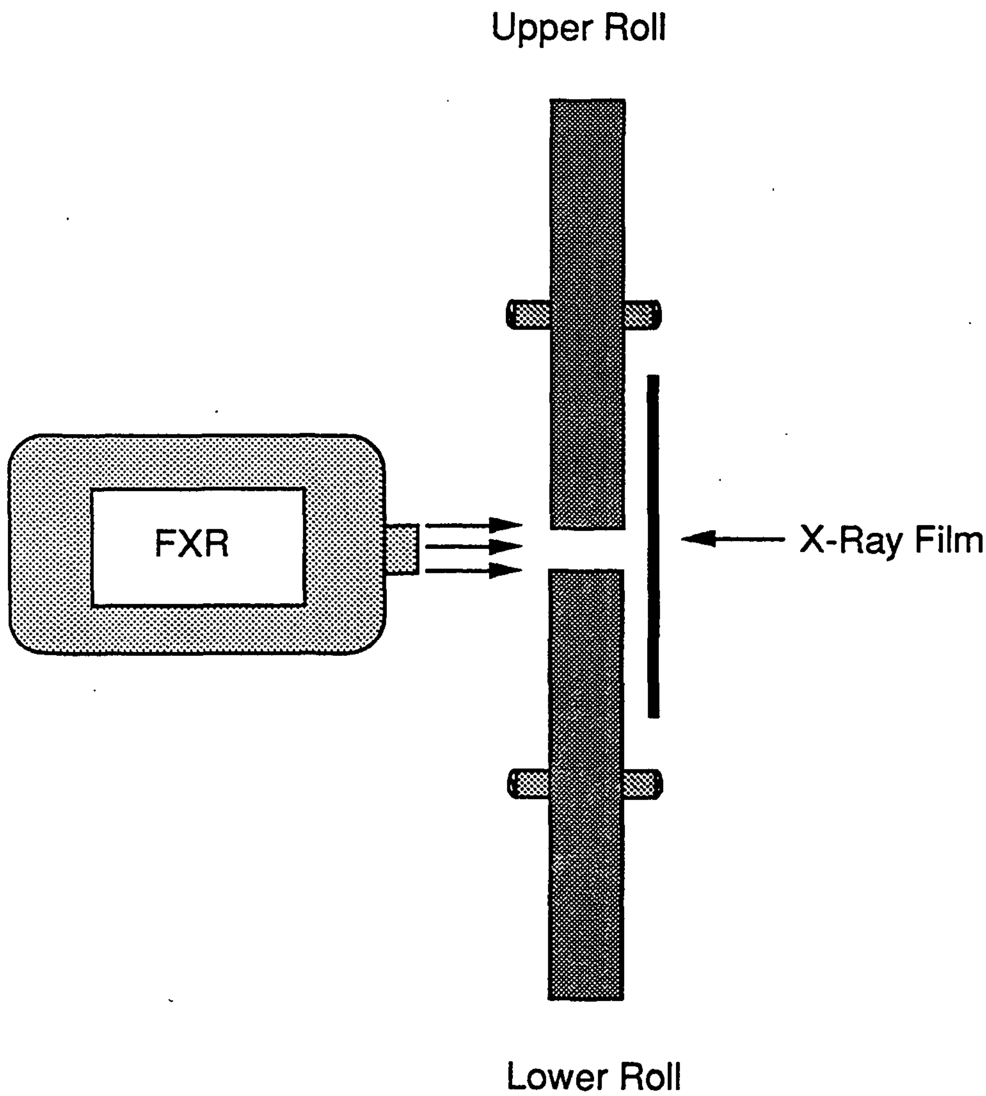

Figure 2. Schematic diagram of the relative position of the x-ray source, x-ray film, and the rolls.

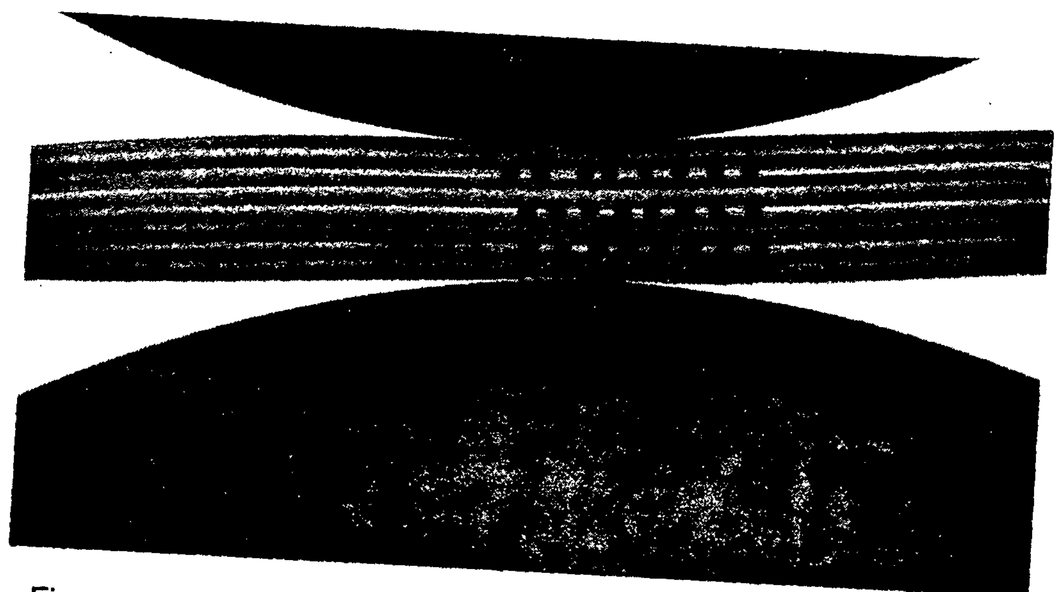

Figure 3a. Flash X-ray Radiograph of Target Particles (zero load)

Figure 3b. Flash X-Ray Radiograph of Target Particles (compressed)

Currently, the impulse drying simulations are possible by using a commercial propane soldering torch to heat the upper roll to a maximum temperature of 550°F. Either liquid silver nitrate could be applied directly on the surface of the sheet before it enters the nip or x-ray tracers (solid, liquid, or both) could be added to the sheet during forming.

For quantitative studies, we adopt the second approach, that is, x-ray tracers in the form of solid particles or fibers are carefully placed in the sheet. By recording their x-ray images before, during, and after the pressing process (be it wet pressing or impulse drying), we will be able to obtain direct quantitative results on local and directional sheet deformation and fluid flow.

Small spherical solid particles (20 to 100 microns in diameter), continuous thin wires (~ 25 microns), and metallic fibers (~ 25 microns in diameter, 1 mm long) have been used. An image analyzer is used to enhance the contrast in the x-ray image and assist in measuring the local deformation of the sheet. This process is demonstrated in Figures 4 and 5. The first figure is an x-ray image of tungsten particles in a sheet, and the second figure is the same picture when magnified and processed by the image analyzer.

The actual particles are smaller than their enhanced (in contrast) image in Figure 5. This is partly because of the relatively poor resolution of the x-ray film which causes a blurring effect. In actual measurements, the image analyzer will be used to pinpoint the center of mass of each particle and to measure their relative distance from each other and from the rolls.

Figure 6 shows the enhanced x-ray image of three 50-micron tungsten wires implanted in a sheet of paper (~ 30% solids). Here the wires are also much smaller than their enhanced image. Both continuous and discontinuous target fibers have been used in the measurements outlined in the next section.

DEFORMATION MEASUREMENTS OF INDIVIDUAL SHEETS IN WET PRESSING OF A MULTILAYER ARRANGEMENT

The purpose for this set of measurements is to show whether the current resolution of the system is sufficient for measuring local densification in a relatively heavy sheet. The main

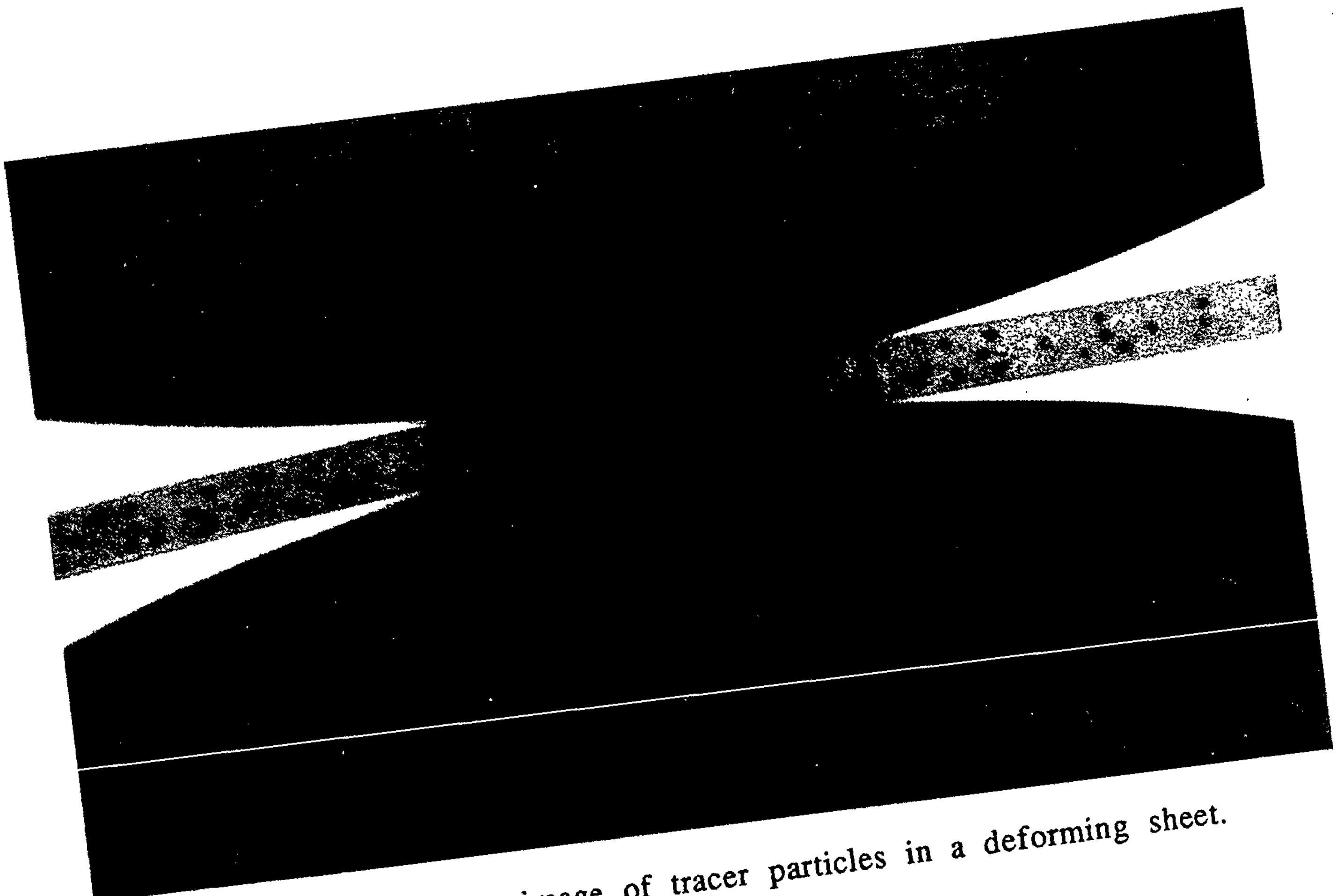

Figure 4. X-ray image of tracer particles in a deforming sheet.

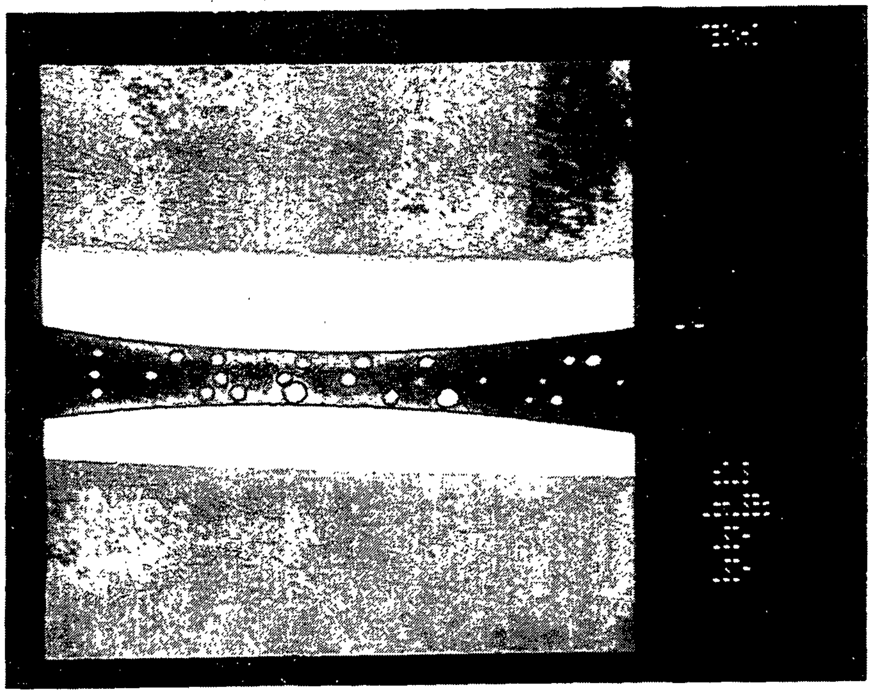

Figure 5. X-ray image of solid particle tracers in a sheet inside the nip of a roll press.

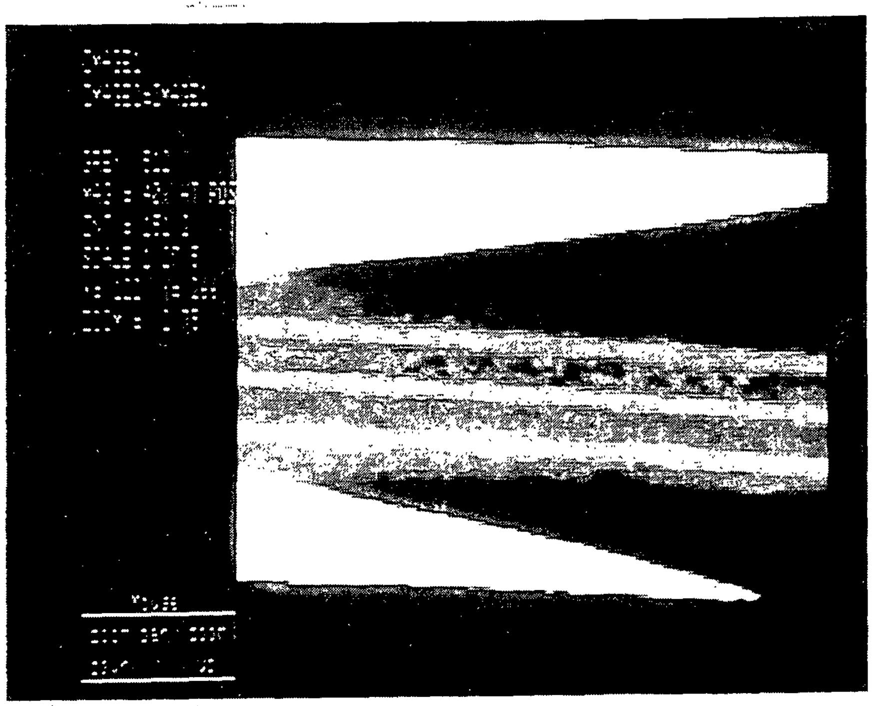

Figure 6. X-ray image of continuous tungsten wires in a sheet at the exit side of the nip.

(a)

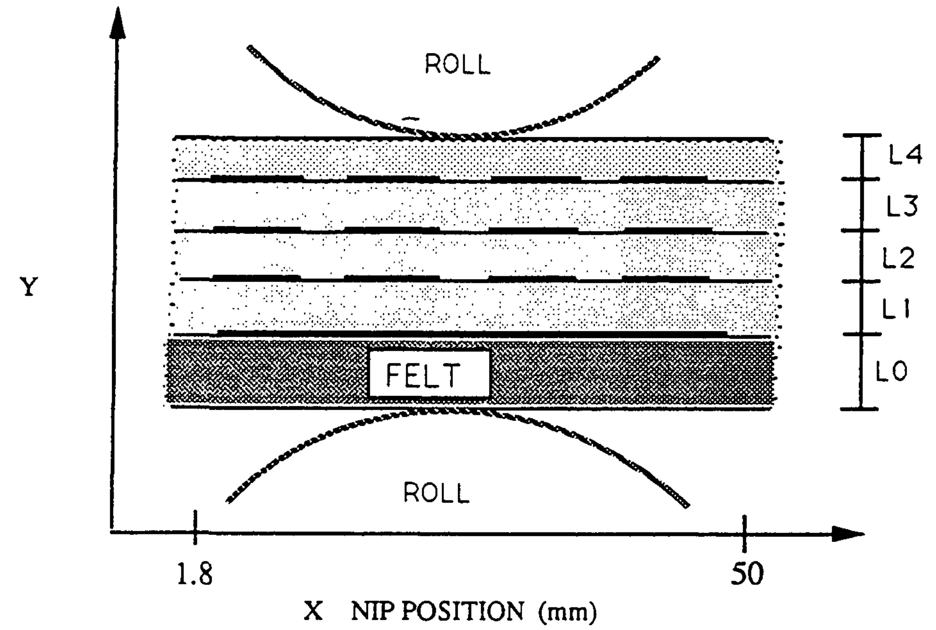

(b)

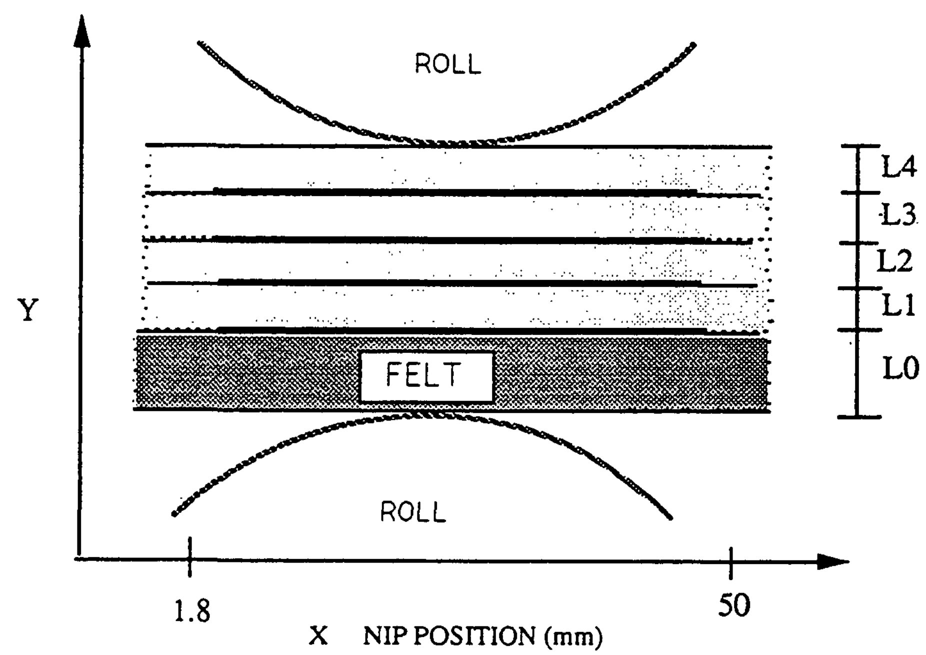

Figure 7. Schematic of the test samples.
4 layers of paper, L1 through L4, each with 150 g/m2 basis weight, 28% solids.
X-Ray shuts are at two different pressures, 50 and 60 psi. Roll press speed is at 17 ft/min.
Selection of axes for analyzing the x-ray films and the thickness measurements with the image analyzer are also shown. Targets : 50 microns, tungsten wires (99.95%) are located between the sheets in two different arrangements : (a) Discontinuous wires 5 mm long and 2 mm apart, and (b) Continuous wires 4 " long. Also a continuous wire is placed between the sheet and the felt in both sets.

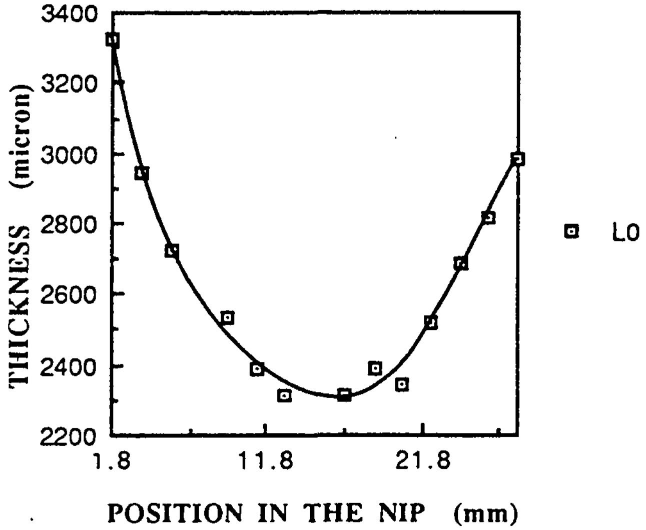

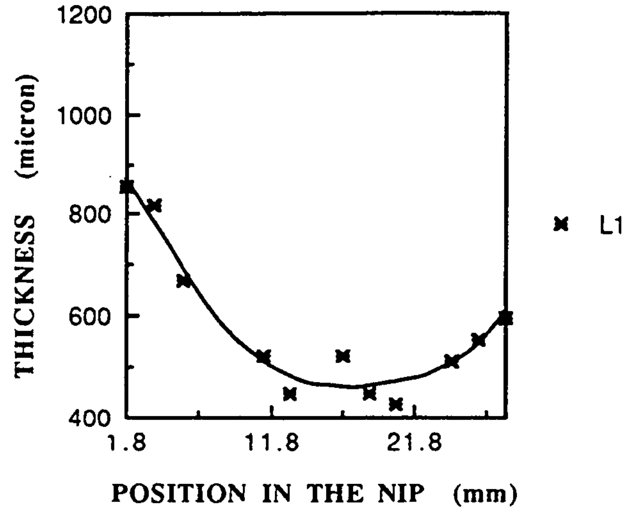

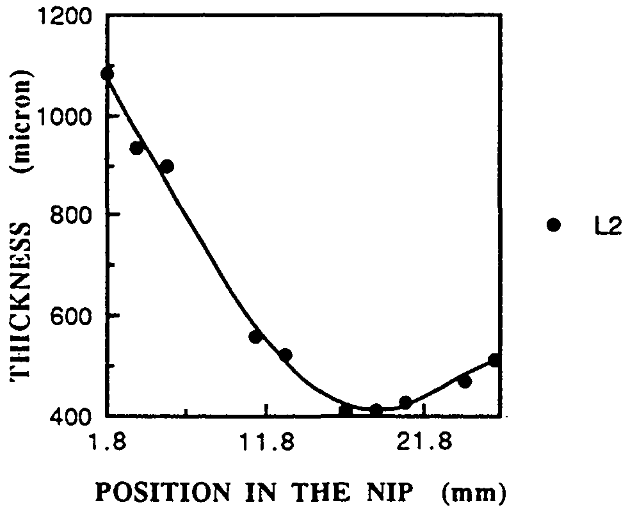

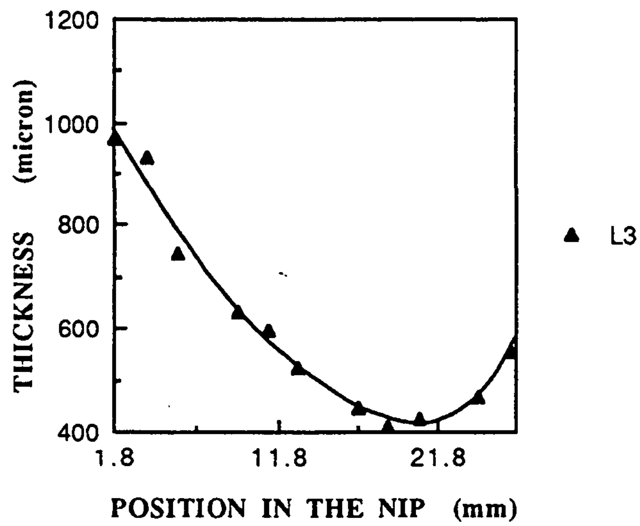

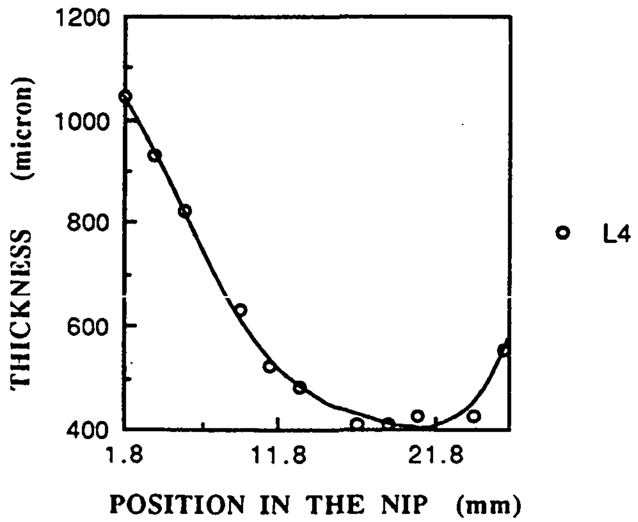

Figure 8. Thickness variation of individual free sheets in wet pressing at 60 psi, discrete target arrangement. For sample description, see Fig. 7a. Graphs show first half of the nip .

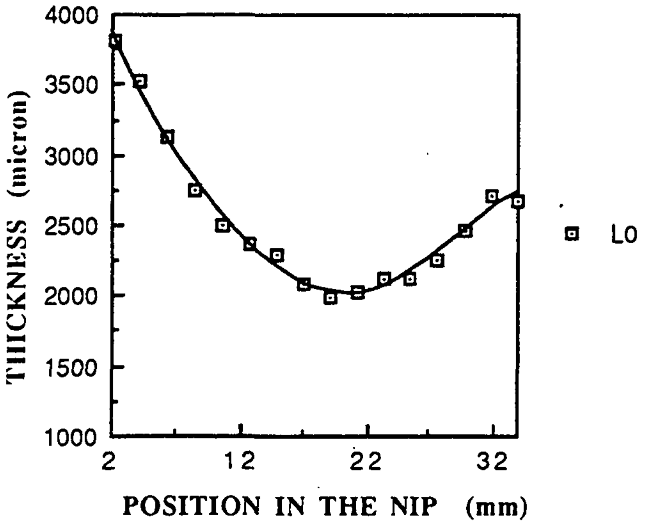

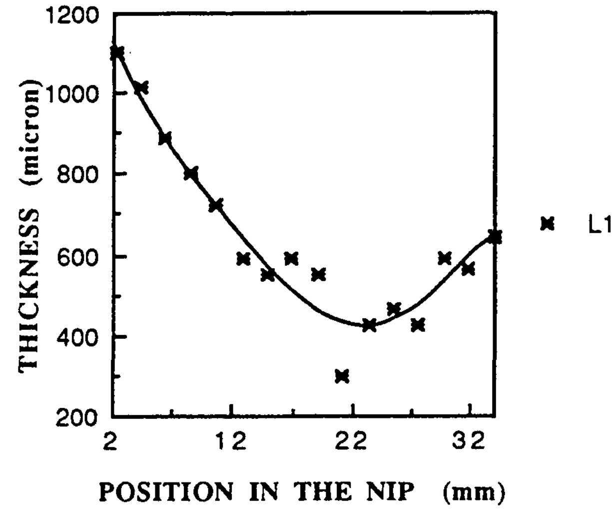

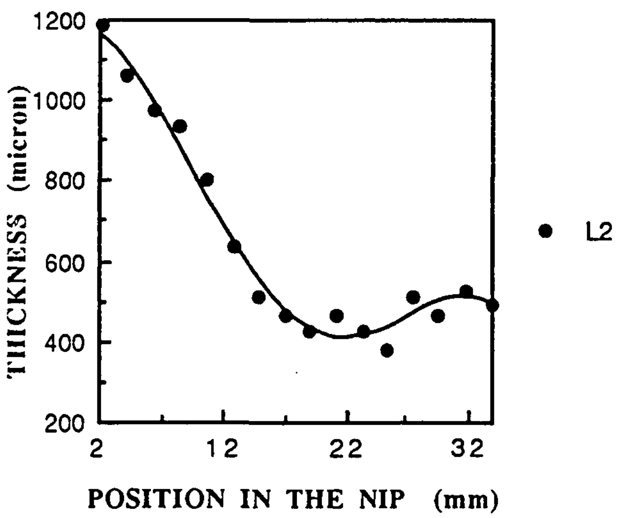

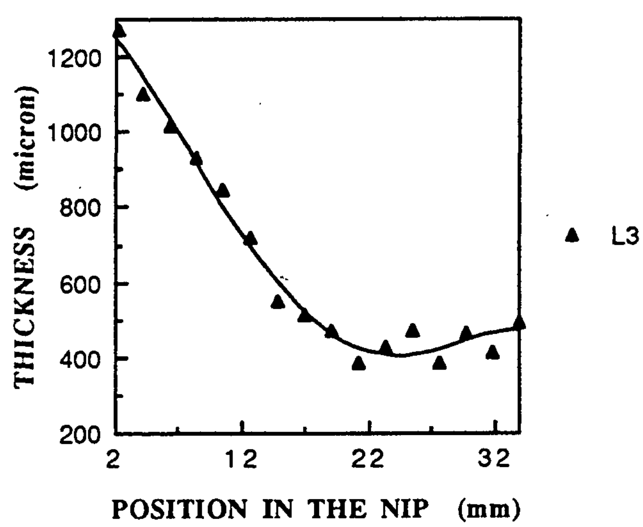

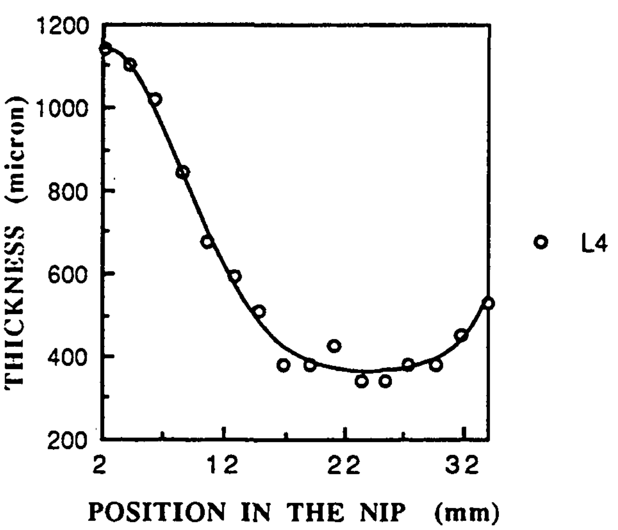

Figure 9. Thickness variation of individual free sheets in wet pressing at 60 psi, continuous target arrangement. For sample description, see Fig. 7b.

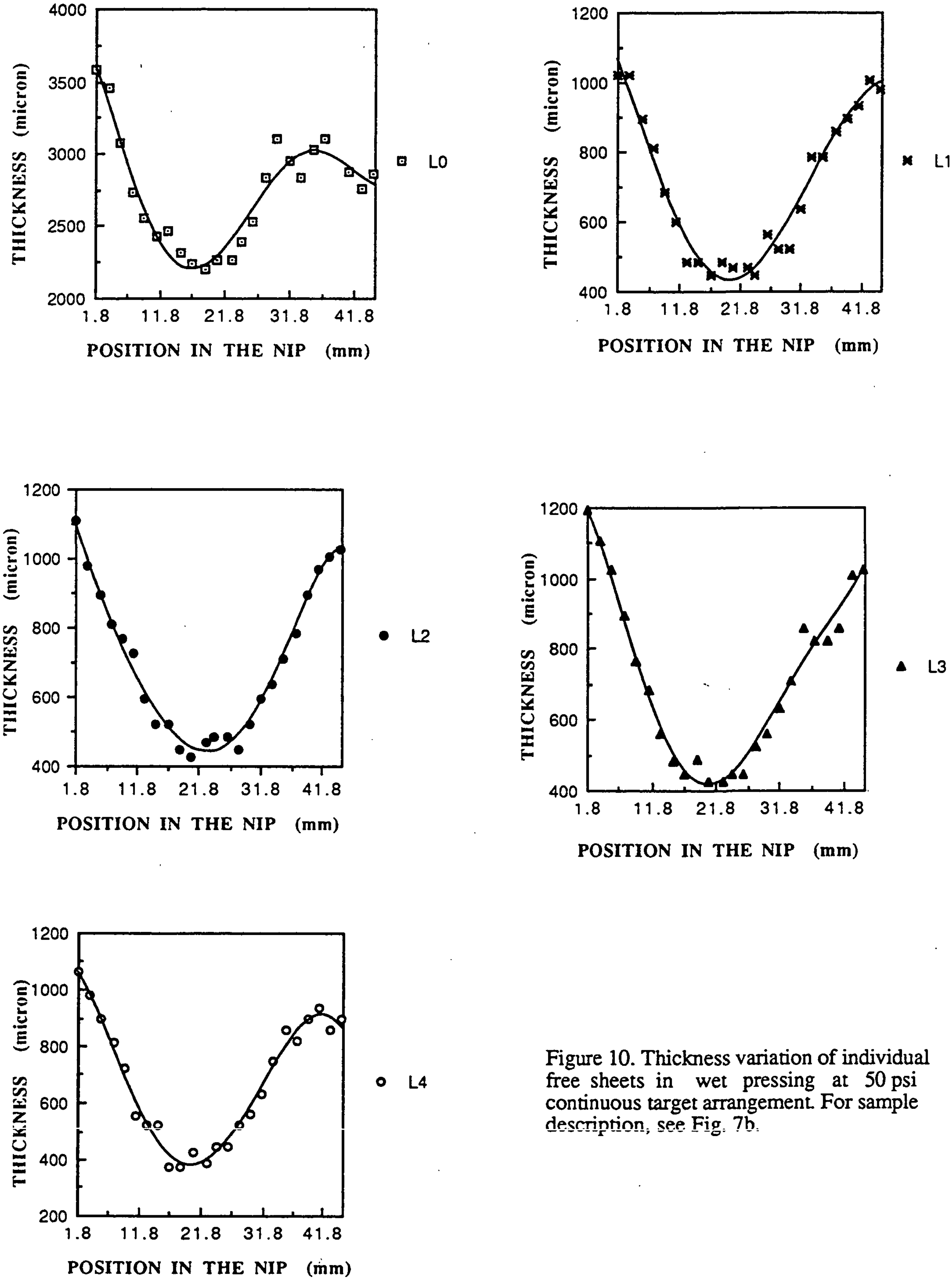

Figure 10. Thickness variation of individual free sheets in wet pressing at 50 psi continuous target arrangement. For sample description, see Fig. 7b.

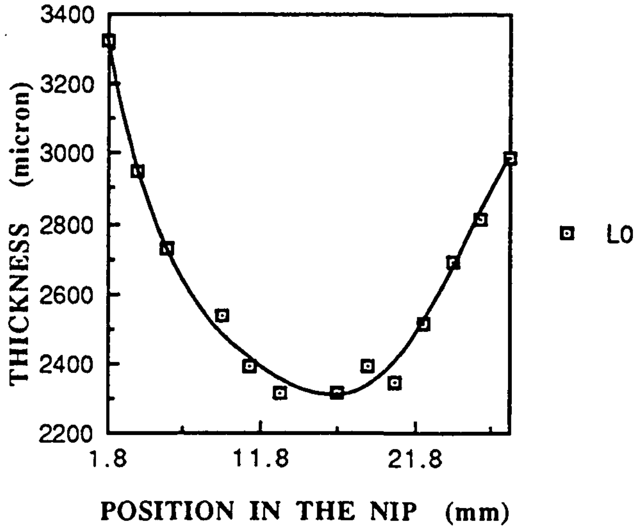

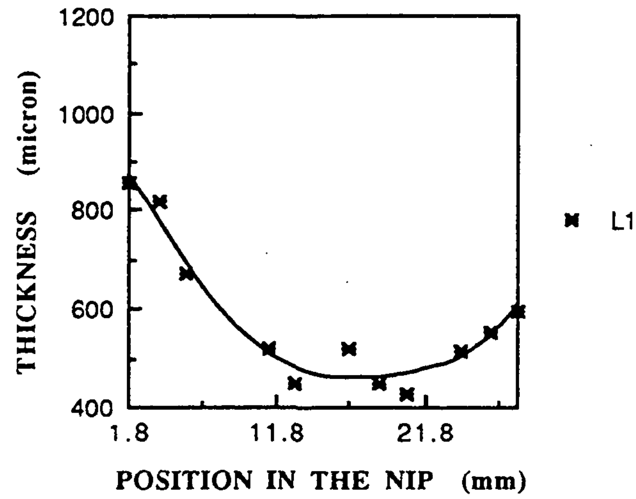

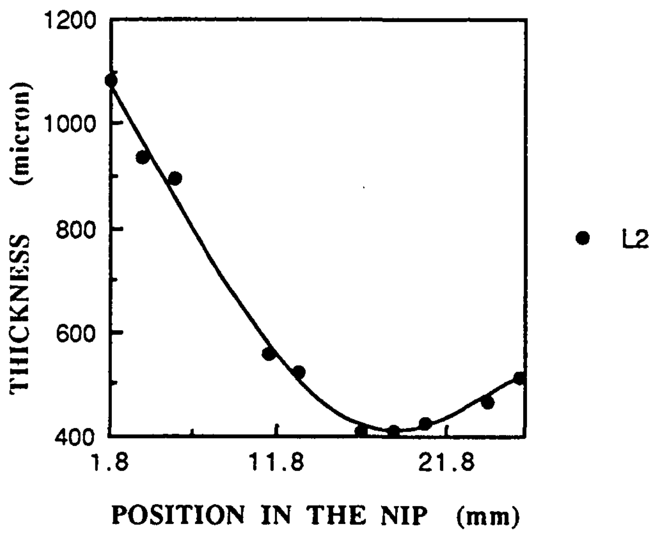

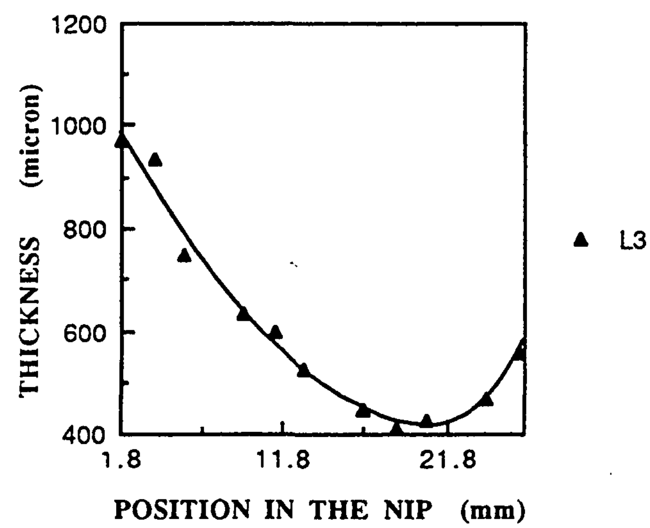

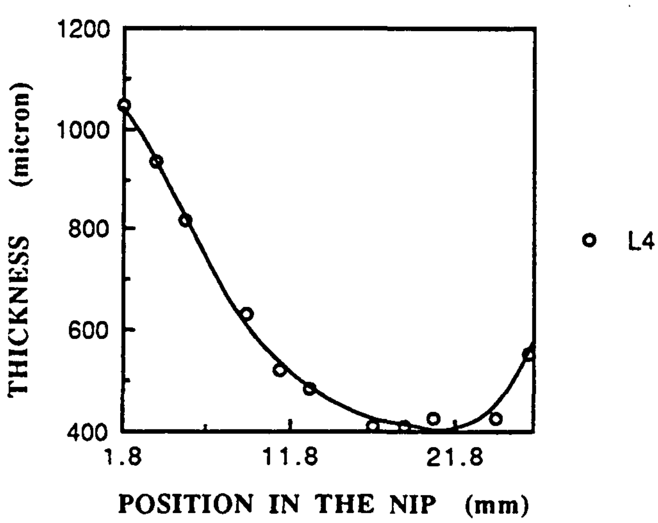

Figure 11. Thickness variation of individual free sheets in wet pressing at 50 psi, discrete target arrangement. For sample description, see Fig. 7a. Graphs show first half of the nip .

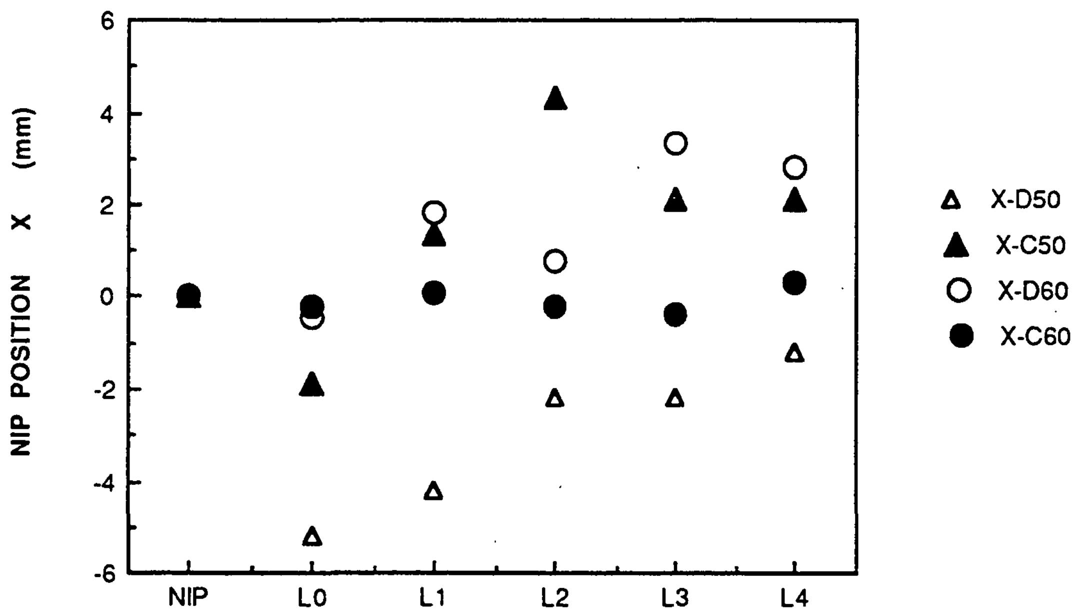

Figure 12. Location of the minimum sheet thickness relative to the mid-nip at 0.

investigators have over the phase-lag between the mid-nip and the maximum hydraulic pressure in pressing. Issues related to local densification profile at mid-nip can also be studied from the minimum thickness measurements of each layer as shown in Figures 13 and 14.

As stated before, the quantitative values of the current measurements cannot be related to single sheet pressing, since the samples were prepared by stacking four individual sheets on a felt. With this arrangement, the sheets can separate from one another just before or after the nip, and targets are also free to follow each adjacent sheet.

CONCLUSIONS

- The thinnest target wire which can be resolved inside a sample sheet is 50 μm in diameter.
- The resolution of the flash x-ray is not sufficient to measure deformations in single light-weight sheets.
- The technique can be used to study multi-layer sheet pressing of large basis weight sheets.

SIGNIFICANCE TO THE INDUSTRY

Even modest improvements in the dewatering processes are extremely important to capacity, drying energy reduction, better property development, and removing bottlenecks. Development of the techniques to understand the interaction between the fluid flow and the deformation of the porous network could lead to improved property control, enhanced dewatering, reduced drying energy and increased capacity.

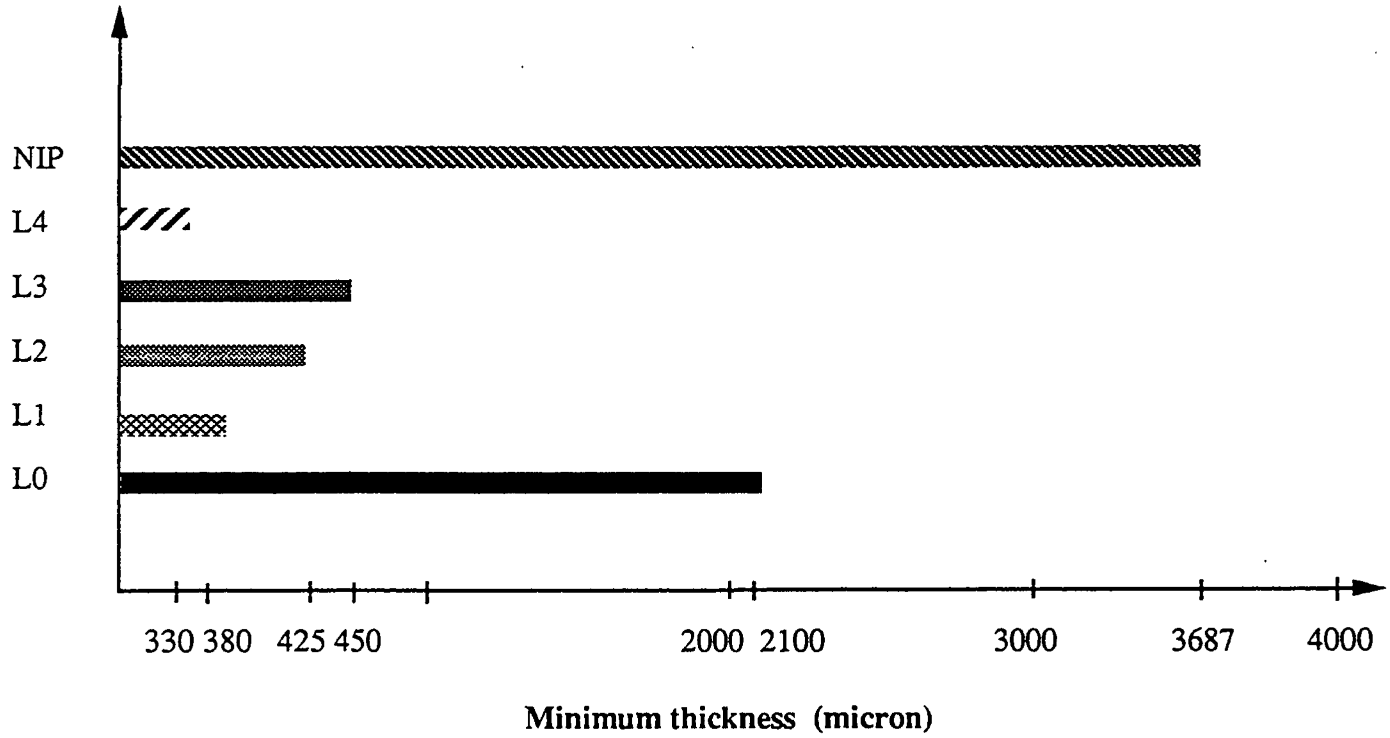

(a)

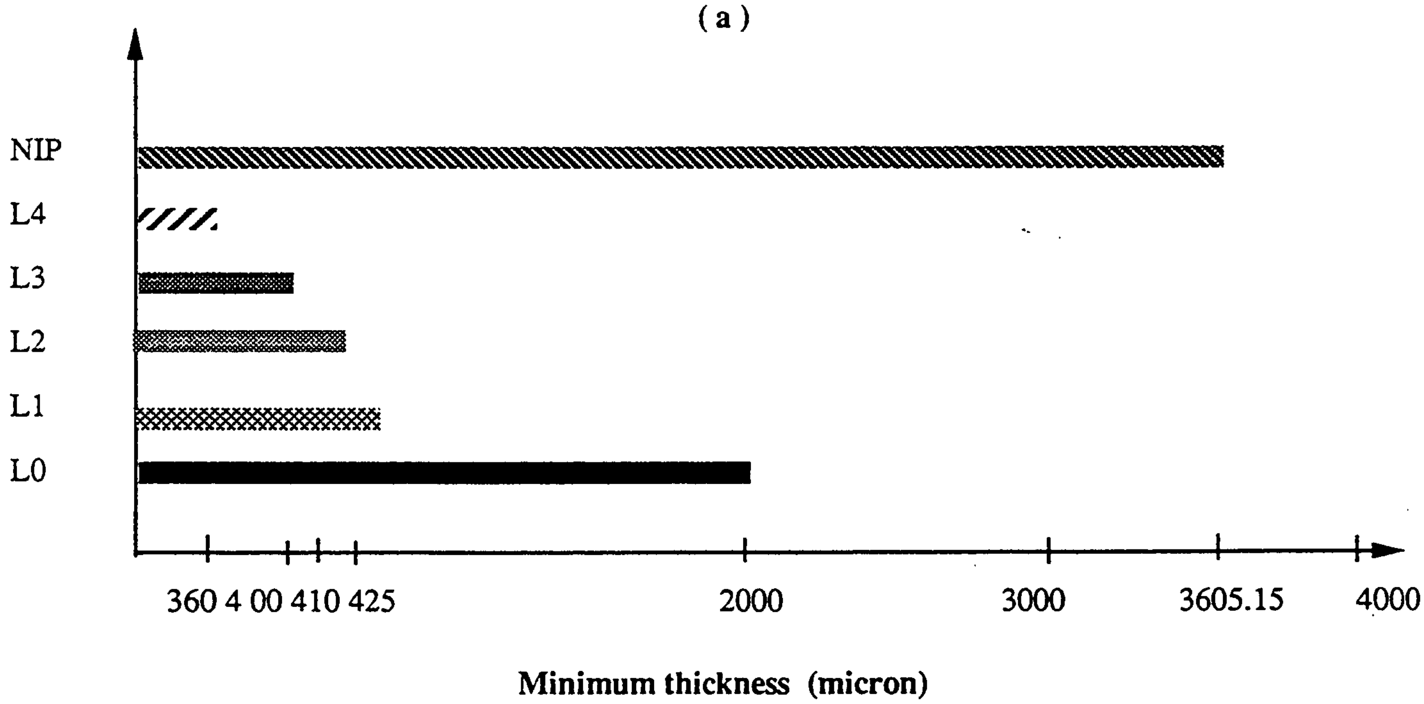

(b)

Figure 13. Minimum thickness of each individual sheet.
(a) Discontinuous wires at 60 psi and (b) Continuous wires at 60 psi.

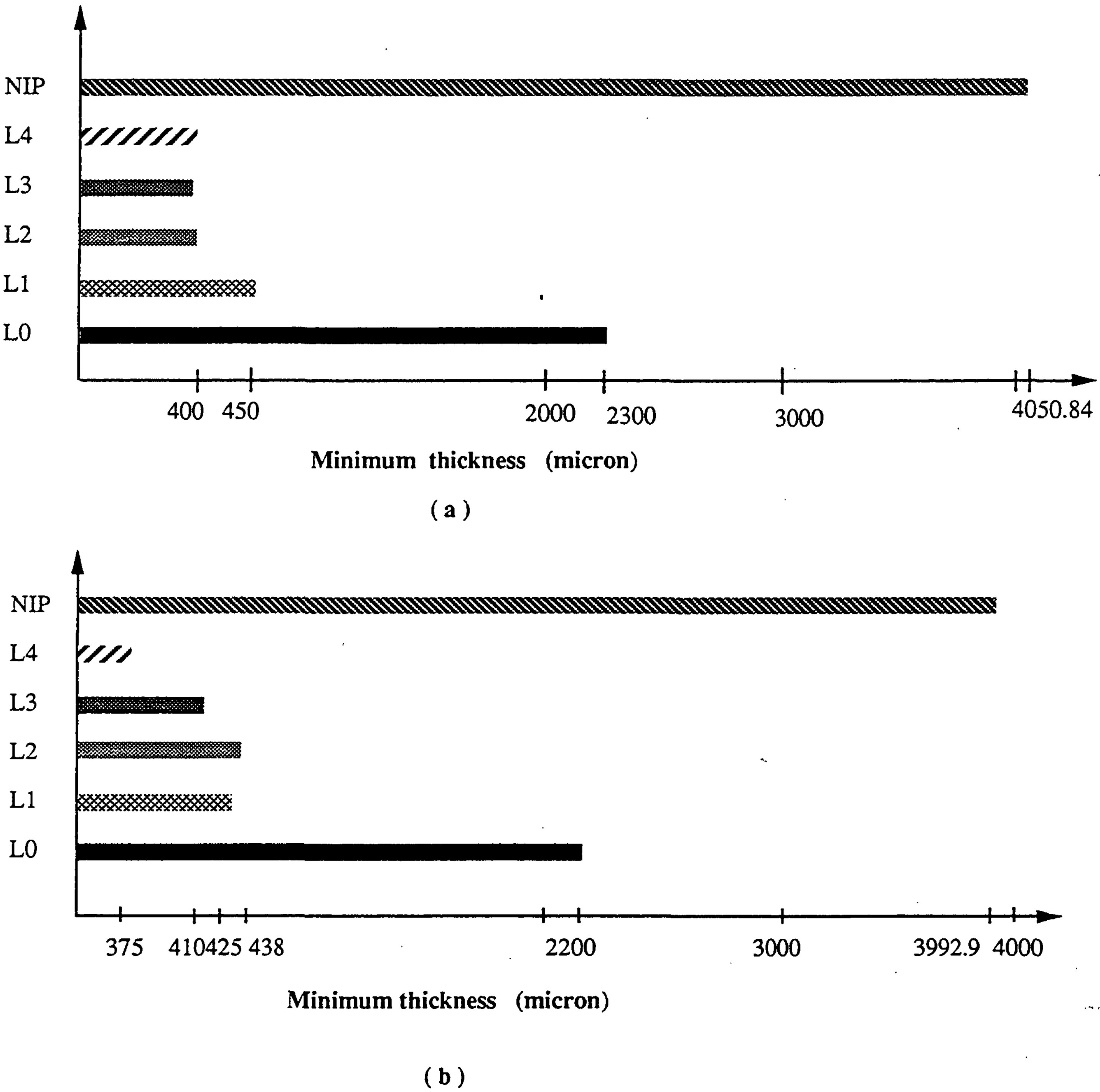

Figure 14. Minimum thickness of each individual sheet.
(a) Discontinuous wires at 50 psi and (b) Continuous wires at 50 psi.

REFERENCES

1. Aidun, C.K., "A Technique for Measurement of Local Deformation in Composite Sheet Pressing," presented at the 1990 Annual AIChE Meeting, Nov. 11-16, 1990.

2. Burns, J.R., Conners, T.E., and Lindsay, J.D., "Dynamic Measurement of Density-Gradient Development During Wet Pressing," *TAPPI J.*, April 1990.

FUNDAMENTALS OF COATING SYSTEMS

STATUS REPORT

FOR

PROJECT 3674

April 4, 1991
Institute of Paper Science and Technology
Atlanta, Georgia

PROJECT SUMMARY FORM

Project Title:	Fundamentals of Coating Systems
Project Number:	3674
Project Staff:	Cyrus K. Aidun
Fiscal Budget:	$100,000
IPST Goal:	Develop the technological foundation for the design of the next generation of high-speed coaters.

OBJECTIVES:

(1) To investigate the cause and origin of coat weight nonuniformities reported in high-speed blade coating of paper and board; (2) to explore novel coating systems for application of a more uniform coat weight profile at higher machine speeds.

RECENT PROGRESS:

- Initial studies of a hot-film anemometer system for measuring the dynamics of coating colors in pilot and full-scale systems have been completed. A flow loop for calibration of this system is constructed and calibration curves for isothermal systems are obtained.

- A cavity with variable aspect ratio ($0 > S/D > 10$) has been designed, built and installed for measuring the influence of geometry on the critical machine speed for the onset of time dependent flow in the pond of short-dwell coaters. The system is currently being tested for leakage and other operational defects.

- The computational fluid dynamics analysis of the short-dwell coater has been extended to include the free-surface flow at the blade and the rheological properties of the coating color. The pressure field, shear rate, and viscosity have been computed for one set of parameters using the Carreau model.

- A new coater is being designed for superior performance. The flow field in an initial design has been obtained and design modifications are in progress.

- The roll coating simulator has been modified in order to obtain accurate quantitative measurements of flow rate and the critical speed for the onset of coat-weight nonuniformities. A complete data acquisition system has been added along with digital speed control and an accurate (<0.5% error) on-line flow meter. The critical roll speed for the onset of unsteady state flow has been measured as a function of fluid viscosity and net mass flow rate using the new system with a fixed span-to-width aspect ratio (S/D = 3/1) cavity.

- A proposal is submitted to the Chemical Sciences Division of the National Science Foundation for global stability analysis of flow in a cavity simulating the pond of a short-dwell coater. A proposal is also submitted (with H-C. Chang, U. Notre Dame) to TAPPI for air entrainment studies.

CONTENTS

1. INTRODUCTION

Short-dwell coaters (SDCs) enjoy several advantages over roll applicators. Contrary to roll coaters where frequent breaks occur at high speed (particularly with light weight papers), SDCs do not exhibit this problem; they are compact and easy to operate. In practice, at high machine speeds SDCs experience runnability problems when the machine speed exceeds a certain limit. Surface nonuniformities are the main obstacles which limit the maximum machine speed for high solids concentration in the coating color. We have shown in previous reports [1-7] how the rheological properties coupled with the flow instabilities in various regions of the system play an important role in creating these limitations.

In high-speed blade coating, surface nonuniformities can appear in the form of streaks and/or regions of high and low wet film thickness in MD and/or CD. Nonuniform structures, where the length scale is the same order of magnitude as the fluid/substrate contact region, are categorized as macroscale. There are also problems with "randomly" spaced variations in surface coat weight which have small length scale characteristics and are independent of the base paper formation. Examples of nonuniformities are shown in Figure 1.

Conclusions from recent pilot coater trials are analyzed and presented in the next section. A possible explanation of the dynamics of the pilot coater trials with the short dwell coater is presented in reference [3].

In a previous meeting, we showed that the time-periodic motion of fluid inside the puddle of a coating system can result in chaotic solid particle trajectories [4]. We have proved this claim by calculating the appropriate measures of the rate of divergence of neighboring particles (Lyapunov exponents).

In addition to flow instability and nonuniformities in coat weight distribution, most high-speed coating systems suffer from an additional constraint - air entrainment at the contact line between the coating liquid and the substrate. Some new results were presented in the previous reports [4].

The connection between the fluid dynamics in the pond and the appearance of streaks needs to be further explored. Dynamic interaction between the eddies inside the pond with the wetting line at the overflow baffle shall be further investigated.

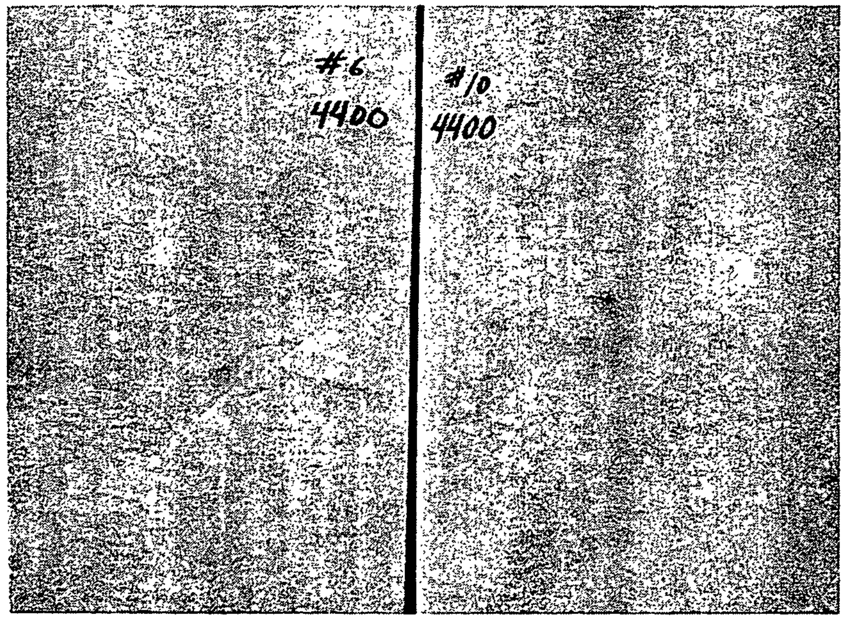

(a)

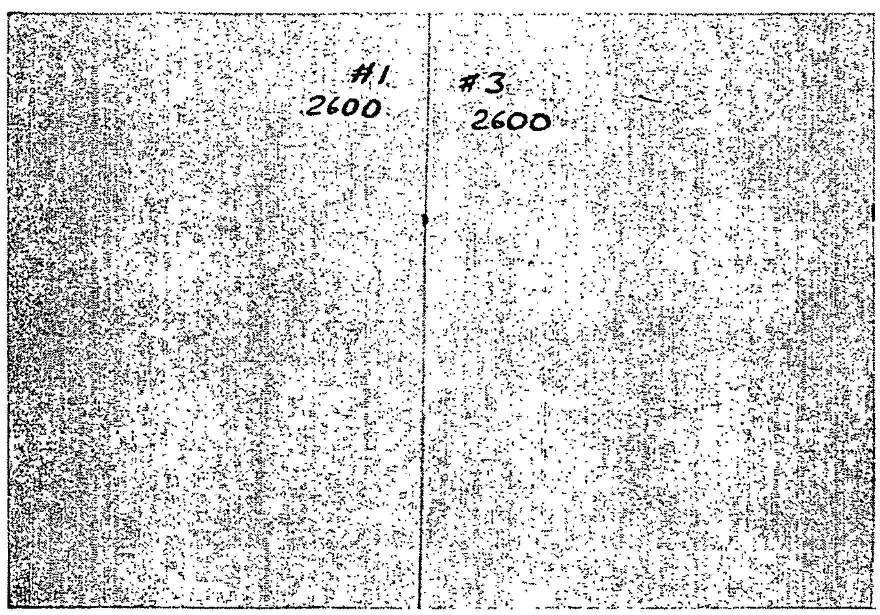

(b)

Figure 1. Macroscale and microscale nonuniformities in coat weight (or solids content) distribution for a LWC paper coated at (a) 4,400 fpm and (b) 2,600 fpm machine speeds.

Section 2 presents new quantitative measurements of the critical roll speed for the onset of time-periodic flow with the mass flow rate as a varying parameter. Also, the effect of small nonuniform blade deflection in CD due to nonuniform normal stress caused by flow instability in the pond is examined below (section 3).

2. NONUNIFORMITIES IN BLADE COATING

High aspect ratio clay particles (e.g., delaminated English China clay) in coating color provide a relatively superior surface quality for printing purposes. However, problems due to coat weight (CW) nonuniformities prevent application of these coating formulations at high solid levels (>58%) and desired machine speeds (~5000 fpm). In general, with short-dwell coaters (perhaps the most favorable system for light weight coated products, i.e., <12 gsm) application of highly viscous colors will result in macroscopic nonuniformities in the cross-machine direction (CD). These nonuniformities appear in the form of visible streaks which run along the machine direction. These streaks signify regions (patches) of high and low coating weight concentration on the surface of the paper.

Through systematic pilot coater trials (at Beloit Corp.), we are documenting the influence of various parameters on the onset and severity of the CW nonuniformities. Laboratory experiments (at IPST) provide the fundamental physical information required to pinpoint the origin of this problem. The complete results from the pilot coater trials and laboratory experiments to date are presented in various reports [1-6].

3. MORE CONCLUSIONS FROM PILOT COATER TRIALS

The ongoing pilot coater trials are adding to our understanding of the general behavior of pigment coating with contact application systems. A number of conclusions are listed below:

- The comparable length scales between the flow patterns and the streaks suggest that a connection exists between the coat weight nonuniformities on the web and the instabilities in the flow upstream of the blade.

- Trials with various formulations show that streaks appear regardless of the particle aspect ratio and concentration.

- Reducing the color viscosity increases the critical machine speed for the onset of streaks.

4. NEW QUANTITATIVE RESULTS FROM LABORATORY EXPERIMENTS

Previously, the experimental facilities could only be used to obtain a qualitative understanding of the coating process. In addition to this, it was recommended that accurate quantitative measurements of the stability bounds and flow parameters would also be of use to the industry. Therefore, during the last period, major modifications were made to allow more accurate quantitative measurements of the operational parameters in the experiments. These modifications include a digital speed control unit, an accurate flow meter, and a complete data acquisition system (Fig. 2).

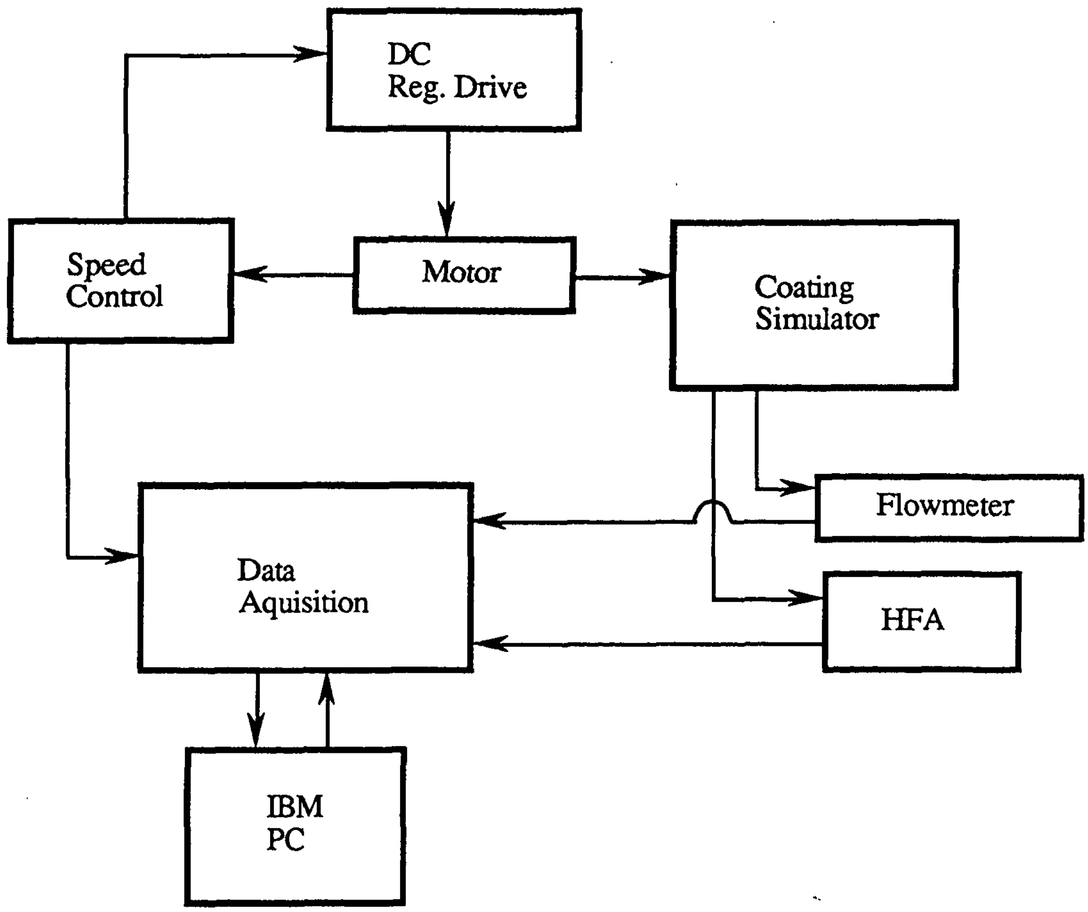

Fig. 2. Coating Simulator Facility.

The critical machine speed, V, for the transition from steady state to an unsteady flow in the cavity is measured as a function of fluid viscosity and the net mass flow rate, m, in a 3:1:1 aspect ratio cavity. The objective is to investigate whether the magnitude of the through-flow has any significant influence on the critical speed for the onset of time dependent flow in the pond of a short-dwell coater (Newtonian model fluids were used in these initial measurements). The data are plotted in Fig. 3 using two nondimensional parameters: (1) the cavity Reynolds number, $R=VD/\nu$, where ν and D are the fluid kinematic viscosity and the cavity depth (5.08 cm), respectively; and (2) the through-flow Reynolds number,

$R' = \frac{m}{S\,\mu}$, where S and μ are the cavity span (15.24 cm) and the dynamic viscosity of the fluid, respectively. The data show that at this small rate of through-flow, the effect of R', on the critical roll speed is insignificant. The effects of new mass flow rate at higher values of R' which includes flow through the overflow baffle, will be investigated in future experiments.

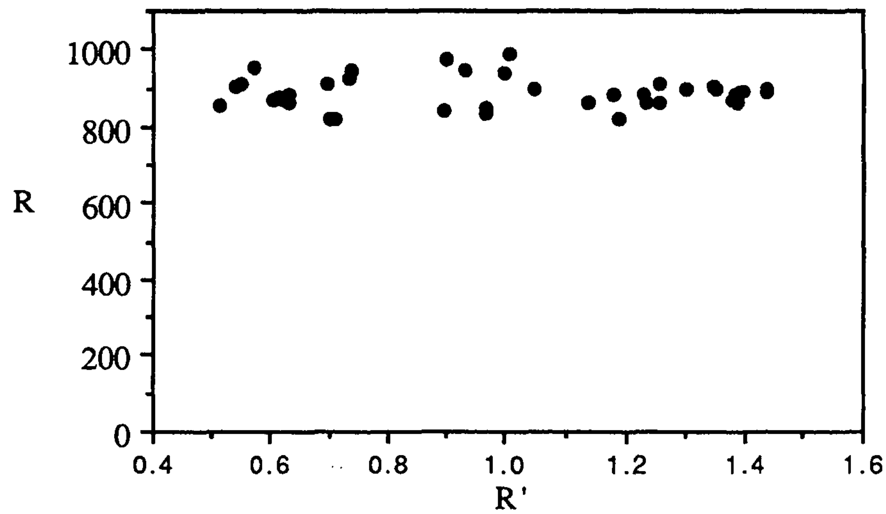

Figure 3. The critical cavity Reynolds number for transition to time-dependent flow as a function of through-flow Reynolds number.

5. HOT-FILM ANEMOMETER

We are currently in the process of adding Hot-Film Anemometer (HFA) to this system for velocity measurements of flow inside the cavity. In contrast to optical methods (e.g., LDA), this technique can be applied to opaque fluids such as coating colors. Once the HFA system is fully implemented in our laboratory experiments and its signal behavior fully understood and documented with transparent model fluids, it will then be used in conjunction with a pilot coater to study the behavior of actual coating systems in industrial operations. The HFA signal is sensitive to any changes in temperature. A thermocouple is being installed adjacent to the HFA probe to correct the signal for variations in temperature. A master calibration data base will be constructed and stored as reference for future measurements.

The equipment used in calibrating the hot-film anemometer consists of an eleven foot, 3/4-inch diameter Plexiglas pipe mounted to an optical bench. Before the pressure drop measurements, an entry length of four feet is allowed. The length between the two pressure ports, P1 and P2, is five feet. The pressure differential transducer used in this experiment is a Schaevitz model P-3091 which provides a DC output voltage linearly proportional to applied pressure. Recording the pressure difference across the pipe is necessary since the pressure difference is linearly proportional to shear stress by the equation for steady flow in a circular pipe given by

$$\tau = r\Delta p/2\iota$$

where r, radius of the pipe; and

ι, distance between the two pressure ports, P1 and P2.

Halfway between P1 and P2 we have installed a TSI model 1237 standard flush-surface hot-film sensor. The hot-film sensor, which is perfectly flush with the inside tube wall, is .005 by .04 inches in size. The output signal from the hot-film sensor is received by a TSI Model 1750 constant temperature anemometer. The main purpose of the temperature anemometer is to transmit high level signals from the hot-film sensor into a voltage signal, which can be measured on any chart recorder. The hot-film anemometer system operates on a +15 VDC (.7 amps) power supply. The probe which holds the hot-film sensor is 3.2 mm in O.D. and is designed to be mounted flush with a surface or wall where the flow is perpendicular to the axis of the probe body. The collected data from the hot-film anemometer are recorded in millivolts on a chart recorder.

During the calibration experiment, the pressure difference across the pipe and the shear stress reading from the hot-film anemometer are recorded during each change in temperature of the fluid. The temperature of the fluid steadily increases from 20 ºC to 25 ºC and readings are taken in increments of .2 ºC. The temperature readings are taken from the main tank which houses the fluid being pumped into and out of the pipe. It is assumed that the local temperature at the hot-film sensor is equal to the temperature of the fluid at the main tank. After all readings are taken, the actual shear stress, τ, is calculated from the given equation and plotted versus the hot-film sensor reading in millivolts (figures 4 and 5). Graphs need to be plotted for every change in temperature since the hot-film sensor varies linearly with temperature. Since temperature change is proportional to both shear stress and viscosity of the fluid, it has been found experimentally that as temperature increases, shear stress decreases. The main purpose of these calibration graphs is to accumulate a reference data base. The hot-film anemometer can then be used to measure the shear stress at the walls of coaters or other hydrodynamic systems such as headboxes.

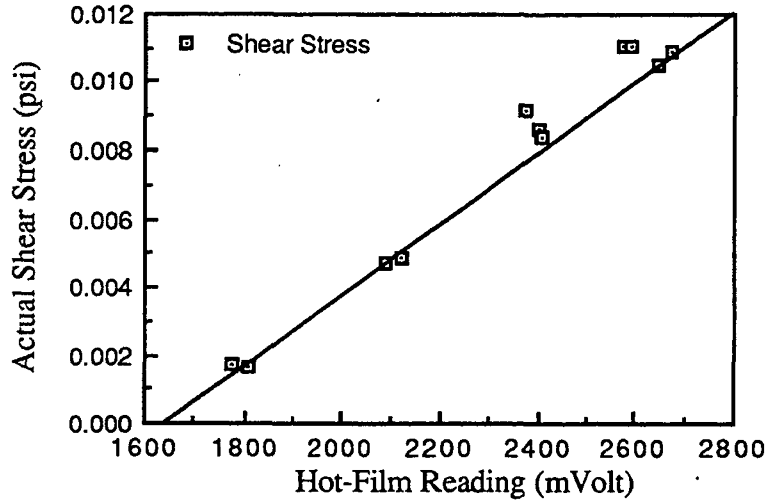

Figure 4. Hot-film calibration data at 20ºC

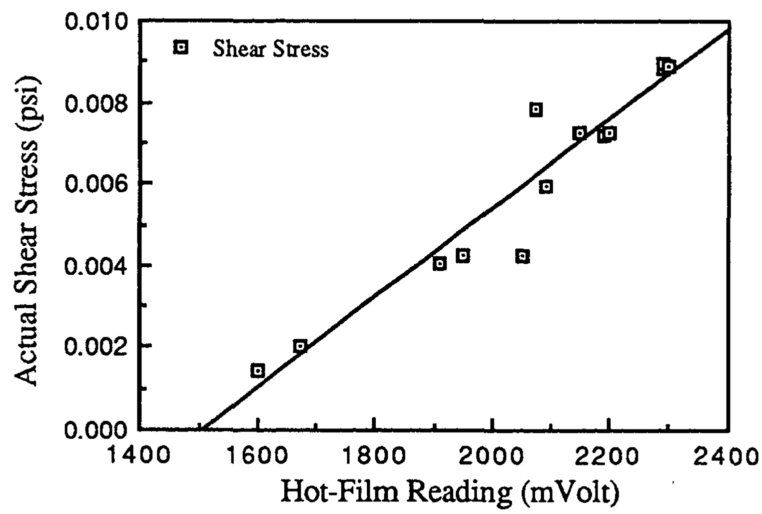

Figure 5. Hot-film calibration graph at 25ºC

6. A NOTE ON WET STREAKS

The wet streaks which appear at high-speed in blade coating with a short-dwell application are believed to be related to the flow instability and appearance of recirculating vortices with strong rate of change of velocity and momentum components in CD upstream of the blade. In order to design a superior coating system, it is also necessary to establish the mechanism by which these disturbances result in wet streaking. These streaks should not be confused with the streaks and scratches that are caused by blade imperfections, stalactites, or foreign material entrapped at the blade tip. Wet streaks occur as a result of increasing the machine speed beyond a limit regardless of the solid aspect ratio or concentration, although the limiting speed tends to decrease with increasing concentration. With a SDC having a pond about 5 cm deep, they typically appear as elliptical strips of lower coat weight about 2 - 3 cm wide and 20 - 40 cm long. At 1200 m/min it takes about .015 seconds to generate a typical streak. The 3-D vortices in the pond, for example the Taylor-Görtler-like [1] vortices, are 2.5 cm in diameter. Therefore, the comparable length scale between the 3-D flow structures and the streaks suggests a connection between the two.

Now consider the shear-induced clustering mechanism we have proposed in past reports [4-5]. In blade coating, the coating color at the tip of the blade experiences an enormous amount of shear (10^5 - 10^6 sec^{-1}).

Experiments indicate that when a high concentration of solid particles in a coating color is placed under large shear in a narrow gap, the particles tend to cluster into patches forming a bridge between the two boundaries of the gap; in our case, the cluster forms between the web and the tip of the blade. When there is no other physical influence from the upstream side of the blade, these clusters have length scales in the order of the blade gap believed to be about .01 cm. Their length scale is therefore two orders of magnitude smaller than the smallest length scale of the wet streaks. Therefore, without any hydrodynamic influence from upstream, at best, these clusters can cause microscale nonuniformities. In fact, these clustering actions occur at small shear rates and, therefore, start at low to moderate speeds and do not significantly affect the surface quality.

However, recirculating vortices (eddies) forming upstream of the blades due to 3-D instabilities may promote clustering layers with the length scale in CD equal to the eddy length scale, about 1 - 2 cm. Now, as soon as this clustering layer (a 1x100 plane) forms, it will act as a filtering screen and the following sequence of events can occur in 15 milliseconds:

- Particles start to accumulate at the clustered layer due to its filtering action.

- The accumulated solid particles form a porous layer which allows the fluid phase to pass only and this causes lower solid deposition on the web surface.

- The pressure builds behind the solid formation which eventually is forced through the gap.

A second mechanism is due to different modes of air entrainment which have been discussed in previous reports [4-5].

Nonuniform blade deflection in CD resulting in streaks can also be caused by several mechanisms. A detailed two-dimensional analysis of blade deflection is given in reference [9].

Quantitative values of the stress distribution on the surface of the blade are given, respectively by

$$\frac{d^2K}{ds^2} + KT + N_{el}\,\hat{n}\,\hat{n} : \tau = 0 \tag{1}$$

and

$$\frac{dT}{ds} - K\frac{dK}{ds} + N_{el}\,\hat{n}\hat{t} : \tau = 0 \tag{2}$$

where the stress tensor t for a Newtonian fluid is given by

$$\tau_{ij} = -p\,\delta_{ij} + \mu\left(\frac{\partial u_i}{\partial x_j} + \frac{\partial u_j}{\partial x_i}\right)$$

and K = surface curvature of the blade
T = tangential stress resultant measure

N_{el}	=	elasticity number
$\hat{n}$	=	unit normal vector to the blade surface
$\hat{t}$	=	unit tangent vector to the blade surface
p	=	hydrodynamic pressure
μ	=	viscosity
u_i	=	velocity component in direction x_i

The subscripts i and j are the tensorial indices representing the spatial direction of the surface forces.

In order to obtain the surface curvature of the blade, one needs to have the fluid stress tensor evaluated at the blade surfaces. This is extremely difficult if not impossible to measure experimentally. One has to rely on Computational Fluid Dynamics (CFD) simulation and analysis of the system to evaluate the hydrodynamic forces. We are working on a 3-D CFD program (through student research) for this analysis. In the meanwhile, the development of the Hot-Film Anemometer technique for experimental analysis of hydrodynamic behavior of coating systems will provide valuable information which can be used to evaluate and verify the computational analysis.

7. COMPUTATIONAL ANALYSIS OF A SHORT-DWELL COATER

Through experiments during the past two years, we have gained a better understanding of the three-dimensional instability of the flow in the pond of short-dwell coaters and formation of eddies upstream of the blade. Another issue which is also of considerable importance is the possibility of generating subambient pressure in the pond or at the blade and subsequent promotion of flow cavitation. Since it is not practical to measure the pressure field throughout the coating head and the blade tip, we resort to computational analysis of the flow in the coater. The full equations governing the flow of the coating color are solved using the fluid dynamics package (FIDAP) which uses the Galerkin finite element technique (Engelman and Sani, 1986). The advantage of this approach is that the solution provides the complete field values such as pressure, velocity, and shear rate. Other practical issues, such as blade deformation, substrate porosity and deformation, can also be included in the computational model as demonstrated in [9,11].

We start with a simplified version of a short-dwell coater with rectangular walls and a blade perpendicular to the sheet, as shown in Fig. 6. The flow inlet is at the middle of the bottom wall, the overflow baffle at the upper left corner is about 3mm, the blade gap is 0.1 mm, and the blade thickness is .5 mm. The purpose of these calculations is to obtain the hydrodynamic information otherwise unavailable experimentally.

The computations presented in Fig. 6-8 are for constant viscosity fluids and correspond to the following dimensionless parameters:

Cavity Reynolds number, $R = \rho UD/ = 666.6$
Capillary number, $Ca = \mu U/ = 600$
Stokes number, $St = \rho g D^2/\mu U = .8167$
Through-flow Reynolds number, $R' = \rho m/\mu = 1.85$

The physical conditions can then be evaluated from these parameters. For a coating color having a low-shear-rate viscosity of 1500 mPa.s, the results correspond to:

machine speed, $U = 1200$ m/min	viscosity, $\mu = 1{,}500$ mPa.s
net flow rate, $m = 166$ l/min.m	surface tension, $\sigma = .05$ N/m
pond depth, $D = .05$ m	gravity = 9.8 m/s^2
blade gap = .1 mm	density = 1000 kg/m^3

The general flow direction can be determined from the streamlines plotted in Fig. 6. The downstream secondary eddy at the lower right corner of the pond counter rotates with the primary eddy. Most of the flow entering the pond leaves through the left side without interacting with the primary eddy. Some of the fluid, however, is driven by shear along with the sheet, generating a relatively large shear at the overflow baffle. The pressure close to the wetting point, as shown in Fig. 7, does become subambient, promoting cavitation.

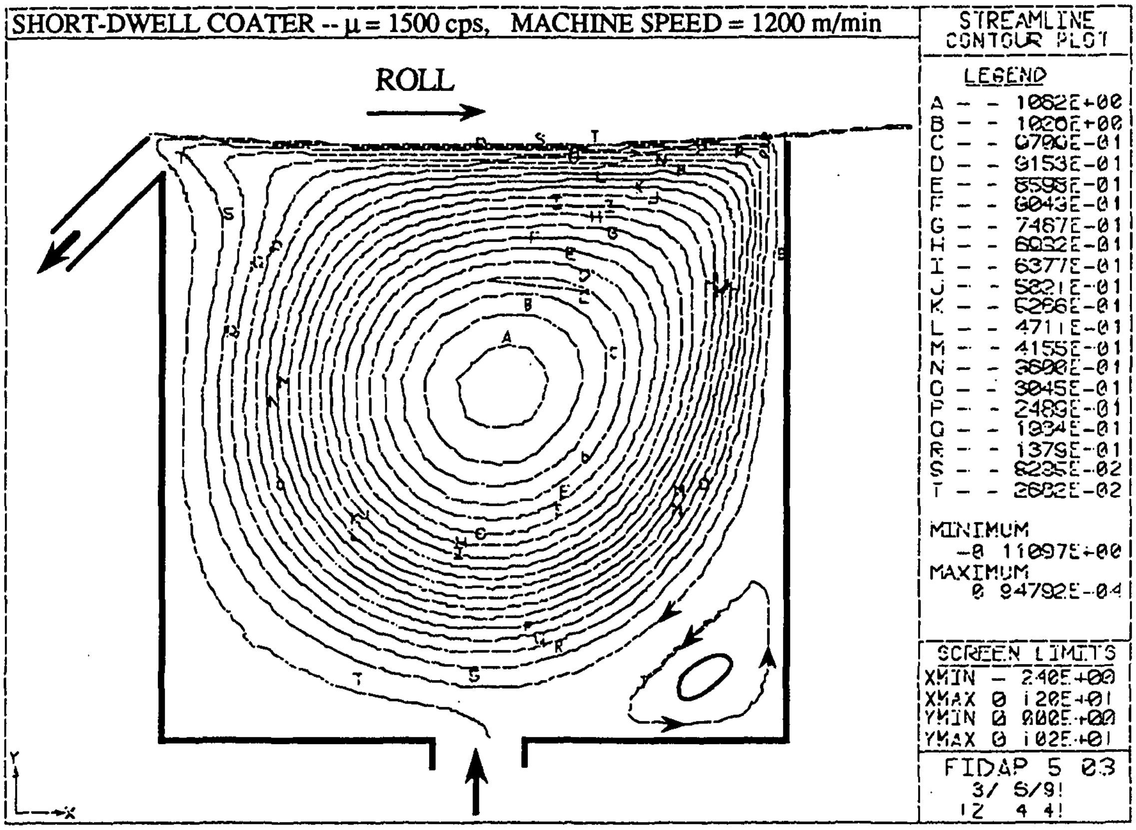

Figure 6. Streamline contour plot of flow in a short-dwell coater (constant viscosity).

Another location with even larger pressure variations is the blade gap. Here we have simulated a blade running on its heels, forming a diverging channel in the gap. The velocity vector plot in Fig. 8 shows the general flow field while the pressure and shear contour plots show the more interesting details of the flow. As the flow reaches toward the outlet tip of the blade, the pressure decreases, forming a rather large subambient pressure region. With the parameters considered in this simulation and the diverging gap configuration, cavitation is likely to occur at the blade tip. The highest shear rate occurs near the blade surface at the upstream side of the gap. With the above parameters, the maximum shear rate is about 1.5×10^5 (1/s).

Since the coating colors are generally shear thinning, the viscosity decreases significantly at the blade. We have used the Carreau model to investigate the effects of rheology on the flow. This model can be written as

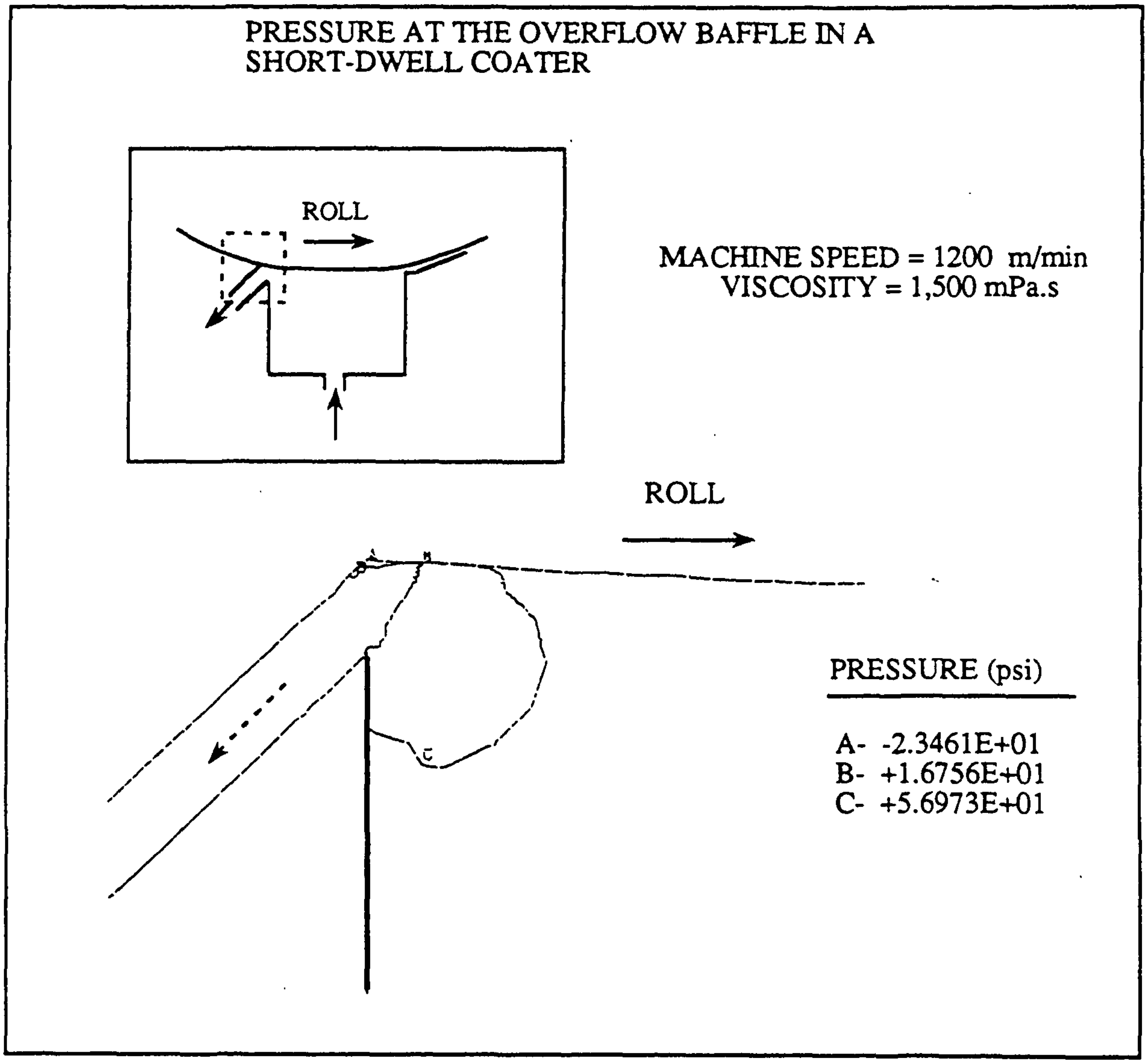

Figure 7. Subambient pressure at the overflow baffle in a short-dwell coater (constant viscosity).

DIVERGING BLADE IN A SHORT-DWELL COATER

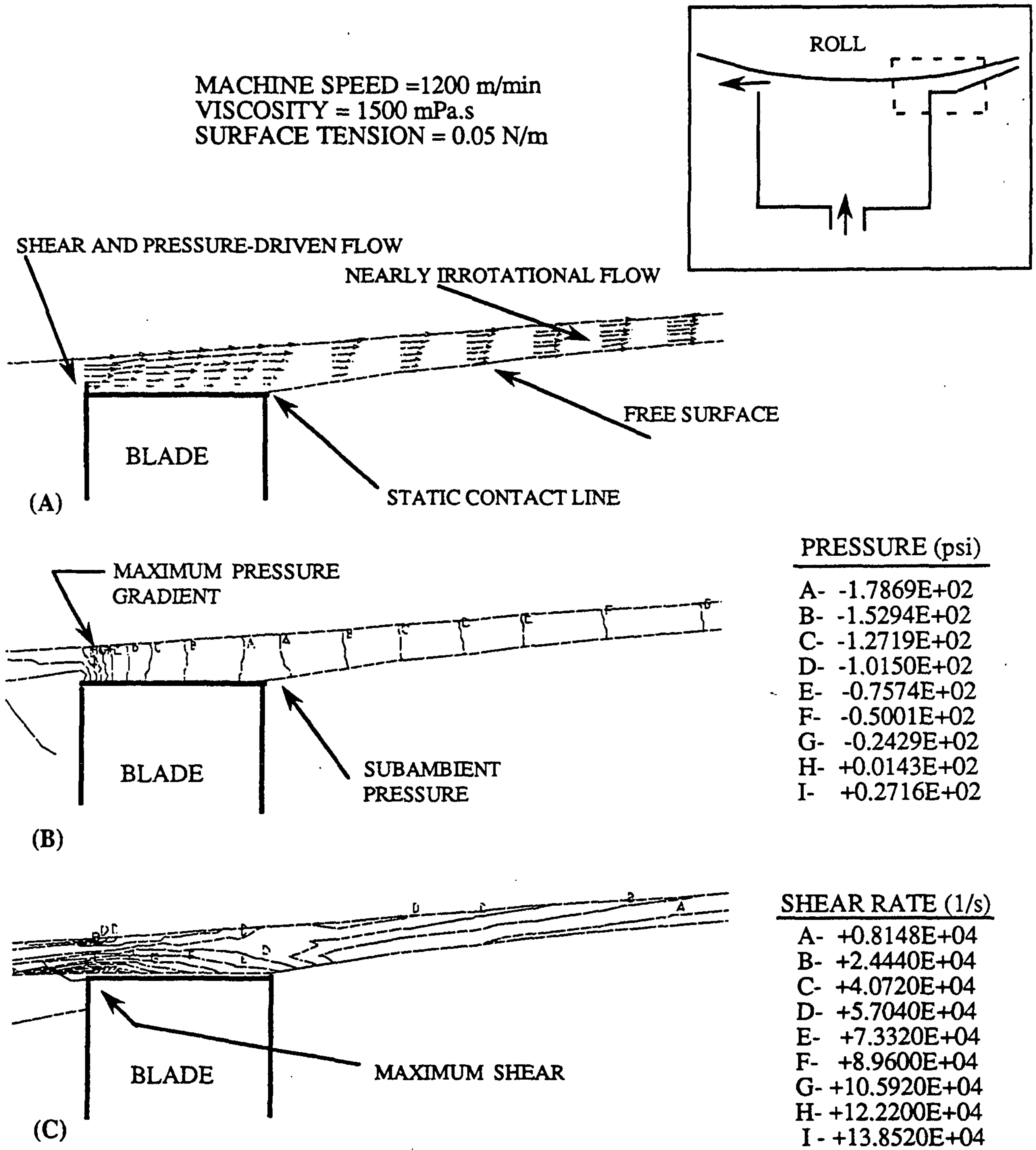

Figure 8. Constant viscosity fluid flow at the blade of a short-dwell coater; (A) velocity vector plot, (B) pressure contour plot, and (C) shear rate contour plot.

$$\frac{\eta - \eta_\infty}{\eta_o - \eta_\infty} = \left[1+(\tau\dot{\gamma})^2\right]^{\frac{n-1}{2}}$$

where $\dot{\gamma}$ shear rate
τ time constant
n Carreau index
η_o zero-shear-rate viscosity
η_∞ infinite-shear-rate viscosity.

In the preliminary simulations shown in Fig.9, the zero-shear-rate viscosity was kept at 1500 mPa.s and the infinite-shear-rate viscosity was set at 150 with .01 for the time constant and .7 for the index. The fluid remains, in general, more viscous than typical coating colors. We have deliberately started with a worst case scenario in order to better establish the limiting factors in terms of flow parameters which result in hydrodynamic cavitation.

Relative to the constant viscosity case, the pressure at the blade becomes less negative due to decrease in viscosity at that region, as shown in Fig. 9a. Therefore, higher shear rate reduces the possibility of cavitation. The minimum viscosity in this case is about 900 mPa.s at the upstream tip of the blade.

8. DESIGN OF A SUPERIOR HIGH-SPEED COATER

Our past research on short-dwell coaters [1-7] was mainly focused on establishing a better understanding and documenting various sources of problems in this system. Although this work is continuing and expanding to other types of coaters, we are now in a position to focus part of our efforts toward developing a new superior application system. The problem areas with the current system are identified as three-dimensional instability of recirculating eddies in the pond, dynamic contact line instability and air entrainment at the overflow baffle, and flow cavitation. One approach is to modify the existing short-dwell pond by adding baffles or screens in the pond. This type of modification, we believe, will only be marginal at best and may cause additional problems such as excessive pressure drop and generation of micro-eddies. Also, in practice, complicated geometries are difficult to clean and maintain. Therefore, our objective here is to design an application system

DIVERGING BLADE IN A SHORT-DWELL COATER

MACHINE SPEED = 1200 m/min
VISCOSITY; CARREAU MODEL
μ_o = 1500
μ_∞ = 150
n = .7
τ = .01

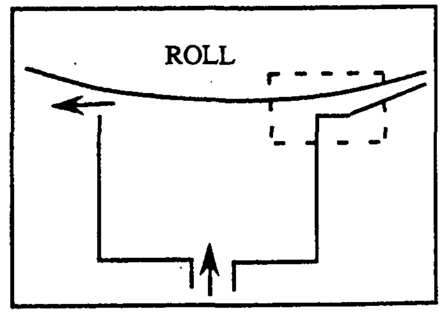

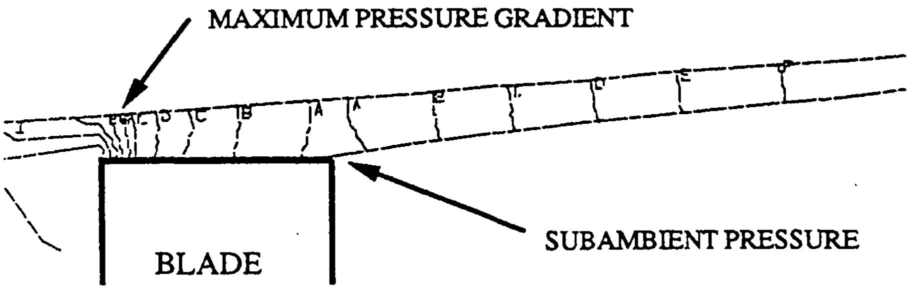

(A)

PRESSURE (psi)

A- -1.4923E+02
B- -1.2702E+02
C- -1.0474E+02
D- -0.8253E+02
E- -0.6026E+02
F- -0.3803E+02
G- -0.1579E+02
H- +0.0645E+02
I- +0.0286E+02

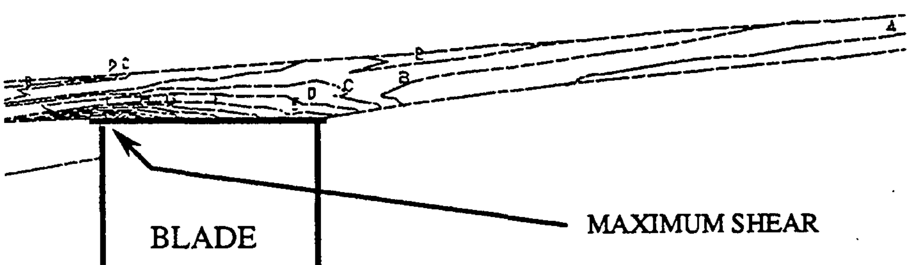

(B)

SHEAR RATE (1/s)

A- +0.9608E+04
B- +2.8824E+04
C- +4.8040E+04
D- +6.7240E+04
E- +8.6480E+04
F- +10.5680E+04
G- +12.4920E+04
H- +16.3360E+04

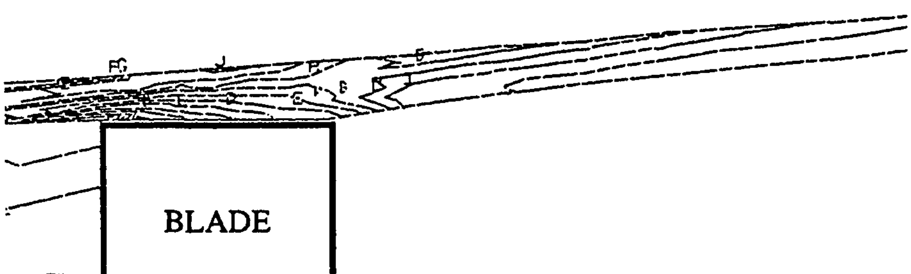

(C)

VISCOSITY (mPa.s)

A- +1.013E+03
B- +1.065E+03
C- +1.116E+03
D- +1.167E+03
E- +1.218E+03
F- +1.269E+03
G- +1.321E+03
H- +1.372E+03
I- +1.423E+03

Figure 9. Flow of shear-thinning coating color at the blade of a short-dwell coater; (A) pressure, (B) shear rate, and (C) non-newtonian viscosity contour plot.

HIGH-SPEED COATER

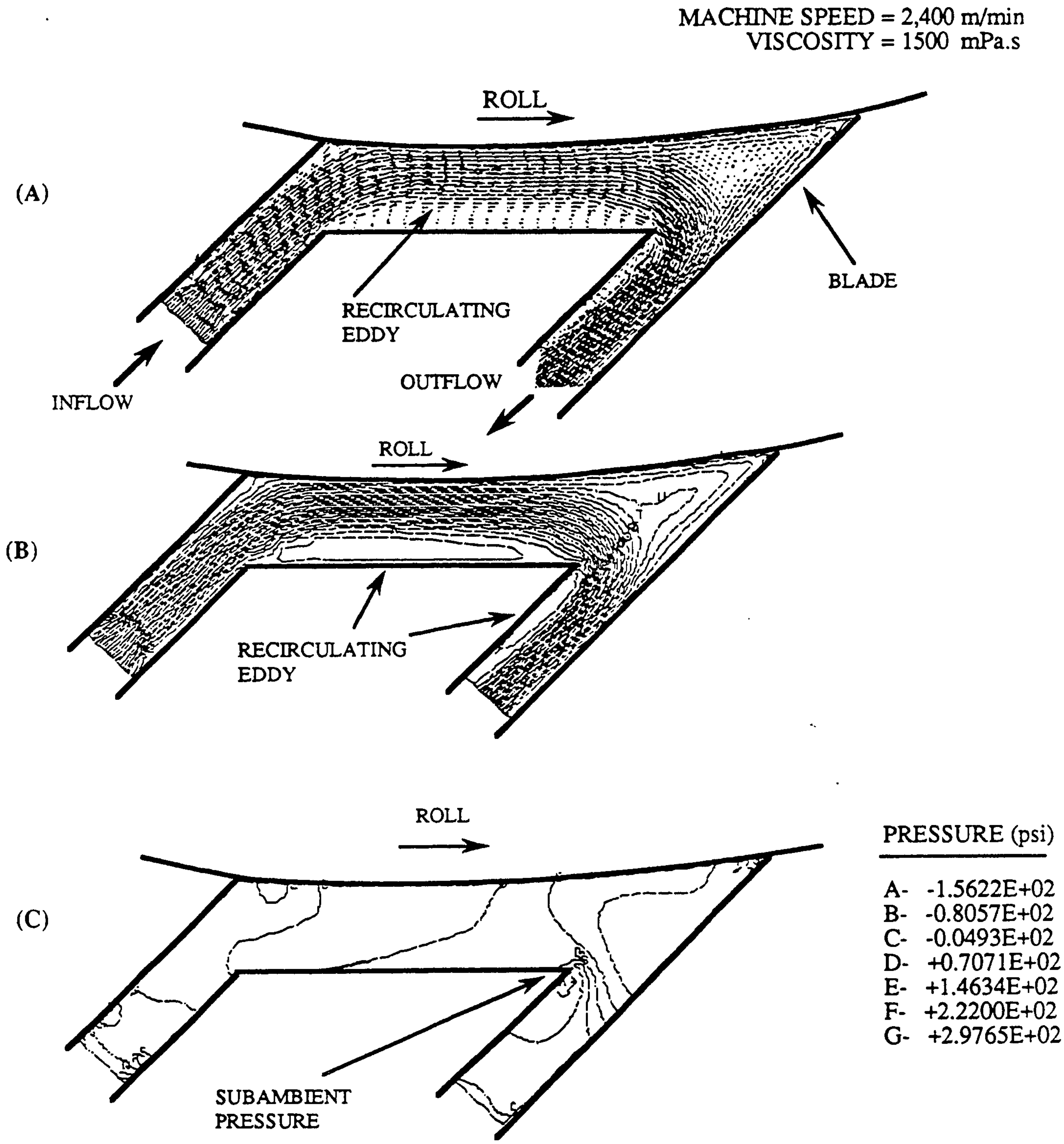

Figure 10. Parallel-flow coater; (A) velocity vector plot, (B) streamline contour plot, and (C) pressure contour plot.

HIGH-SPEED COATER

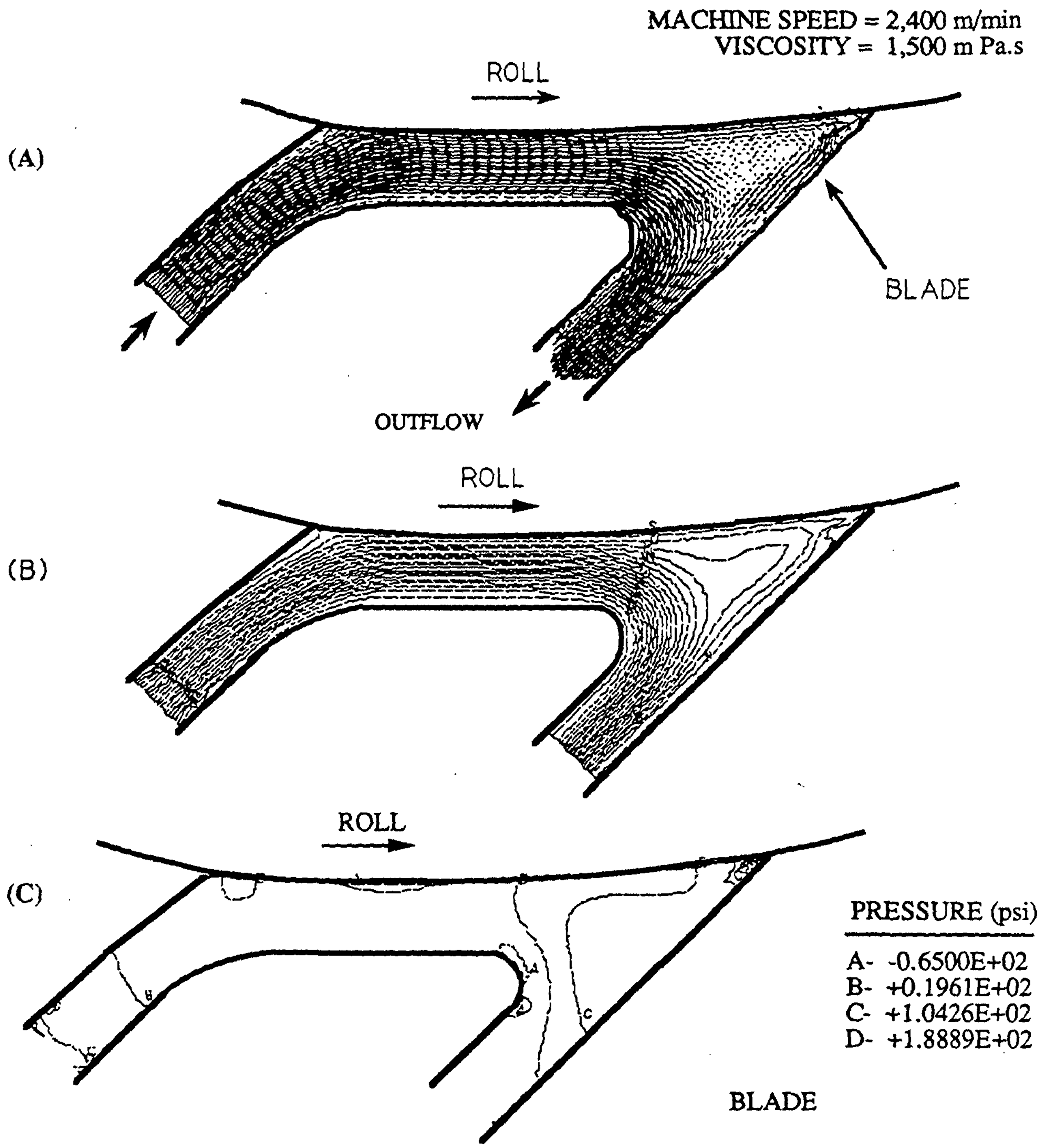

Figure 11. Modified parallel-flow coater; (A) velocity vector plot, (B) streamline contour plot, and (C) pressure contour plot.

which is simple and not adversely affected by instability of recirculating eddies, flow cavitation, or air entrainment .

We use the computational technique explained in the previous section for this study. The first system under investigation is based on the idea of parallel shear flow, that is, a flow system with no recirculating eddies. One such system is shown in Fig. 10 where the fluid enters from one side and leaves the pond from the other in the same direction of the substrate. In these calculations, for a viscosity of 1500 mPa.s, the machine speed is 2400 m/min. At this high speed, the jetting action near the horizontal plate results in flow separation and generation of an eddy. Another eddy also forms at the outlet section as pointed out in Fig. 10a and 10b. The pressure calculations, shown in Fig. 10c, indicate a large pressure drop at the sharp corner near the exit side. Flow cavitation is very likely to occur in this region.

To prevent these problems, we have modified this application system such that the flow generally follows the streamlines in Fig. 10a. The velocity and streamline contour plots in Fig. 11a and 11b show that this modification does indeed result in a smooth flow with no eddies. The pressure calculations in this system show that the subambient pressure is also improved by 50%.

The future work in this area is to include the rheological properties of the coating color in the calculations of the flow field and also to address the air entrainment issue.

FUTURE PLANS

1. Calibrate a hot-film anemometer (HFA) for non-isothermal conditions by attaching a thermocouple to the HFA probe. This device shall be used to analyze the dynamics of flow field of coating colors (opaque) in various coating systems.

2. Measure the effects of span aspect ratio on the critical speed for the onset of time dependent flow in the pond of short-dwell coaters using (a) viscous Newtonian fluid and (b) shear-thinning fluids with typical coating color rheological characteristics.

3. Extend the computational fluid dynamics techniques to study and compare the rheological behavior of coating colors in a SDC for various sets of parameters, such as blade angle and physical properties of the fluid.

4. Install an actual SDC head (being built by Beloit) on the experimental roll coater to investigate problems with flow cavitation.

Long-term:

5. Develop a computational technique based on spectral decomposition for stability analysis of rheologically complex coating colors in various coating systems.

6. Modify the application technique in a blade coating system for superior performance. This is an exploratory research within the project for development of novel coating systems. The current computer aided design techniques will be used to continue modification of the new coating head design.

TIME TABLE

```
Tasks     April   May    June    July    Aug.   Sept.   Oct.
  1       +------------ 1 ------------+
  2                     +--------------- 2a --------------->
  2                                             +--- 2b -->
  3        +---------------------- 3 --------------------+
  4                  +----------------- 4 ------------------>
  5       +-------------------------- 5 ----------------------->
  6       +-------------------------- 6 ----------------------->
```

SIGNIFICANCE TO THE INDUSTRY

High quality coated paper products are a significant segment of the total paper market. The goal of this research project is to contribute to the development of a cost- effective coating process for products with superior quality and more flexibility. This will provide the industry with a competitive edge in an ever growing market.

REFERENCES:

1. Aidun, C.K., "Principles of Hydrodynamic Instability: Applications to Coating Systems -- Part I Background," *TAPPI J.*, 74(2), 213, 1991.

2. Aidun, C.K., "Principles of Hydrodynamic Instability: Applications to Coating Systems -- Part II Examples of Coating Flow Instability," *TAPPI J.*, 74(3), 1991.

3. Aidun, C.K., "Principles of Hydrodynamic Instability: Applications to Coating Systems -- Part III Generalization of Coating Flows as Dynamical Systems," *TAPPI J.*, 74(4) to appear, 1991.

4. Aidun, C.K., Institute of Paper Science and Technology, Project 3674- Fundamentals of Coating Systems, Status Report to PAC, pages 51-71, October 1989.

5. Aidun, C.K., Institute of Paper Science and Technology, Project 3674- Fundamentals of Coating Systems, Status Report to PAC, pages 61-87, March 1990.

6. Triantafillopoulos, N.G., and Aidun, C.K., "Relationship between flow instability in short dwell ponds and cross directional coat weight nonuniformities," Technical Report number 352, Institute of Paper Science and Technology, 1990; also *TAPPI J.*, 73 (6), 127, 1990.

7. Aidun, C.K., and Triantafillopoulos, N.G., "Global stability properties of flow structures in the pond of a short-dwell blade coater," Int'l Symp. Mech. of Thin-Film Coating, AIChE Meeting, March 18-22, 1990.

8. Gane, P.A.C., and Coggon, L., "Coating Blade Geometry: Its Effect on Coating Color Dynamics and Coated Sheet Properties," *TAPPI J.*, 87-96, 1987.

9. Pranckh, F.R., and Scriven, L.E., "The Physics of Blade Coating of Deformable Substrate," 1988 Coating Conference Proc., TAPPI Press, Atlanta, GA, 1988.

10. Engelman, M.S., and Sani, R.I., "Finite Element Simulation of Incompressible Fluid Flows with a Free/Moving Surface," In: Taylor, C., Johnson, J.A., and Smith, W.R. (eds.), *Computational Techniques for Fluid Flow*, 47-74, Pineridge Press, Swansea.

11. Chen, K.S.A., and Scriven, L.E., "On the Physics of Liquid Penetration into a Deformable Porous Substrate," 1989 Coating Conference Proc., TAPPI Press, Atlanta, GA, 1989.

DISPLACEMENT DEWATERING

STATUS REPORT

FOR

PROJECT 3680

April 4, 1991

Institute of Paper Science and Technology

Atlanta, Georgia

Project Summary Form

Project Title: Displacement Dewatering
Project Number: 3680
Project Staff: Jeffrey Lindsay
FY Budget: $160,000
Project Goal: Develop techniques to efficiently dewater paper while maintaining bulk.

ABSTRACT

In the last period, a displacement dewatering process for paper dewatering has been experimentally evaluated. The process uses a pressurized air or steam phase to expel free liquid water from paper while the paper is simultaneously under mechanical pressure. The objective is to efficiently dewater paper while maintaining bulk, in contrast to conventional pressing operations which remove water solely through volume reduction of the web. Displacement dewatering also differs from through-drying, in which a gas phase blows through the paper to evaporate water. In displacement dewatering, a true displacement process is desired in which a gas-liquid interface is maintained.

The results to date suggest that displacement dewatering can be a useful dewatering process for some grades of paper and for some specialty products. However, if displacement dewatering is considered as a replacement for conventional wet pressing, the objective of achieving higher bulk may not be realized, at least for some furnishes. In particular, subjecting paper to low mechanical pressure for the relatively long nip residence times required in displacement dewatering can induce creep effects which can lead to higher than expected densification. This creep effect is still subject to question and needs further verification; it may have been due to experimental artifacts. However, densification can be especially severe when superheated steam is used due to thermal softening of the fibers. Improved strategies are being explored to tap the potential of a displacement dewatering process.

INTRODUCTION

The capabilities of the press section have progressed significantly in the last several decades, allowing ever higher dryness levels to be achieved. However, higher dryness typically means higher sheet density. For those grades of paper where high density is not desirable, the trade-off between bulk and dryness poses unwanted constraints on the papermaker. Energy-efficient dewatering techniques which decouple density and dryness could be of significant benefit to the industry. One proposed means of achieving this objective is through displacement dewatering, in which a pressurized gas phase is used to drive liquid water out of a mechanically compressed sheet. The externally imposed gas pressure could supplement the normal hydraulic pressure gradient in a sheet that forms as the sheet is compressed. Because gas pressure would increase and extend the usual hydraulic pressure, driving more water out of the sheet, higher dryness levels could be achieved without further mechanical compression of the sheet. Dryness and density could thus be decoupled to a degree, potentially giving the papermaker added control over sheet properties and possibly a lower energy demand in the dryer section.

In most pressing operations, increasing the press impulse is not effective in raising the outgoing dryness beyond about 45-50%. The details vary widely from press to press, but once a compression-controlled regime is reached, higher impulse brings only marginal dryness gains. Displacement dewatering, however, has the potential of increasing the dryness to even higher levels, for the free water in a sheet can still be removed by the gas in a compression-controlled regime. If displacement dewatering could be commercially implemented, it may give the papermaker a new choice between higher dryness at the usual density or lower density at the former dryness level, or something in between.

In this paper, displacement dewatering refers to a process in which a gas phase is used to drive out a liquid layer in a compressed sheet. If true displacement dewatering is achieved, relatively little vapor would be required to pass through the sheet - ideally only enough to uniformly displace the free water in the interconnected pores of a compressed sheet. This concept, at least in its idealized form, differs from through-drying or impingement drying, in which large volumes of heated air are used primarily to evaporate water in the sheet, although the process of through-drying also removes some water by entrainment. While the objective is to decouple density and dryness, displacement dewatering still requires substantial applied pressures to saturate the sheet and create an interconnected liquid layer which can be displaced by gas. In practice, the gas is likely to break through some pores in the sheet and remove water by entrainment and evaporative drying, but the objective is uniform displacement.

Such a displacement process would be of interest in grades such as linerboard, boxboard, and some printing papers and specialty products where the sheet is too heavy for through-drying or other techniques suitable for lightweight, highly porous paper, but where bulk is still desired. Piece goods such as paper plates may also benefit from displacement dewatering. In the displacement process under consideration, a sheet would be subjected to moderate mechanical pressures to increase sheet saturation, probably in the range of 30-300 psi, while simultaneously being exposed to compressed gas. One possible implementation is shown in Figure 1. The apparatus envisioned here is like a suction roll operating in reverse, with multiple low-pressure long nip shoes to maintain the displacement process for a sufficient time.

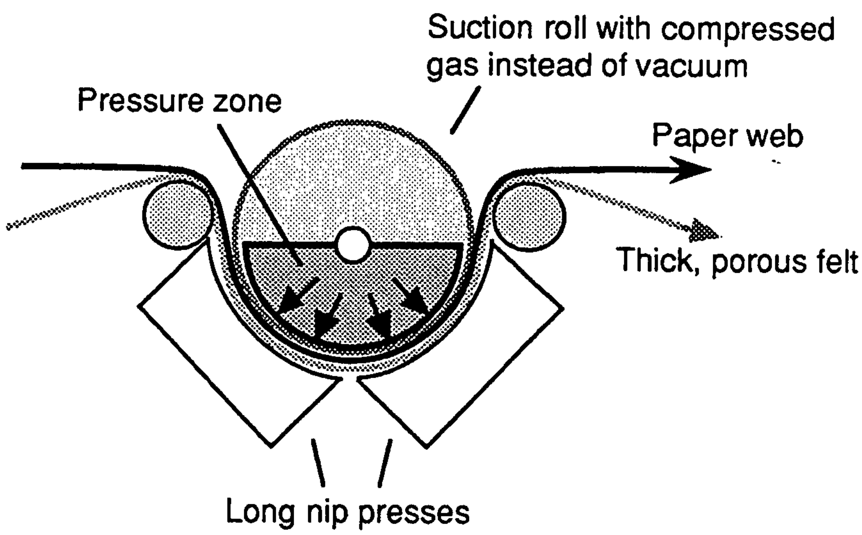

Figure 1. Possible implementation of the displacement dewatering concept.

This paper describes the recent results of an on-going study on the potential of displacement dewatering, and attempts to evaluate the possible commercial importance of this technology.

PREVIOUS WORK

The use of gas to assist dewatering is hardly new. Indeed, a number of the concepts explored in this study were found to have been proposed, if only in passing, in a variety of prior patents and articles. A careful discussion of what has been done in the past is thus needed to clarify the contributions of the present study.

Through-drying Concepts

Entrainment and Displacement

In a patent granted in 1966, Holden (1) proposed several devices which would blow air through a wet web to remove water. Holden's concept was to dislodge and entrain water in a porous sheet by blowing air through the z-direction over a sufficiently long time (>50 ms). While he proposed several devices, the one most relevant to the present study is shown in Figure 2. In this apparatus, light mechanical pressure was to be applied to the sheet by felt tension as the sheet received air flow from a perforated roll.

Holden's concept was extended by Kawka and co-workers (2-9) over a number of years. Kawka used some of the devices as proposed by Holden, such as that in Figure 2, and invented others which also passed gas through a sheet under low mechanical pressures applied by porous belts, wires, or felts (2-4). Kawka's work focuses on blowing air through paper, especially absorbent papers and boards. In one study, for example, unheated air pressures from 0.01-0.08 MPa were used with exposure times of 0.1-1.0 s to dry absorbent papers (5). Solids content was raised from 10% to 30-40%, although a 28 gsm napkin tissue was dried from 18% to 87% solids in 0.5 seconds using air heated to 130°C.

In general, the blow-through process, with light mechanical compression, is severely limited in the dryness that can be achieved in short times. For example, with bag paper of 70 gsm, Kawka reports solids out of up to 43% obtainable with an 0.6 second exposure time of room-temperature air passing through the sheet (6). Initial solids content was 31%. In a thorough, recent study of through-drying with room-temperature air, Kawka reports that the time required to remove the free water in paper is about 5 seconds with air pressures on the order of 0.1 MPa (7). (As will be seen below, any blow-through or displacement process will not be able to remove much water on the short time scales characteristic of conventional wet pressing.)

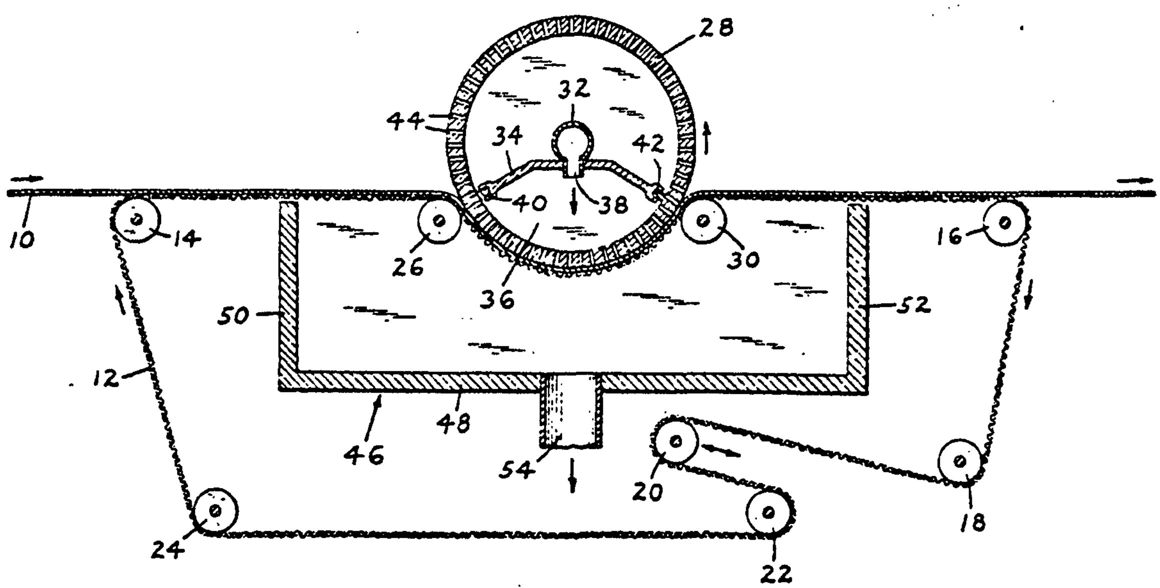

Figure 2. A blow-through dryer proposed by Holden (1).

The theory of through-drying is treated in (8). While Kawka claims that displacement of water from pores takes place in wet sheets with initial solids below 25%, more important seems to be the entrainment of water particles which occurs as air passes through the sheet with velocities on the order of 100 m/s (9). He states that the process works best at solids contents around 35%.

All devices used by Kawka and Holden have the following characteristics:

- low mechanical compression (e.g., < 0.1MPa) on the sheet
- long exposure times (0.05 - several seconds)
- modest applied gas pressures (typically < 0.2 MPa)
- air as the displacing medium, typically unheated
- low operating speeds (< 300 m/min).

The blow-through concept has been aimed primarily at lightweight grades such as towel and tissue as well as bag papers. One article mentions application to heavyweight board, but no data are given (9).

Thermal Processes (Evaporation)

Through-drying is a well developed technology in which heated air is passed through a highly porous sheet under minimal compression (10-13). Because the hot air contacts water across a large surface area inside the sheet, evaporative heat transfer is very efficient. Displacement is not likely to occur, but some liquid may be removed by entrainment. Tissue and toweling are prime grades for through-drying, although various filter grades, roofing felts, wiper grades, and many wet-laid nonwovens can be used (12).

Both cylindrical and flat bed through-dryers are used. One example of a cylindrical though dryer is shown in Figure 3. A porous roll can be sufficiently strong to withstand high pressure differentials. Using a roll with a highly open honeycomb structure, Randall (14) reports pressures up to about 0.03 MPa or 5 psi, while a drilled suction role could support still higher pressures at the cost of less open area. With high differential pressures, sheet transfer may be impaired. Flat bed through-dryers, as shown in Figure 4, pass the sheet between high and low gas pressure zones on a conveyor device. Sheet transfer is easy, but the process is limited to lower pressures.

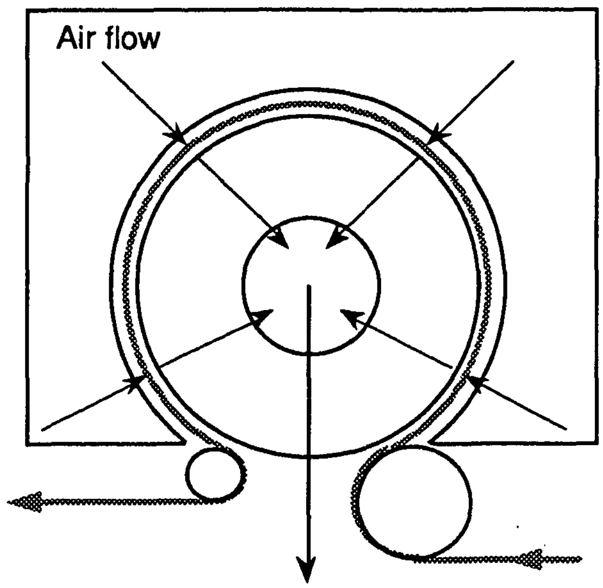

Figure 3. A cylindrical through-dryer.

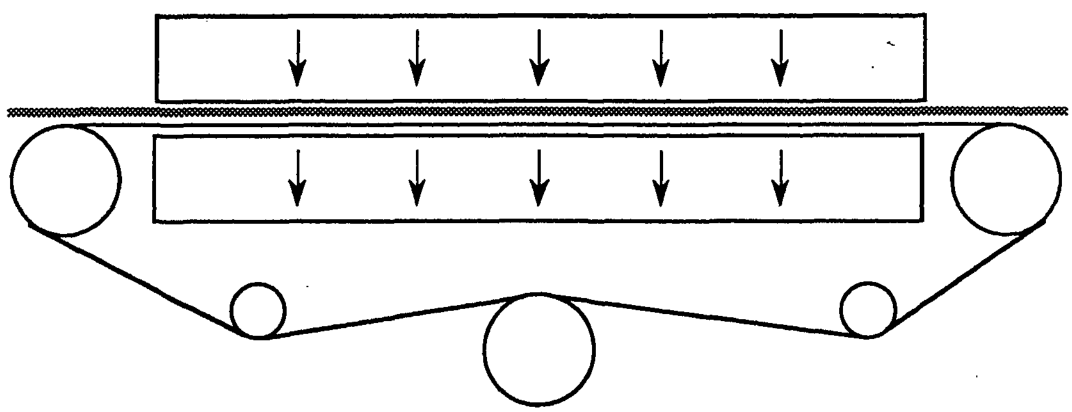

Figure 4. A flat bed through-dryer.

High velocity gas impingement in tandem with through-drying has been investigated and patented by Burgess et al. at the Pulp and Paper Research Institute of Canada (15,16). In this "Papridryer" system, vacuum pressure inside a drilled suction roll pulls hot air through the sheet, decreasing boundary layer heat transfer resistance in impingement and causing internal heat transfer in the sheet.

Other Dewatering Processes

Impulse drying, a novel thermal dewatering process under development at The Institute of Paper Science and Technology, may induce a displacement process which enhances liquid water removal from a sheet. In this process, a web and a felt pass through a nip in which one roll is heated to around 250°C (17,18). During the period of brief but intense heat transfer, with peak heat fluxes on the order of 4 MW/m^2, a high-pressure steam zone may form in the nip which can displace some liquid water or at least resist rewetting (19,20).

A related concept of gas-liquid displacement in dewatering was addressed in a patent awarded to Gottwald, et al., in 1967 (21). Their proposed device was a heated drum at 120-250°C, wrapped with a wet web held in place by a porous belt under enough tension to cause at least 0.03 MPa (5 psi) of pressure on the web. They claim that vapor generated at the drum-web interface would drive liquid water into the porous belt, reducing the evaporative load on subsequent dryers. The proposed physics seem questionable, as a saturated liquid layer is not likely to exist under these conditions, but the possibility of *in-situ* steam-liquid displacement clearly was envisioned.

Use of a high velocity gas nozzle to remove water by atomization was patented by Clemens and Morton (22). This method is related to some versions of through-drying in that entrainment of liquid water takes place, but Clemens and Morton use a small, high-pressure, high-velocity jet from a nozzle which is claimed to remove water from low-density webs at web speeds as great as 6,000 feet/min (30 m/s). Their objective was to remove water without decreasing bulk. The process is intended for very light grades such as tissue.

The IPST Displacement Concept

The displacement dewatering concept discussed here employs conditions well outside the realm of the through-drying processes discussed above. Specifically, the dewatering process under consideration:

- employs mechanical pressures great enough to liberate a substantial amount of water in the sheet, with conventional pressing pressures being possible;
- is intended to use brief intervals of time, less than 0.3 seconds and preferably under 100 msec to permit operation at practical speeds;
- seeks to raise solids levels of incoming sheets at 20-30% solids to beyond 40-50% to save drying energy as well as offer better control over bulk.

The current study actually began in 1985 with exploratory work done by Wahren, Ahrens, and Sprague at the Institute of Paper Chemistry in Appleton, Wisconsin (now IPST in Atlanta, Georgia). The work reported here is a continuation of the same project, resumed in 1987, which has suffered a number of major delays and interruptions over the past several years. Early results of this study were reported by Sprague (23). Room temperature air only was used in a series of brief experiments using lightweight sheets with several displacement devices. The equipment used posed a number of problems. In particular, drying was nonuniform due to improper air flow distribution. Large drilled holes in the platens led to nonuniform mechanical pressures. Air leakage around the edge of the sheet during displacement also appears to have been a problem. The new equipment for this phase of the study was designed to overcome these problems, as described below.

Sample results from the early portion of this project (23) are shown in Figure 5. Here a sheet was subjected to mechanical compression between plates with a number of holes. After 60 ms of compression, a valve released a burst of compressed air which continued for another 60 ms, with gas pressure maintained past the end of the pressing event. The low gain in solids when no air was used must reflect the inefficiency of wet pressing between two drilled platens; conventional wet pressing under similar press conditions would have undoubtedly given much better dryness levels.

In examining trends in density and dryness, Sprague found evidence that gas displacement can allow significant water removal to be achieved without the normal degree of densification. This possibility will be examined in more detail in this paper.

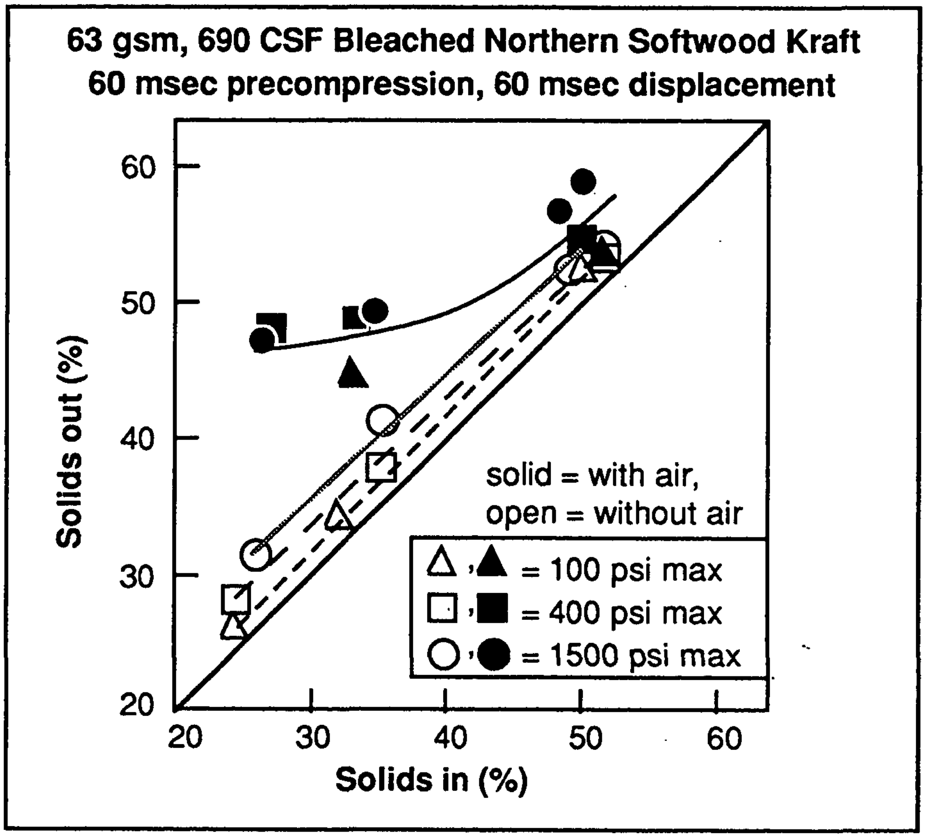

Figure 5. Dewatering results obtained with early displacement dewatering equipment at the IPST (23).

THEORY OF DISPLACEMENT DEWATERING

Limits to Water Removal: The State of Water in the Sheet

The interaction of gas with water in a sheet of paper depends on a number of factors. Most critical, perhaps, is the state of the water with respect to the porous structure of the paper. Gas displacement will not remove water that is chemically or physically bound to the fibers or water that is trapped in dead-end or isolated pores. The potential of displacement dewatering is limited by the amount of water available for flow at a given compression.

A possible indication of the water that could be removed by air flow alone, apart from drying, can be found in a study of White and Marceau (24). They applied fully saturated, room-temperature air at low pressure differentials (< 0.02 MPa) to saturated sheets of blotting and filter papers. Air flow rates remained low (0.5-3 liters/min cm^2) for long times (several hours in some cases), until a point was reached at which the air flow rate rapidly increased to an equilibrium value (4-7 liters/min cm^2). During such tests, the water content of the sheet decreased slowly, but when the water content fell to 50-60%, the air flow rate experienced the rapid increase and the water removal rate likewise increased rapidly until an equilibrium moisture content of less than 30% was achieved (see Figure 6). These results were presented as unexpected and puzzling, although the authors surmised that water removal was by air drag and that the final equilibrium level of water in the sheet represented pendular water that could not be removed by air flow.

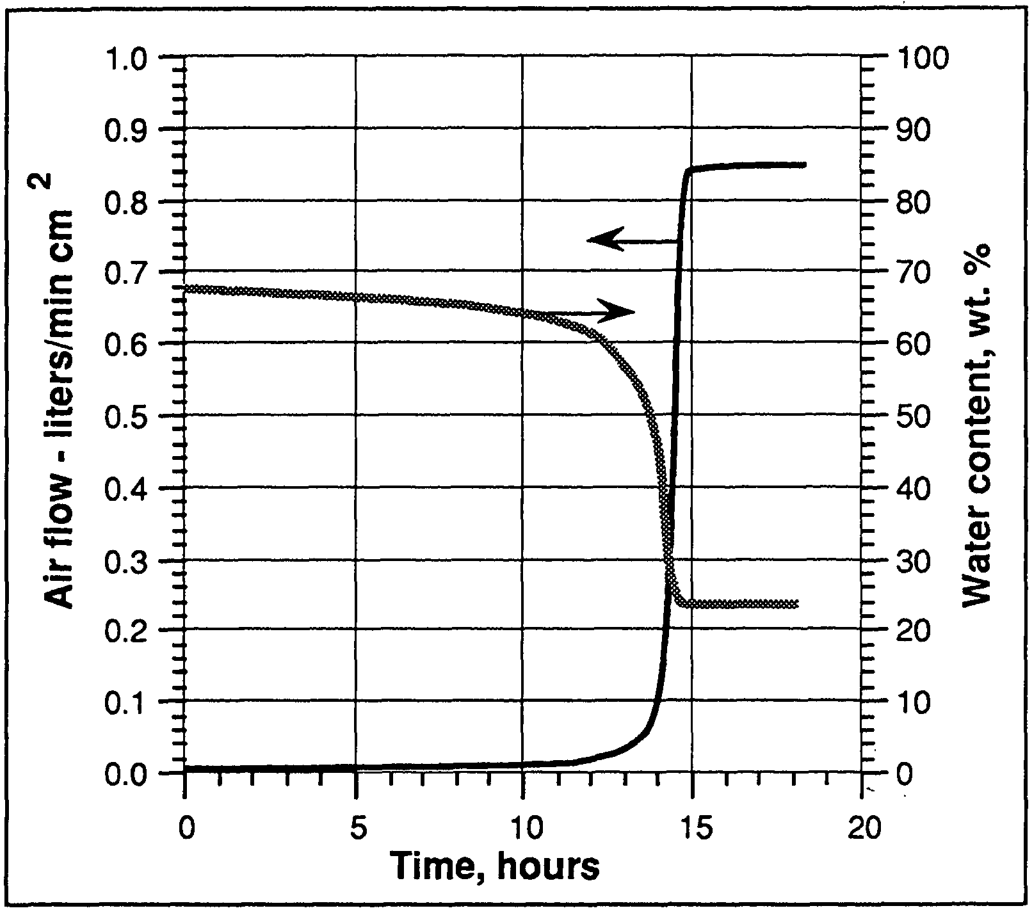

Figure 6. Data from White and Marceau (24) for air flow rates and water content of a 100-lb blotting paper as a function of time. Air pressure differential was 5 in Hg (1.7×10^4 Pa).

In spite of the long times required, one might still conclude from the above study that a combination of displacement and entrainment could remove a substantial portion of the water, with dryness levels above 70% being possible without evaporative drying. Such optimism is unwarranted, however. It seems unlikely that entrainment from low velocity air in an uncompressed sheet could lower the moisture content to the level of about 24% indicated in Figure 6 without evaporative drying. Estimates of the amount of water associated with the swollen fibers of paper and thus unavailable for flow suggest that much higher equilibrium moisture levels should have been obtained. It is thus hypothesized that the air passing through the sheet was not fully saturated, and that a gradual reduction in moisture content by evaporative drying occurred until the equilibrium vapor pressure of the moisture in the sheet equalled the vapor pressure of the incoming air. Note that capillary effects and liquid-solid interactions in small pores lower the equilibrium vapor pressure of water in cellulose (25,26). The air in this experiment passed through heated water to saturate it, then through a cooler and condensate trap before entering the sheet. A temperature increase between the cooler and the sheet may have made the air unsaturated.

If some drying did occur, then the change in flow at a moisture content near 50-60% may be due to the change in pore structure which occurs as some of the water of swelling (gel water or water associated with the fibers) evaporates. Upon deswelling, the pore structure in the sheet should become more open, yielding a higher air flow rate and thus more rapid evaporation.

Understanding the swollen state of cellulose fibers is relevant to displacement dewatering. A variety of studies have been conducted to understand where the water is in the sheet and how much might be available for removal. Lindström (27) provides an excellent review of this topic. Useful information can be obtained from water retention values, solute exclusion measurements (28,29), and from values of specific volume (a better term would be "associated volume") of fibers from permeability measurements (30,31). Based on such information, a perfectly efficient displacement dewatering method without high mechanical compression is unlikely to exceed dryness levels of 50% in typical papers. As with conventional wet pressing, much of the water to be removed may need to be pressed out of the cell wall (32). The potential advantage of displacement dewatering is that more of the free water can be removed, so a given solids level may be obtained at lower pressures than required in wet pressing.

The Physics of Gas-Liquid Displacement

Gas-liquid displacement flows in porous media pose a challenging problem in analysis. The problem involves the unsteady flow of two immiscible fluids through a non-homogeneous solid matrix, with capillary and viscous forces that are linked to the porous structure, to the local values of saturation, and to the history of the domain (i.e., hysteresis effects can be significant). An accurate prediction of gas-liquid displacement in this case becomes computationally unfeasible and would still require measured parameters that are generally unavailable for paper. However, simple limiting estimates of performance are possible if one assumes that a sharp interface separates the gas and liquid phases. This commonly employed assumption may be useful in some simple cases when high displacement velocities occur (33), although it is expected to be only a crude tool for the problem at hand.

Speed of Displacement

One simple but key issue in displacement dewatering is the length of time the gas pressure must be applied. The sharp-interface assumption may be applied to give a *lower* limit. Consider the one-dimensional motion of a sharp, stable gas-liquid interface driven by constant gas pressure through a uniform porous medium of thickness L and permeability K. The gas liquid interface is at position x, with x = 0 at the flow exiting side of the sheet. The pressure drop across the sheet is ΔP. Neglecting inertial effects and the viscosity of the gas phase, we can apply Darcy's law to determine the interface velocity:

$$V = -\frac{dx}{dt} = \frac{K}{\varepsilon\mu}\frac{\Delta P}{x} \quad (1)$$

where V is the interface velocity, e is the sheet porosity, and μ is the liquid viscosity. The time required for the interface to move across the entire porous medium beginning at the upper surface (x=L) is given by integration:

$$\int_L^0 -x\,dx = \int_0^t \frac{K\Delta P}{\varepsilon\mu}\,dt' \qquad (2)$$

resulting in

$$t = \frac{\varepsilon\,\mu\,L^2}{2K\,\Delta P} \qquad (3)$$

where t is the required time. Let us apply typical conditions for a linerboard sheet. The viscosity of the warm water could be 0.0007 Pa-s, the compressed sheet might be 0.2 mm thick with a permeability of 4.0×10^{-16} m^2 and a porosity of 0.6. If gas is applied at a pressure of 0.5 MPa (73 psi), Equation (3) predicts that the gas-liquid interface will move across the sheet in 42 ms. A thicker or less permeable sheet will require more time. In reality, the displacement process will not be so efficient. The gas-liquid interface will not move smoothly but will break up because of inherent instabilities, which are discussed next.

Interface Stability

When a liquid is displaced in a porous medium by another immiscible fluid of lower viscosity, the interface between the phases is frequently unstable. This can be shown by simple stability analysis based on the sharp-interface assumption (34). Any small perturbation on the initially smooth interface will accelerate because of the lower pressure drop in the more mobile fluid, creating "viscous fingers" that penetrate into the phase being displaced, as shown in Figure 7 (35). For secondary oil recovery, this means that displacement of oil by water or gas will be inherently inefficient, since large portions of the oil may be bypassed by fingers that break through to the production well. In the paper industry, this means that a gas phase will tend to simply blow through certain paths in the paper, leaving much of the water behind. Based on the work of Lenormand et al. (36), who numerically examined displacement processes for a wide variety of conditions, the conditions typical to air-water displacement in paper clearly fall in a regime where significant viscous fingering is likely.

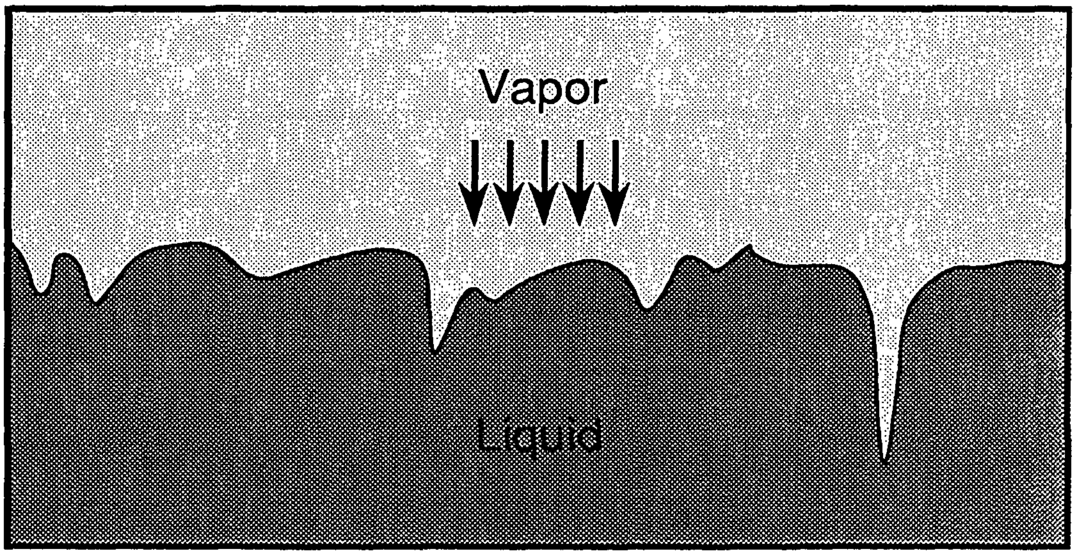

Figure 7. Viscous fingering in a porous medium as a gas displaces a liquid.

However, a number of factors have been shown to enhance stability. For example, if the viscosity of the displacing phase can be "artificially" increased, interface stability can be achieved. This artificial increase in viscosity can be achieved by using foams, which are mostly low-viscosity air but behave like a fluid with a very high viscosity due to the structure of the foam. In secondary or tertiary oil recovery, for example, foams have been used to increase the stability of displacement (37). In the paper industry, Skelton (38) has reported that application of foam to paper increases water removal by suction. Skelton writes that the reasons for this effect are unknown. The analogy to oil recovery, however, would appear to provide at least part of the explanation. The stability of the displacement process in suction is increased, and water removal becomes more efficient. Experimental work with stabilizing foams is planned for the current study, but has not yet been conducted.

Anisotropic permeability in paper can also enhance displacement stability. If the lateral permeability is greater than the normal permeability, a viscous finger could tend to spread out in the plane of the paper, thus creating a more uniform surface. Measurements of the full permeability tensor have been conducted in conjunction with the present study (39,40).

The results to date indicate that the ratio of in-plane to transverse permeability is greater than unity, with an observed range of about 2-10. Paper made from TMP pulp had the greatest anisotropy ratios observed, near 10, while kraft pulps gave values consistently near 2 (40). Papers with higher lateral permeabilities may yield improved interface stability in displacement dewatering.

Heat transfer can also play a role in decreasing instabilities. If transient heat transfer from the vapor to the liquid is occurring, the interface becomes more stable (41). As a hot viscous finger penetrates into cooler liquid, the gas begins to cool and contract, thus decreasing the growth rate of the viscous finger.

When steam displaces water, the condensation of steam can significantly improve the stability of the vapor/liquid interface (41). For instance, as steam breaks through and contacts cooler liquid, it will condense. The viscous fingers become "self-sealing" to some extent, making the interface more stable. The combined effects of heat transfer and condensation are believed to make superheated steam a good candidate for displacement dewatering.

EXPERIMENTAL APPROACH

Equipment

An experimental displacement device (Figure 8) was constructed for this study. The displacement device consists of two heads installed in an MTS hydraulic press (Figure 9). The hydraulic ram drives the upper head, and can control the motion and applied mechanical pressure to simulate pressing conditions. The upper head consists of a hollow chamber above a drilled bronze plate. The plate can apply mechanical pressure to paper, and at the same time allow gas pressure to be applied. High-pressure gas is released from a pressure vessel into the upper chamber by a rapid solenoid valve. The extended, tapered sides of the upper head fit over the lower head and form a seal with an O-ring that encircles the lower head. The lower head is also a hollow chamber with a drilled bronze plate on top to allow gas to pass from the upper into the lower head, and from thence into the atmosphere through a hole in the lower frame of the MTS system. If desired, the volume of gas passing through the sheet can be measured with a collection bag at the end of the exhaust line from the lower head. The gas pressure in the upper head can be released by gas passing through the sheet and into the lower head, by escaping at the end of a press event when the O-ring seal is broken, or by passing through an opening in the side of the upper head.

The bronze plates are drilled with 0.09-in (0.0023 m) holes, with a center-to-center distance of 0.125 in (0.0032 m). The open surface area is 47%. The plates are sufficiently thick (1 in or 0.0254 m) to prevent significant bowing during compression. Carbon paper imprints between the platens were used to check head alignment in order to get a uniform applied pressure.

For displacement dewatering of paper, a 3-in (0.076 m) handsheet disk is placed on a 3-in felt. A fine, stiff disk of either a plastic forming fabric or copper mesh is placed on top of the paper to help distribute the gas pressure uniformly over the paper and to prevent embossing the paper with the pattern of the drilled upper plate. A felt could also be used. Tests have indicated that the gas pressure is applied evenly to the paper in the tests of this study. The fabric-paper-felt stack is placed on the lower drilled plate. An electronic switch then drives the upper head downward to apply a controlled pressure pulse typically lasting for 20-100 ms. As the mechanical pressure pulse begins, a relay opens the solenoid valve for a specified time and the pressurized gas then fills the upper chamber and begins to assist the dewatering of the paper. Gas pressures of 0.14-0.75 MPa (20-110 psi) have been used.

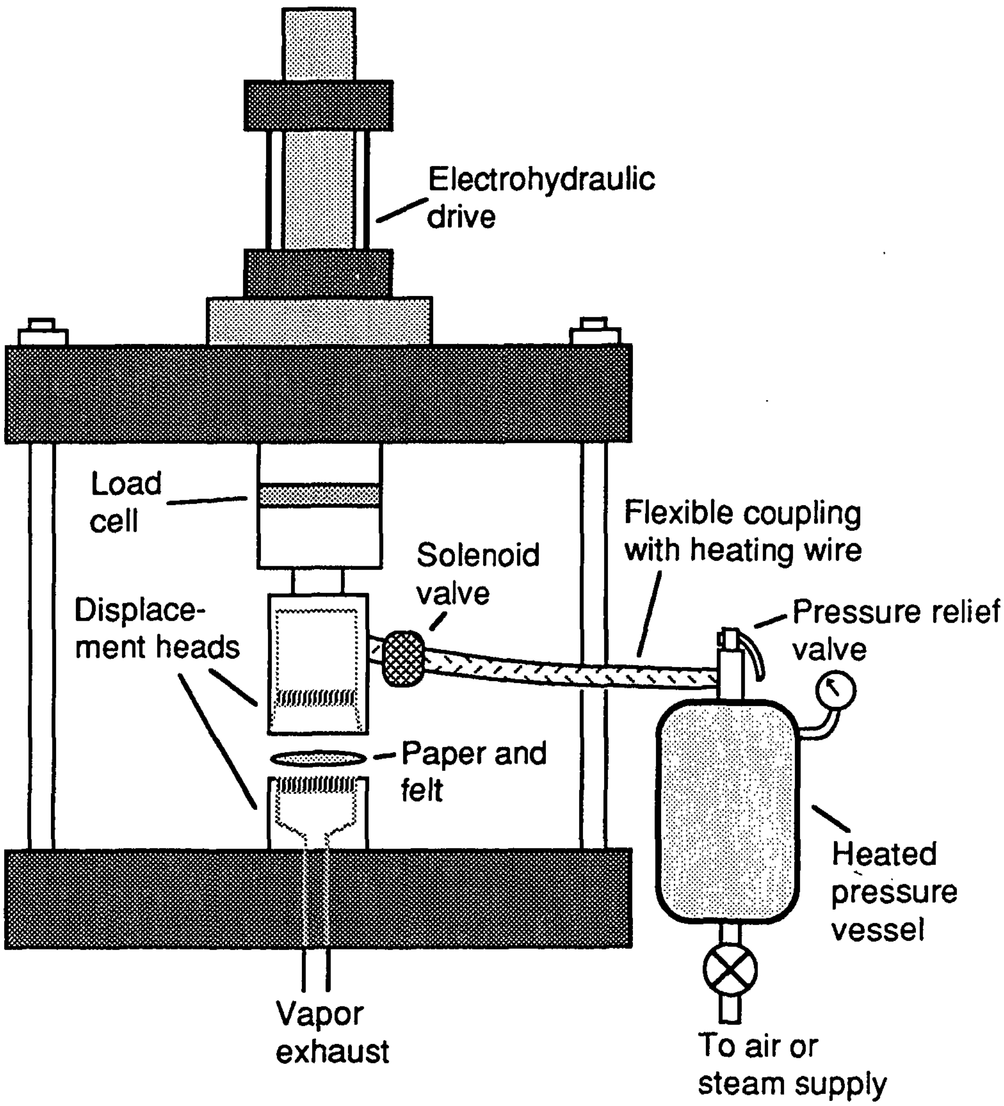

Figure 8. The experimental displacement apparatus.

Unfortunately, the fastest solenoid valve which could be purchased still had a lag time of about 20 ms before the valve is fully open. Once the valve is open, the chamber reaches full pressure in about 5 milliseconds. A control system was thus devised which could trigger the solenoid valve within a range of over 100 ms before sheet compression begins to over 100 ms after compression ends. Generally the solenoid was fired 10-20 ms before the beginning of the mechanical pressure pulse, providing a gas pulse to the sheet that began only after substantial compression had occurred.

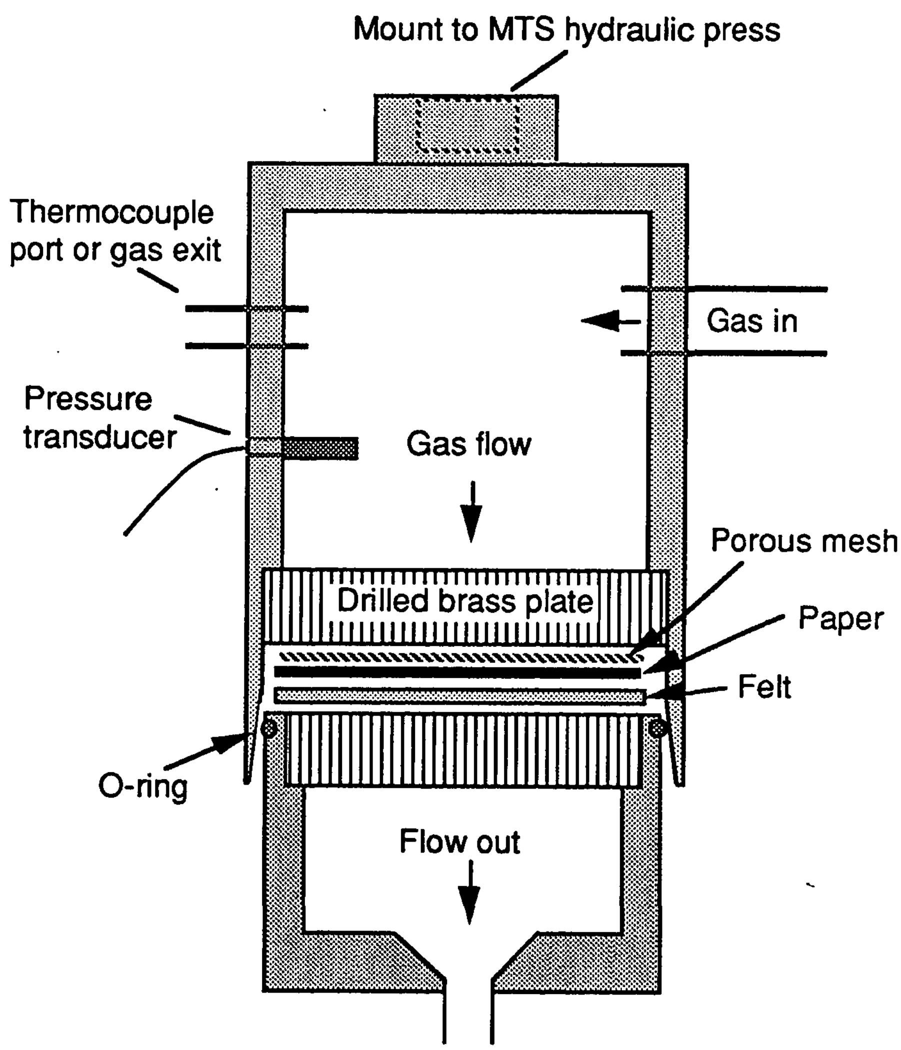

Figure 9. Detail of the displacement heads.

The new displacement heads overcame the problem of nonuniform gas pressure by providing a large chamber above the sheet to allow the applied gas pressure to become spatially uniform during displacement. An O-ring assembly prevented gas leakage from the upper chamber during displacement.

"Unconfined" Displacement Dewatering

The greatest difficulty with the new equipment, which also appears to have been a problem with the previous equipment used for this project, was controlling the duration of the applied gas pressure. We wished to release the gas pressure before the expansion phase of the press event began; this would keep the gas application time low and prevent significant blowing as the sheet decompresses and becomes more permeable. (Blow through should not harm the sheet and will increase the dryness by water entrainment and evaporative drying, but we wished to avoid significant air flows through the sheet.) Controlling the gas pressure proved problematic, however. We attempted to use a second fast-acting solenoid valve on the upper head to release the gas at a specified time. Unfortunately, even the best solenoids that we could locate did not perform as required. Solenoid valves require upstream pressure or flow to become properly seated; the sudden burst of pressure as the first solenoid opened blew open the second solenoid before it could seat, releasing the vapor pressure.

The first set of experiments was thus run with only one solenoid valve. The port which had served as the exit port to the second solenoid valve was sealed, and the applied gas remained pressurized until it either passed through the sheet or was released as the two displacement heads separated (usually a combination of both). As a result, the vapor pressure duration in the first set of experiments was undesirably long, ranging from 100 to 350 ms, and exceeded the duration of the mechanical pressure pulse. Since the gas pulse was not confined within the time of the mechanical pressure, these runs are termed "*unconfined*" displacement dewatering. Figure 10 shows pressure pulses during a typical unconfined run.

The long gas pulse in the unconfined runs allowed us to test the upper limits of the displacement process: if the process appears economically inviable at these conditions, there is no reason to explore it at shorter durations.

"Confined" Displacement Dewatering

Following the somewhat favorable results of the first series, a second series of experiments was launched in which the duration of vapor displacement was made shorter by leaving an opening in the gas exit/thermocouple port of the upper head. The open time of the inlet solenoid was also shortened as much as possible (too short a signal would lead to closing before the solenoid was fully open). With this arrangement, a series of tests with more desirable gas pulses could be achieved. Figure 11 shows the typical gas and mechanical pressure pulses for such a run. Since most or all of the gas pulse is confined within the mechanical pressure pulse, these runs are termed "confined" displacement dewatering.

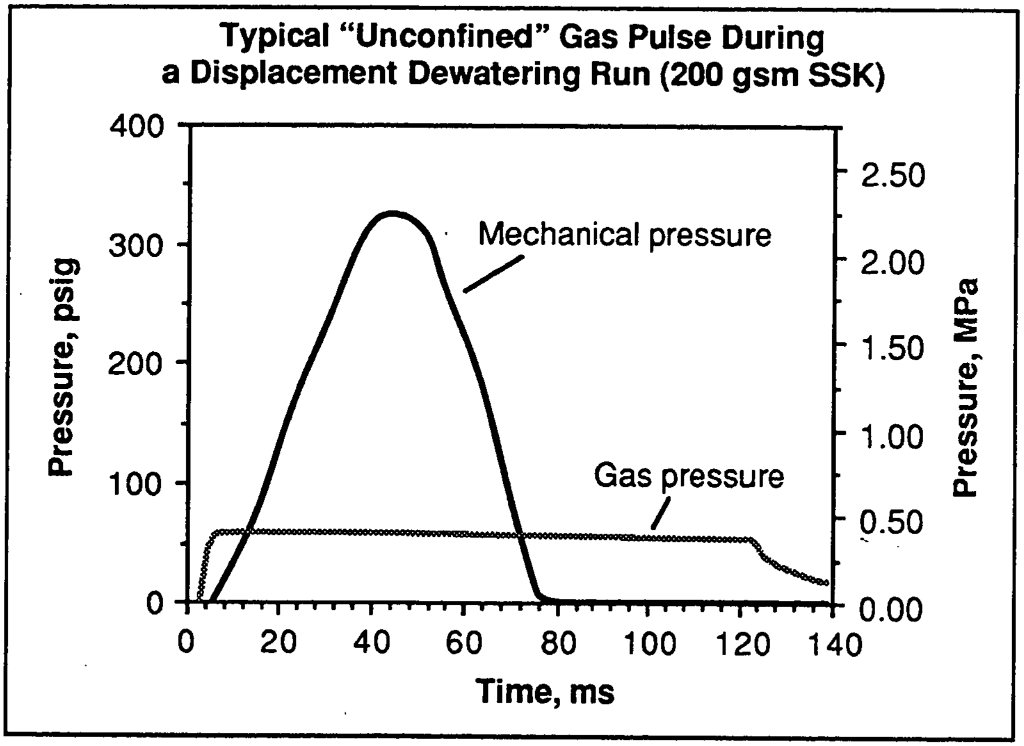

Figure 10. Applied gas and mechanical pressure pulses during a typical "unconfined" displacement dewatering run. The gas pulse is not confined within the mechanical pressure pulse, but extends well beyond.

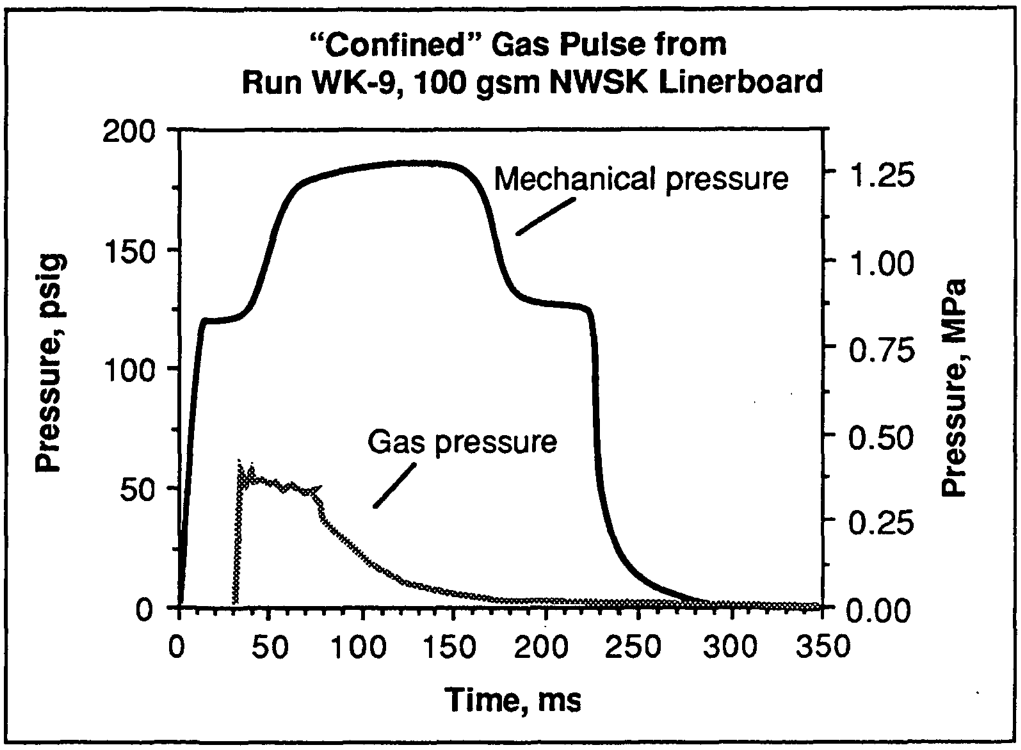

Figure 11. Applied gas and mechanical pressure pulses during a typical "confined" displacement dewatering run.

Run Procedures and Conditions

Displacement dewatering and wet pressing runs were made in a variety of handsheets, primarily linerboard grades. The two main linerboard furnishes were a Northwestern softwood unbleached kraft (NWSK) and a Southern softwood unbleached kraft (SSK). Both furnishes had freeness levels of about 700 CSF. Some runs were made in handsheets from an unbleached thermomechanical pulp (TMP). The TMP had a freeness of about 100 CSF. Saturated 240 gsm commercial blotter paper was also used as an example of a heavy but highly permeable material.

In each run, a wet sheet was weighed, then placed between a dry felt and the fine plastic or copper mesh, and the assembly was set on the drilled bronze plate of the lower displacement head. The MTS control system was activated, which would cause the pressing and displacement event to occur. As the upper head retracted, the sheet was removed and weighed again. The sheet was then dried at about 100°C under mild constraint, and its thickness was measured at 4-10 random sheet locations to obtain an average. From this information the solids in, solids out, and sheet density could be determined.

Displacement was done with both room temperature air and superheated steam. When steam was used, the pressure vessel and the flexible coupling to the upper displacement head were heated and insulated. The pressure vessel was heated with a band heater near the centerline, and temperatures measured there were typically 315-330°C. The heated flexible coupling to the solenoid valve was at about 175°C. The temperature inside the upper head just prior to displacement was 120-150°C, achieved by passing some pressurized steam through the head while compressing a disk of blotter paper on a felt. This head temperature was usually sufficient to prevent significant condensation in the head during a displacement event. Without this preheating of the head, condensate drops would often be found on sheet after displacement.

The use of steam posed a number of problems. While condensation was prevented by heating the displacement head, the MTS system also warmed up. This often played havoc with the dynamic response of the system. The solenoid valve, rated for high temperatures, also tended to behave erratically with steam, frequently misfiring. A number of good runs were possible with steam, however.

The peak mechanical pressures in the displacement runs ranged from 180 to 400 psi (1.2-2.8 MPa), well below what is typically used in wet pressing. Nip residence times were large, however, with a range of about 70-300 ms. The lower limit is due both to control problems encountered in the MTS at low mechanical pressures, and the dynamic limits in the gas application system.

The applied gas and mechanical pressure pulses were measured with a load cell and pressure transducer, respectively, and monitored with an oscilloscope. Digital readings of peak mechanical pressure and total pressing impulse were available.

<u>Wet Pressing Variants: Normal, Low Pressure, and Open Surface</u>

To compare the densification of displacement dewatering with the densification of conventional pressing operations, we wished to press a number of sheets without any gas being applied. If displacement dewatering is done in the normal manner, but with gas at zero or very low pressure, the pressing efficiency is low. In such a pressing event, termed "open-surface wet pressing," the sheet is pressed by an open wire surface backed with an open drilled platen. (In Figure 5, for example, the data labeled "without air" represent open surface wet pressing.) Without significant gas pressure being applied, water may pool above the sheet and cause rewetting, or sufficient hydraulic pressure for dewatering may not be generated. The low dryness levels achieved in this manner are an artifact of the experimental setup, and would be different if another gas delivery and distribution system were used, such as a porous platen composed of sintered metal without a layer of wire or fabric on the paper. Comparison of displacement dewatering to open-surface wet pressing is an inappropriate means of evaluating process performance.

To create a true wet pressing effect, the pressing surface of the sheet must be solid. By replacing the wire mesh with a rigid disk of acrylic plastic, wet pressing could be simulated in the displacement apparatus. Gas was not applied, of course, during such runs. During a series of displacement dewatering runs, occasional wet pressing results would be obtained using this method. The wet pressed sheets were thus subject to essentially the same mechanical pressure pulse as was used in the displacement dewatering tests of that particular run. Because the peak mechanical pressures were lower in these runs than is typically used in commercial wet pressing, this method of wet pressing is termed "low-pressure wet pressing." In the industrial practice of wet pressing, it is commonly noted that wet pressing density-dryness data tend to fall on the same curve, regardless of the details of the wet press operation. Therefore, during most of this study, it was simply assumed that the density-dryness data for a given sheet type obtained with low-pressure wet pressing would fall on the same curve as similar data sets obtained under different wet pressing conditions. This assumption was finally tested by obtaining "normal wet pressing" data.

"Normal wet pressing" in this study refers to wet pressing data obtained by pressing paper on a felt between solid platens using peak mechanical pressures from about 2-8 MPa and nip residence times of 20-50 ms. The applied mechanical pressures are higher and the nip residence times much lower in "normal wet pressing" than those used in the low-pressure wet pressing tests, and are closer to the conditions used in commercial operations.

RESULTS

Water Removal and Densification

Unconfined Displacement

The unconfined tests were run to check the upper limits of displacement dewatering. Being "unconfined," the gas exposure times were longer than the nip residence times, with total gas exposures on the order of 350 ms. Peak mechanical pressures were about 2.3 MPa. The results from this series gave positive indications that displacement dewatering could effectively remove water, and did not serve to disprove the concept. To further test the concept, it was necessary to run tests under the more critical confined conditions. Since the confined displacement results provide the most useful data for evaluating the proposed process, they will be emphasized in this paper.

One key set of data from the unconfined series with superheated steam is given in Figure 12, where density-dryness relationships for three batches of 100 gsm handsheets are examined. Two batches of sheets were made from a Southern softwood unbleached kraft (SSK) furnish, and the other was from unbleached TMP. Most runs employed an 80 ms nip residence time, although in SSK batch 1, times up to 200 ms were used. Steam exposure times were on the order of 100-150 ms longer than the nip residence time. The enclosed shaded area contains the low pressure wet pressing results (same mechanical pressure pulses as the displacement runs, with a solid surface in contact with the upper sheet surface), and the other data points give the steam displacement results.

The two linerboard batches give consistent results, indicating that lower densities are achieved than is possible with low-pressure wet pressing, and also indicating that high dryness levels can be achieved. Even more encouraging are the TMP steam results, where the density-dryness curve is flat. This suggests that high solids levels can be achieved with no significant losses in bulk. However, given the long exposure times of unconfined displacement, these results were probably achieved largely by thermally drying the sheet with steam rather than by displacing the liquid water. An energy balance has not been done, but this particular process is not likely to save energy costs. To more realistically explore the potential of displacement dewatering, we must consider results with confined displacement, where shorter gas exposure times are used and less gas is wasted by blowing through the sheet after the end of the nip.

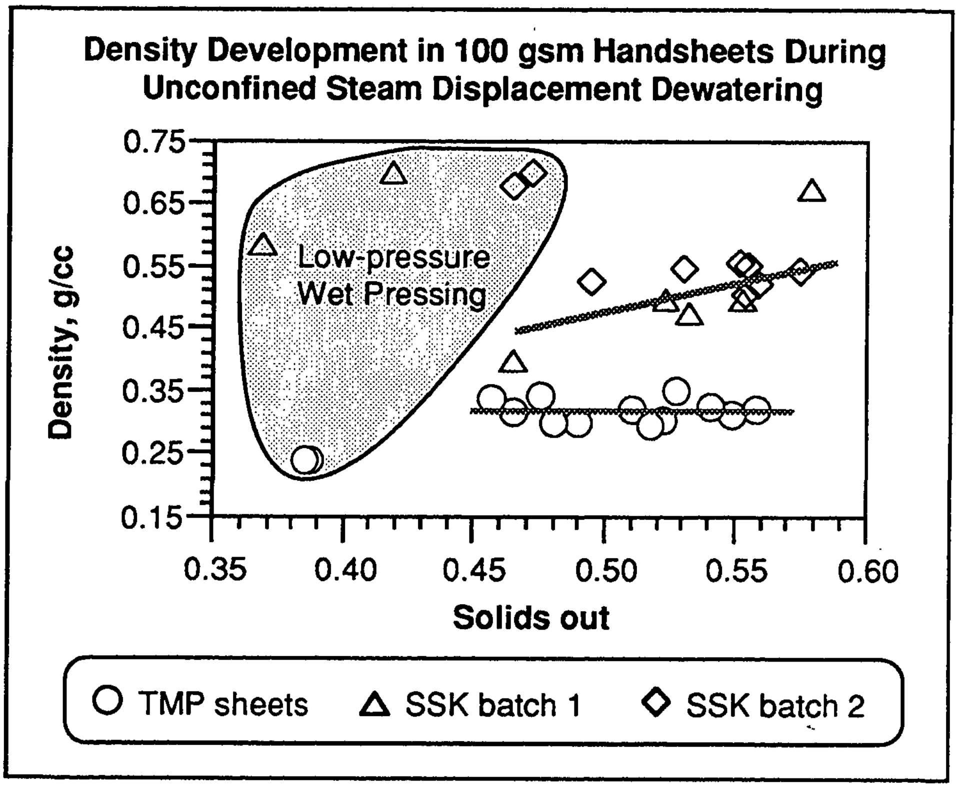

Figure 12. Density-dryness relationship for unconfined displacement dewatering with superheated steam.

Low Pressure, Confined Displacement

In the confined displacement runs, the equipment and the MTS/solenoid valve dynamics were adjusted to ensure that most or all of the gas pressure was contained within the duration of the mechanical pressure pulse (see the discussion in the experimental section above). Low mechanical pressures were used, ranging from 1.2-2.1 MPa peak.

Saturated blotter paper was examined first in the confined displacement series. The data for air displacement in blotter paper are shown in Figure 13. Displacement dewatering yields higher solids levels than low-pressure wet pressing at the same press conditions, but low-pressure wet pressing at a moderately higher pressure (2.34 MPa or 340 psi peak) produces about the same dryness that was achieved with 0.55 MPa (80 psi) of air. Density effects were not considered in the blotter paper, which had already been dried prior to being saturated for this experiment (it was felt that the results would not be of any real value).

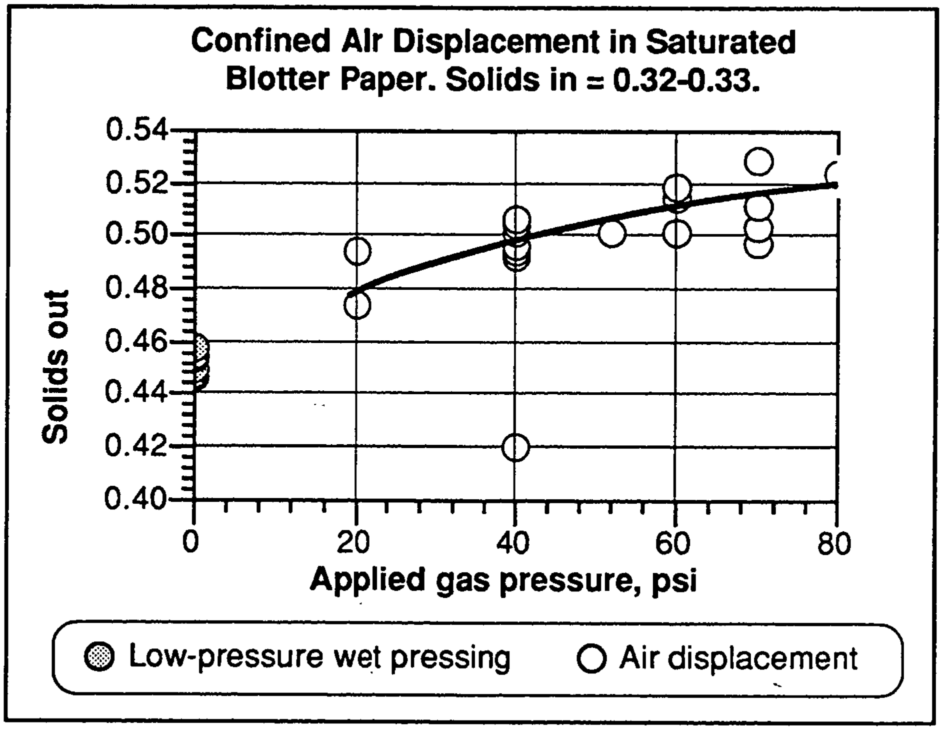

Figure 13. Air displacement results in saturated blotter paper.

More meaningful runs were then done with freshly made linerboard handsheets in order to examine the issue of bulk control with confined displacement dewatering. In particular, it was desired to not only compare displacement dewatering with low-pressure wet pressing under similar press conditions, but also to compare the results with normal wet pressing (done under conditions more closely related to commercial pressing, as described above).

The linerboard handsheets were made from the Northwestern softwood unbleached kraft (NWSK) furnish. First, normal wet pressing data were obtained. A variety of nip residence times and peak pressures were used to obtain a range of dryness values. Peak pressures up to 8 MPa were achieved, with residence times on the order of 20 -60 ms. This was done for 100 and 150 gsm NWSK sheets. The results are given in Figure 14. Both basis weights show similar behavior.

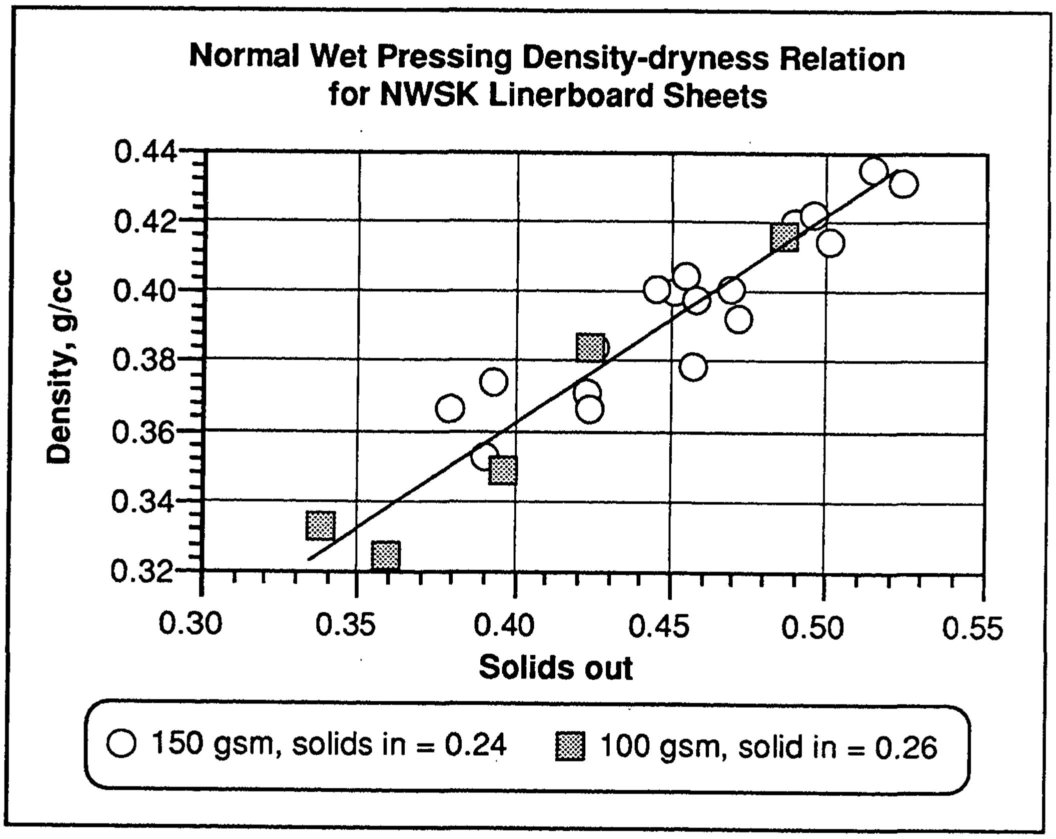

Figure 14. Dryness-density relationship for normal wet pressing in Northwestern softwood unbleached kraft (NWSK) handsheets.

Air displacement was then examined in 150 gsm sheets of this furnish. Nip residence times ranged from 120-140 ms, with peak pressures of about 2.3 MPa. Peak gas pressures lasted for 60 ms and total gas exposure time (gas over 10 psi or 0.07 MPa) was 120 ms. The results, shown in Figure 15, were not encouraging. At 0.55 MPa (80 psi) only a 5% gain in solids was possible over low-pressure wet pressing under the same pressing conditions (including, of course, the long nip residence time). When the density-dryness data were examined, a disturbing result was found. As can be seen in Figure 16, displacement dewatering gives lower density at a given solids than low pressure wet pressing, but compared to the previously collected normal wet pressing data (Figure 14), there is a substantial increase in density. The assumption of a single density-dryness curve for wet pressing is clearly incorrect in this case. Perhaps the long nip residence times (225-240 msec) used in the displacement runs and low-pressure wet pressing runs caused a loss of springback through a creep effect and thus yielded higher density, even though lower mechanical pressures were applied.

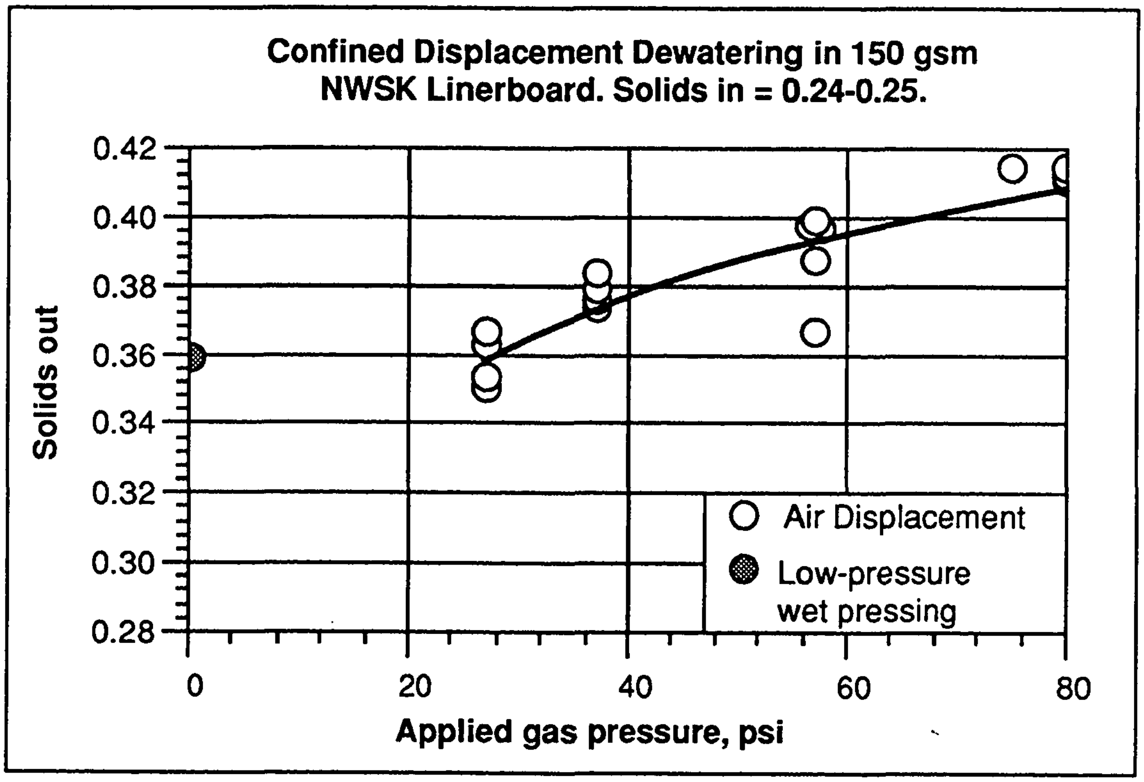

Figure 15. Confined air displacement in 150 gsm NWSK sheets.

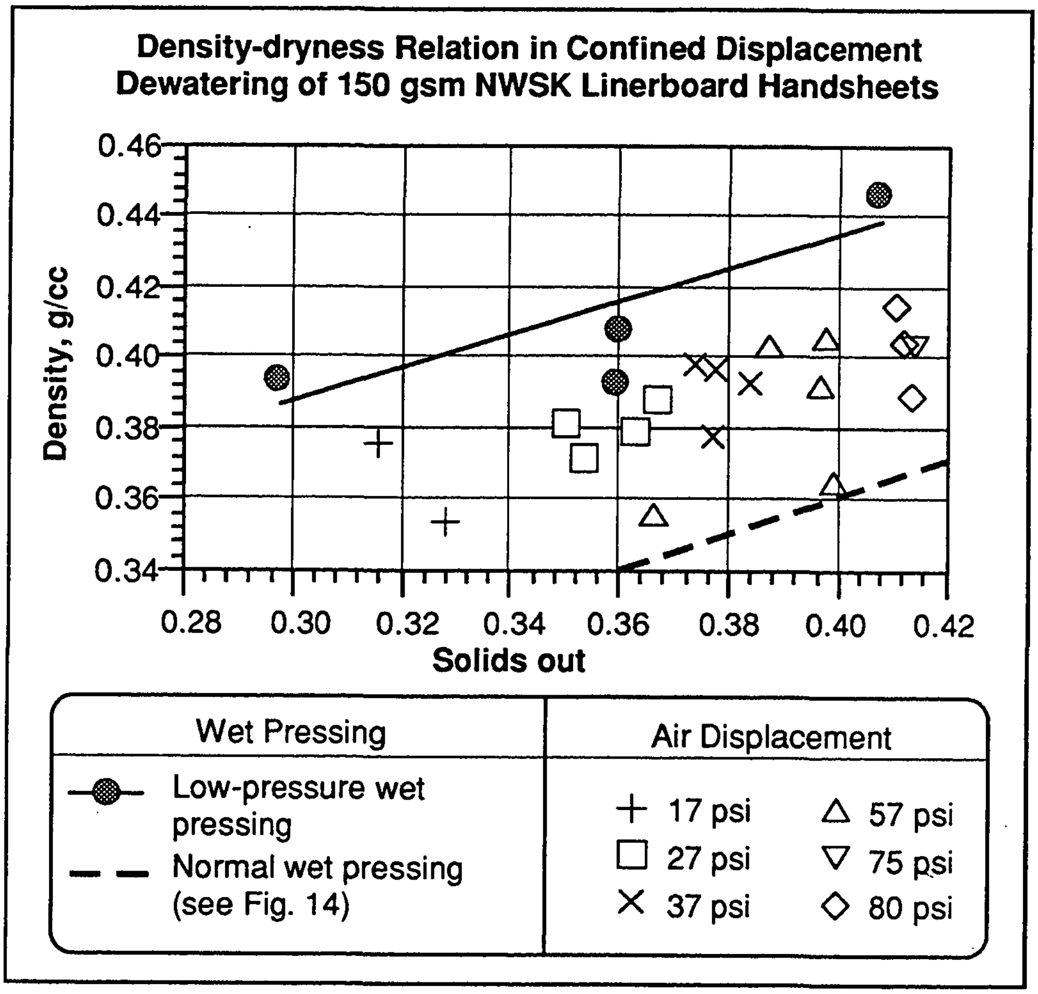

Figure 16. Density-dryness relation for data of Figure 15.

Similar runs were then conducted for 100 gsm NWSK linerboard sheets. Mechanical pressures ranged from 150 to 240 ms, and lower mechanical pressures were used, with peaks of 1.2-1.4 MPa (180-200 psi). Gas exposure times were still at 120 ms, with gas peak pressures lasting for 50-70 ms. In addition to air displacement, superheated steam was also used. The dewatering results for both air and steam displacement are shown in Figure 17, and density information is given in Figure 18. With such low mechanical pressure, low-pressure wet pressing alone raised the solids level from 0.25 to just 0.28. Air displacement was more effective, but the gains are not impressive. Steam dewatering again shows more promise, with over 44% solids possible. The density data, however, are not encouraging. Steam displacement seems to significantly increase the densification of the sheet, probably by thermally softening the sheet and decreasing its resistance to

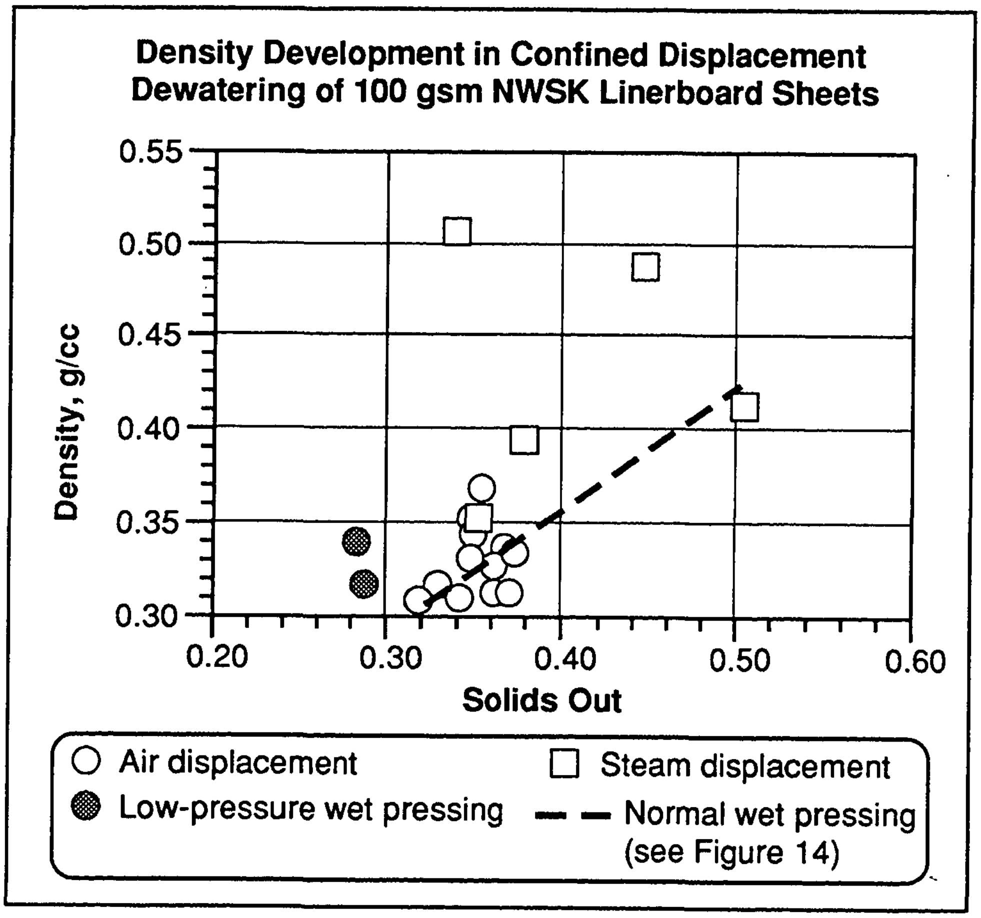

Figure 18. Density-dryness relationship in steam and air displacement dewatering of 100 gsm NWSK sheets.

Path-dependent Density-Dryness Relationships: Further Pressing Work

The possibility that creep effects may lead to higher densities in very long nips needs further experimental verification. Given the constraints of scheduling the MTS equipment and the lack of a technician during the latter part of this period, only one additional body of data could be collected to examine the effect. Several 100 gsm sheets of unbleached Southern kraft, with a freeness of 300 CSF and at 30% solids were wet pressed with a variety of nip residence times and peak mechanical pressures. Press times ranged from 18 to 140 ms, and peak pressures ranged from 200 to 1500 psi. The post-pressing weight was recorded, and the sheets were dried under mild restraint on a steam-filled cylinder. The dry weight was recorded and sheet thickness was measured with an IPC soft-platen caliper device.

The results show path-dependent density-dryness, but are not consistent with the trends noted above. As shown in Figure 19, the data tend to fall onto two curves, with the higher-density curve corresponding to pressing with low nip residence times (and high peak pressures) rather than high nip residence times and low peak pressures. This is in sharp contrast to the results reported above. A creep effect is thus not evident. Perhaps creep would be observed again in different furnishes or at higher pressing times. Further experimental investigation is needed, primarily a detailed and careful study of density development in displacement dewatering.

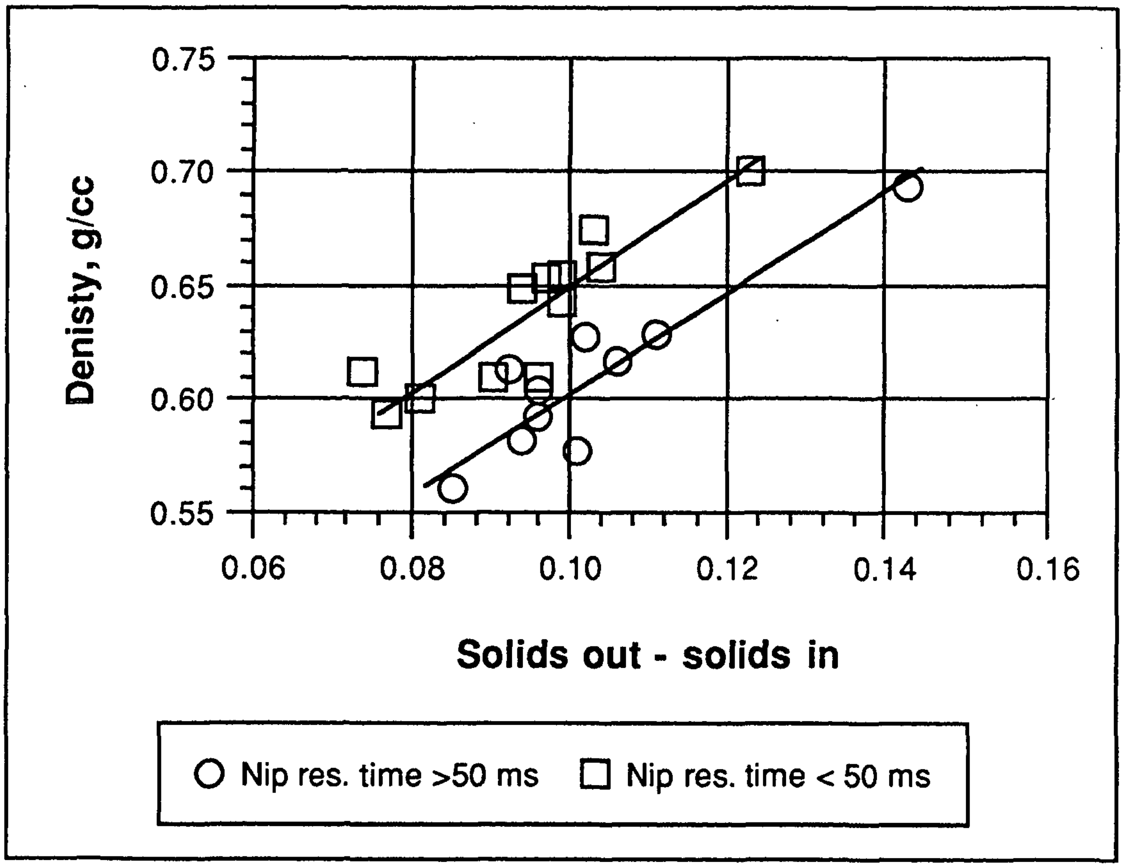

Figure 19. Density-dryness relationships for 100 gsm linerboard handsheets subject to various wet pressing conditions.

Blow Through During Confined Displacement Dewatering

Since gas was primarily applied only while the sheet was under significant compression in the confined series, the resistance to gas flow was high and blow through was relatively low. However, some gas still blew through the sheet. Measurements made during runs with 150 gsm linerboard sheets and 60 psi of air (0.4 MPa) suggested that 0.5-0.8 liters of air at atmospheric pressure were passing into the lower MTS head during a 120 ms pulse of "confined" gas pressure. Not all of this gas had to pass through the sheet, for edge flow around the sheet and through the felt may have been significant. Nevertheless, it is likely that channeling or viscous fingering occurs quickly and permits gas to flow through the sheet. This is in stark contrast to the ideal of displacement dewatering, namely, that the amount of gas required is the minute amount corresponding to the volume of the water being displaced.

Experimental Artifacts at Low Gas Pressures

In the figures above, results from open surface pressing have not been included because such a pressing operation has little relevance to practical water removal. The low dryness levels achieved are an artifact of the experimental setup. A similar artifact occurs when displacement dewatering is attempted with gas at too low a pressure to overcome the adverse effect of using an open pressing surface. In that case, often observed with pressures below 25-30 psi (ca. 0.2 MPa), displacement dewatering appears to give worse results than low-pressure wet pressing with the same nip conditions. For example, Figure 20 shows the full air displacement data set from which Figure 15 above was created. Low-gas pressure displacement data are included here which were discarded in Figure 15 for clarity (i.e., it was desired to save presentation and discussion of low pressure artifacts for later). As Figure 20 shows, over 30 psi (0.2 MPa) was required to overcome the adverse effect of an open upper platen. The "post-nip gas pulse" datum refers to a run in which the solenoid valve did not open until after paper had been pressed. This data point indicates the relative ineffectiveness of applying the gas phase when the sheet is not under a mechanical load.

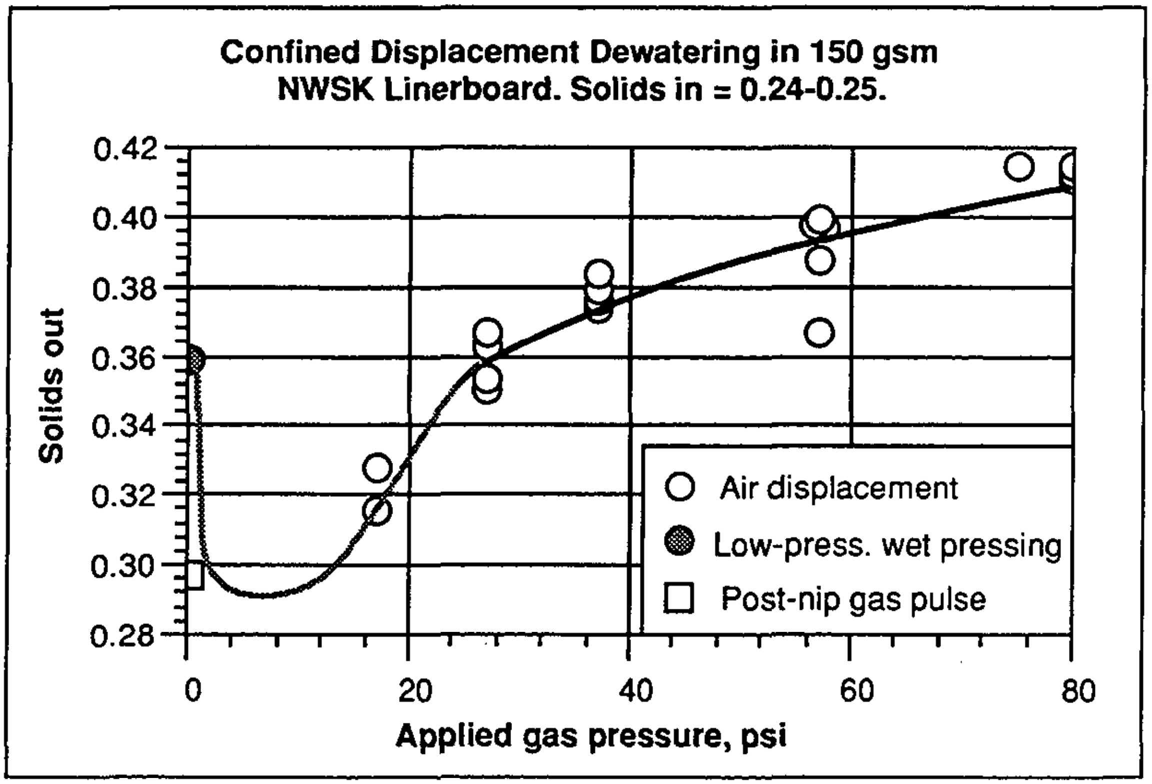

Figure 20. Confined air displacement in 150 gsm NWSK sheets.

Data for confined air displacement in blotter paper, previously shown in Figure 13, are again shown in Figure 21, but now with the full data set from that run. Displacement pressing at low gas pressure is worse than similar low-pressure wet pressing because of the lower hydraulic pressures generated under the open holes of the drilled bronze plate. Figure 21 also includes data for cases when the gas pulse came after the paper had been largely decompressed, but the seal between the upper and lower heads was still intact. These are shown at 0 psi since no gas was applied during the bulk of the mechanical pressure pulse. Such data again show the losses in dewatering when the sheet is not under sufficient mechanical pressure. Two data points are also shown from displacement runs where the solenoid valve failed to open, resulting in open surface wet pressing. The low dewatering (37% solids out) compared to regular wet pressing data (45% solid out) shows the adverse effect of pressing without a solid surface over the sheet.

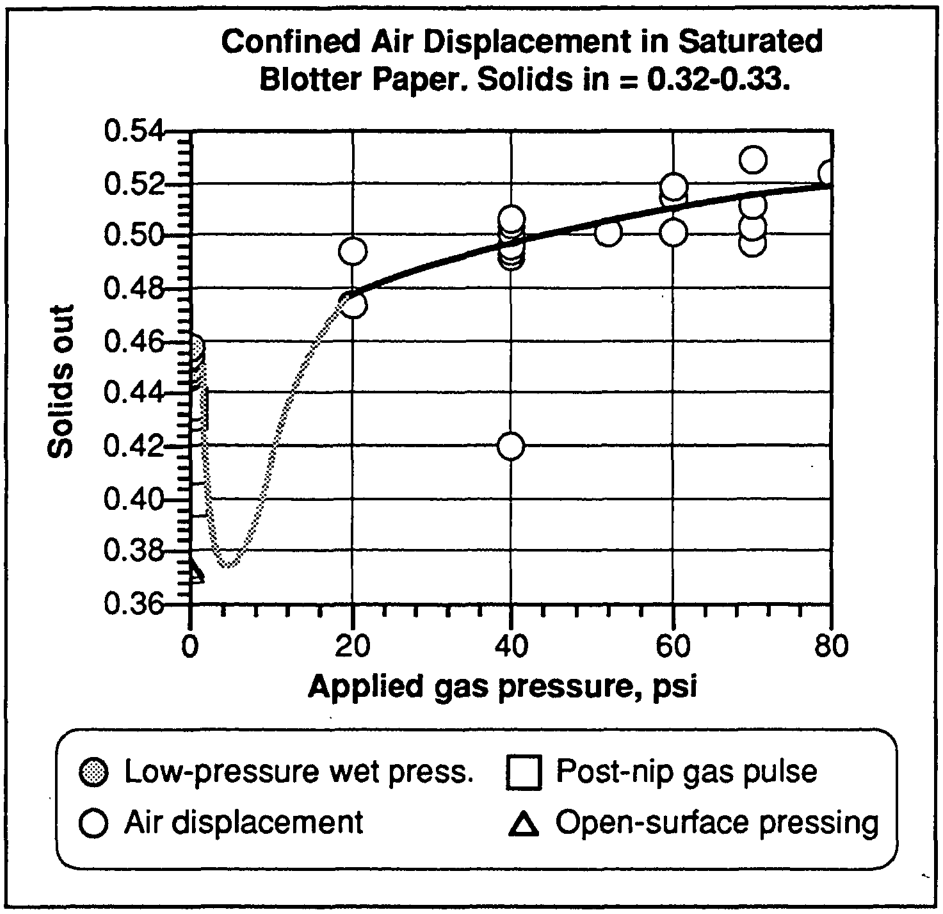

Figure 21. Full data set of air displacement results in saturated blotter paper (partially shown in Figure 13).

DISCUSSION

Improvements in Bulk?

In evaluating the commercial potential of displacement dewatering, we must focus on the ability to give added control over paper properties, with bulk or sheet density being most critical. The degree of water removal is also important. Both can be discussed in terms of density-dryness results.

Based on simple theoretical considerations, improved control over bulk should be easily achieved and has been the primary motivation for this study. The potential to control bulk is best examined by comparing density-dryness data for displacement dewatering and wet pressing. Several pitfalls arise, however, in making this comparison. If displacement pressing is compared to "wet pressing" done in the same way but without any gas (i.e., open-surface wet pressing, as defined above), the results can be impressive. Much higher dryness levels are achieved with no significant loss in bulk. But this is not a proper comparison because of the adverse effect of wet pressing without a solid platen in contact with the sheet.

A more logical evaluation can be made by comparing displacement dewatering with wet pressing (no gas) done under the same press conditions, but now with a solid surface replacing the wire or mesh to generate a wet pressing event. While this is termed low-pressure wet pressing because of the low mechanical pressures that were applied, the long nip residence times used should also be kept in mind. Compared to low-pressure wet pressing, displacement dewatering gives improved water removal once a certain gas pressure threshold is reached (ca. 30 psi or 0.2 MPa here). Higher bulk levels for a given solids content can usually be achieved, and the process thus appears to have promise.

However, the pressing conditions of displacement dewatering are much different than what is used in conventional wet pressing, especially since the nip residence time is extremely long. When "normal" wet pressing is done with shorter times and higher pressures, a different density-dryness curve is obtained. The normal wet pressing density-dryness curve lies below the low-pressure wet pressing curve and is below much of the displacement dewatering data. In other words, displacement dewatering may give worse bulk levels than normal wet pressing, possibly because of creep effects drastically reducing the springback of paper during the long nip. The problem may be exacerbated with steam where thermal softening of the fibers leads to higher compression.

Nevertheless, by using the proper combinations of nip residence time, gas pressure and gas exposure time, the problem with excessive densification may be overcome, and the concept of displacement dewatering may prove viable. Further work is clearly required, and is now underway.

If an existing pressing operation already requires a long nip time, then a retrofit to displacement dewatering could be advantageous. Higher dryness could be achieved with no loss in bulk compared to the normal process. The dryness possible depends, of course, on the permeability of the sheet and the amount of free water available for displacement at a given level of compression. Displacement dewatering may be well suited to the production processes of certain piece goods and specialty papers where low speeds are used.

Inherent Inefficiency

The classical concept of viscous fingering during gas-liquid displacement in porous media may underpredict the problems faced in displacement dewatering. The theory of viscous fingering is based on the concept of a homogeneous porous medium, meaning that for the length scales of interest in the problem, the medium can be treated as a single substance, a smooth blend of solid and void volumes. In such a system a flat interface between two phases during displacement could exist and could propagate without change were it not for unfavorable viscosity ratios. But in a thin structure like paper, where the solid elements are not tremendously smaller than the sheet thickness, the concept of homogeneity becomes inapplicable. Instead, we must realize that there will be some large, easily emptied pores and many small or blocked pores through which displacement cannot occur. As a result, the displacement process considered here is bound to be less efficient than theory would predict. Blow through may always occur under practical conditions. (See Brundrett and Baines [42] for a good discussion of the flow of air through uncompressed but wet sheets.) The mechanism of water removal in "displacement dewatering" is thus likely to be a combination of displacement, entrainment, evaporative through-drying, and rewet resistance. The latter mechanism has been discussed in the context of impulse drying (20), and is likely to apply here: sustained gas pressures existing in the sheet during nip expansion can continue driving water into the felt, resisting any back flows from the felt into the sheet. The importance of rewet resistance, however, has not yet been experimentally confirmed.

CONCLUSION

The concept of simultaneous gas and mechanical pressure to displace water from paper has been tested under several conditions and with several sheet types. The displacement dewatering concept requires further testing, but the data to date raise questions about possible densification effects due to creep. If increased densification does occur in a long-nip displacement process as opposed to a short-nip wet pressing operation, then displacement dewatering may not be suitable as a retrofit for an existing short-nip wet press. In low speed operations, however, where long nip times are already in use, the added dryness without further densification could be beneficial. A variety of piece goods and specialty products may be especially suitable for a retrofit with displacement dewatering.

Displacement dewatering with superheated steam can give very high dryness levels, but the effect is probably largely due to evaporation rather than displacement. Steam displacement can also seriously decrease bulk levels by thermal softening of the sheet under compression. Further research is needed on this issue.

Further tests are underway to determine if bulk can be maintained with efficient water removal in continuous, medium to high speed processes, where displacement dewatering would compete with conventional pressing technology.

PLANS FOR NEXT PERIOD

1. Carefully explore density-dryness relationships in displacement dewatering and compare to various wet pressing operations.

2. Determine optimum operating conditions for displacement dewatering with bench-scale equipment. Specifically, for a given furnish, find the best operating parameters for applied mechanical pressure, nip residence time, and gas phase pressure.

3. Examine the effect of air temperature, and further explore the potential of steam.

LITERATURE CITED

1. Holden, G. R., "Apparatus for Dewatering of Fibrous Webs in Papermaking and Similar Machines," U. S. Patent 3,284,285, (Nov. 8, 1966).

2. Kawka, W., "Theoretical and Experimental Analysis of the Blow-Through Process of Fibrous Web Dewatering" (transl.), Przeglad Papier., 39(11/12): 403-407 (1983).

3. Kawka, W., and Ingielewicz, H., "A New Technology for Producing Porous Papers Using Through Dryers" (translation), Przeglad Papierniczy, 30(1): 10-18 (Jan. 1974).

4. Kawka, W., Ingielewicz, H., and Marek, I., "Study of Equipment for Intense Dewatering and Drying of Porous Paper Products," Przeglad Papier., 34(3): 82-87 (March 1978).

5. Kawka, W., and Szwarcsztajn, E., "Some Results of Investigation on the Equipment for Intensive Dewatering and Drying of Porous Papers," EUCEPA-79, "Web Formation and Consolidation," 18th International Conference, London, May 21-24, 1979 .

6. Kawka, W., and Ingielewicz, H., "Dewatering and Drying of the Paper Web on the Machine by the Method of Air Blowing," Przeglad Papierniczy, 28(11): 381-387 (1972).

7. Kawka, W., "Optimum Consolidation of Absorbent Fibrous Webs on Paper Machines with Air Blow-Through Presses" (translation), Przeglad Papierniczy, 41(5): 163-169 (May 1985).

8. Kawka, W., "Principles of Paper Dewatering by the Air Blow-Through Method" (translation), Przeglad Papier., 34(2): 53-58 (1978).

9. Kawka, W., and Szwarcsztajn, E., EUCEPA-79 International Conference, London, May 21-24, 1979.

10. Walser, R., and Swenson, R. S., "Air Through-Drying of Paper," Tappi J., 51(4): 184-190 (1968).

11. Holik, H., "Zur Durchstromtrocknung von Papier," Das Papier, 26(4): 153-161 (1972).

12. Villalobos, J. A., "Paper Machine Hoods, Pocket Ventilation, Heat Recovery and Thru-dryers," TAPPI 1988 Practical Aspects of Pressing and Drying.

13. Bryand, E. T., "Energy-conserving Drying Methods," Paper Tech. and Ind., 16(1): 24-29 (1975).

14. Randall, K. R., "Using High-velocity Impingement Air to Improve Through Drying Performance on Semi-Permeable Webs," Drying 84. Ed. A. S. Mujumdar, Wash., D. C., Hemisphere Publ. Corp. (1984). pp. 254-263.

15. Burgess, B. W., and Chapman, S. M., "Turbulent Drying Process," U.S. Patent 3,418,723 (1968).

16. Burgess, B. W., Koller, W., and Pye, E., "The Papridryer Process Part II - Mill Trials," Pulp and Paper Mag. Canada, 73(11): 73-81 (1972).

17. Sprague, C. H., "New Mechanisms in Web Consolidation," Pira Paper and Board Division International Conference, Brighton, Sussex, England (May 19-23, 1986).

18. Lavery, H. P., "New Mechanisms for Water Removal From Paper Through Impulse Drying," AIChE Summer Meeting, Minneapolis, Minnesota, Aug. 16-20, 1987. Also printed as IPC Technical Paper Series #251, The Institute of Paper Chemistry, Appleton, WI, July, 1987.

19. Zavaglia, J. C., and Lindsay, J. D., "Flash X-ray Visualization of Multiphase Flow During Impulse Drying," Tappi J., 72(9): 79-85 (Sept. 1989).

20. Lindsay, J. D., "The Physics of Impulse Drying: New Insights from Numerical Modeling," The Ninth Fundamental Research Symposium, Cambridge, England, Sept. 16-22, 1989.

21. Gottwald, B. C., Halsey, B. S., Williams, R. C., and Haigh, J. M., "Continuous Process of Drying Uncoated Fibrous Webs," U.S. Patent 3,354,035 (Nov. 21, 1967).

22. Clemens, M. L., and Morton, W. J., "Method and Apparatus for Continuously Expelling an Atomizing Stream of Water from a Moving Fibrous Web," U.S. Patent 4,157,938 (June 12, 1979).

23. Sprague, C. H., "New Concepts in Wet Pressing," Final report prepared for the US DOE under contract AC02-84CE40685 by The Institute of Paper Chemistry, Appleton, Wisconsin (now IPST, Atlanta), Report No. DOE/CE/40685-T1, U.S. DOE, Office of Industrial Programs, Conservation and Renewable Energy Division, Washington, D.C., March 1986.

24. White, R. E. and Marceau, W. E., "The Capillary Behavior of Paper," Tappi J., 45(4): 279-284 (1962).

25. Udell, K. S., "Heat Transfer in Porous Media Heated From Above With Evaporation, Condensation, and Capillary Effects," J. Heat Transfer., 105: 485-492 (1983).

26. Etzler, F. M., "A Comparison of the Properties of Vicinal Water in Silica, Clays, Wood, Cellulose and Other Polymeric Materials," Water Relations in Food, ed. H. Levine, L. Slade, Plenum Press, 1991.

27. Lindström, T., "The Concept and Measurement of Fiber Swelling," Paper - Structure and Properties, ed. J. A. Bristow and P. Kolseth, pp. 75-97, Marcel Dekker, Inc., New York, NY, 1986.

28. Carlsson, G., Lindström, T., and Scöremark, C., "Expression of Water from Cellulosic Fibres Under Compressive Loading," Fibre-Water Interactions in Paper-

making, Transactions of the Symposium at Oxford, Sept. 1977 , British Paper and Board Ind. Fed., London, 1977.

29. Stone, J. E., and Scallan, A. M., "The Effect of Component Removal upon the Porous Structure of the Cell Wall of Wood. Part III. A Comparison Between the Sulphite and Kraft Processes," Pulp and Paper Canada, 69(12): 69/T288 (June 21, 1968).

30. Carroll, M., and Mason, S. G., "The Measurement of Fiber Swelling by the Liquid Permeability Method," Can. J. Tech., 30: 321 (1950).

31. Mason, S. G., "The Specific Surface of Fibers - Its Measurement and Application," Tappi J., 33(8): 403 (Aug. 1950).

32. Carlsson, G., "Some Fundamental Aspects of the Wet Pressing of Paper," Ph.D. Dissertation, Dept. of Paper Technology, The Royal Institute of Technology, Stockholm, Sweden, 1983.

33. Bear, J., "Dynamics of Fluids in Porous Media.," American Elsevier, New York, NY, 1972, pp. 439-440.

34. Chuoke, R. L., van Meurs, P., and van der Poel, C., "The Instability of Slow, Immiscible, Viscous Liquid-Liquid Displacements in Permeable Media.," Petroleum Transactions AIME, 216: 188-194 (1959).

35. G. M. Homsy, "Viscous Fingering in Porous Media," Ann. Rev. Fluid Mechanics, 19: 271-311 (1987).

36. Lenormand, R., Touboul, E., and Zarcone, C., "Numerical Models and Experiments on Immiscible Displacements in Porous Media," J. Fluid. Mech., 189: 165-187 (1988).

37. P. S. Hahn, Ramamohan, T. R. and Slattery, J. C., "Mobility Control in the Displacement of Residual Oil by an Unstable Foam," AIChE J., 31(6):1029-1035 (1985).

38. J. Skelton, "Foam Assisted Dewatering – A New Technology Emerges," Paper Tech. and Ind., 28: 435-436 (1987).

39. Lindsay, J. D., "The Anisotropic Permeability of Paper," Tappi J., 73(5): 223-229 (May 1990).

40. Lindsay, J. D. and Wallin, J. R., "Characterization of In-Plane Flow in Paper," AIChE Annual Meeting, Chicago, Illinois, Nov. 11-16, 1990.

41. C. A. Miller, "Stability of Moving Surfaces in Fluid Systems with Heat and Mass Transport," AIChE J., 19:909-915 (1973).

42. Brundrett, E., and Baines, W. D., "The Flow of Air Through Wet Paper," Tappi. J., 49(3): 97-101 (1966).